## ABSTRACT

SUI, XINYI. Qualitative and Quantitative Bio-degradation Study of Dyes and Textile Auxiliaries in Soil. (Under the direction of Dr. Nelson Vinueza).

Society has been constantly seeking and making cotton fabrics with better quality and functionality. This includes the alteration of color by using natural or synthetic dyes and the enhancement of commercial and aesthetic properties by applying chemical finishes. One excellent example illustrating this kind of innovation is the discovery of reactive dyes by Imperial Chemical Industries in the 1950s. Reactive dyes use a chemical reaction to create a new covalent bond between the cellulose chain and chromogen, giving the cotton fabric better colorfastness against washing and abrasion. Besides coloration by synthetic dyes, another approach to obtain cotton fabrics with enhanced properties and performance is to apply different chemical finishes onto them like anti-wrinkle and anti-microbial agents. The combination of reactive dye application and chemical finishing has resulted in considerable growth in the use of cotton fabrics. Nowadays, landfilling is the common disposal route for textile fabrics (natural or synthetic), generating an important source of potential contamination due to the migration of dyes and finishes onto soil during the decomposition of these chemicals by microorganisms. The biodegradation of cotton fabrics containing dyes and finishings in a compost is not fully understood. Furthermore, what happens to these chemicals under this decomposition environment is still unknown.

In this project, the chemical changes that happen to cotton fabrics containing reactive dyes or chemical finishes during a small-scale compost process under ASTM D 5988-18 are studied. Analytical methods that include extraction, liquid chromatography, High-Resolution Quadrupole Time-Of-Flight Mass Spectrometry, and tandem mass spectrometry are used in this fundamental study. First, via a joint forces of modified QuEChERS extraction method and QTOF mass spectrometry, four degradation products were identified based on exact mass measurement after a

simulated composting process on cotton fabrics dyed with four commonly used reactive dyes including RO35, RB49, Rblk 5, and RB19. Then a quantification method aiming to measure the concentration of docusate antimicrobial in soil after the simulated composting process was developed through a combination of QuEChERS extraction, quantitative tandem mass spectrometry, and isotopically labeled internal standard. After establishment, this method was validated according to FDA guidelines, and results suggested that this method have good linearity ($R^2 > 0.99$), good accuracy (mean % error less than 15%), good precision (mean % CV less than 15%), good sensitivity (measured docusate concentration is 400% higher than LOD and 100% higher than LLOQ), satisfying matrix effect, and the concentration of docusate (51±5 ng/mL) falls within the linear range of calibration. Finally, two degradation products from the aqueous degradation of RB19-dyed cotton fabric were extracted by QuEChERS extraction and identified based on QTOF mass spectrometry and qualitative tandem mass spectrometry against the standard. The results obtained in this work will provide a better understanding of what happens to certain reactive dyes and finishes in a compost environment.

© Copyright 2020 by Xinyi Sui

All Rights Reserved

# Qualitative and Quantitative Bio-degradation Study of Dyes and Textile Auxiliaries in Soil

by
Xinyi Sui

A dissertation submitted to the Graduate Faculty of
North Carolina State University
in partial fulfillment of the
requirements for the degree of
Doctor of Philosophy

Fiber and Polymer Science

Raleigh, North Carolina
2020

APPROVED BY:

| | |
|---|---|
| _____ | _____ |
| Nelson Vinueza Benitez<br>Committee Chair | Harold S. Freeman |
| _____ | _____ |
| Ericka Ford | Elena Jakubikova |

## BIOGRAPHY

Xinyi Sui was born in Hengshui, Hebei Province, China on October 3, 1993. In the year of 2012, he was admitted by Jiangnan University, which has one of the best-known textile institutes in the country. He earned his bachelor's degree in textile chemistry from Jiangnan University in 2016. During his undergraduate years, he used to work on the synthesis and the applications of bleaching activators. These experiences pushed him to pursue his Master of Science Degree at North Carolina State University (NC State). He obtained a Master of Science degree in Textile Chemistry at NC State in 2017, where his research focused on biodegraded fabrics containing Reactive Yellow 174. After that, he started his PhD program where he studied the degradation of dyes and textile auxiliaries in soil.

## ACKNOWLEDGMENTS

Here I would express my sincere gratitude to my advisor, Dr. Nelson Vinueza, for his visionary guidance, insightful advice, and genuine support in my Ph.D. program, without which this thesis would not have been accomplished to its least content. Additionally, I would like to thank for the help of my graduate committee members including Dr. Harold S. Freeman, Dr. Ericka Ford, Dr. Denis Fourches, and Dr. Elena Jakubikova. I would also like to thank our previous and current group members including Julio Teran, Zoe Millbern, Morgan Demmler, Dongyan Shao, Yixin Liu, Chengcheng Feng, Dr. Emily Lichtenberger, Dr. Kelsey Boes, Dr. Nadia Sultana, and Dr. Yufei Chen, all of whom have been always very supportive, helpful and collaborative to me and my research work. Also, I appreciate the kindness, care, and helpful experience offered by Wilson College of Textile staff including Traci Figura and Joyce Cole. Finally, I would like to thank my parents for their consistent support of my life and studies at NC State, and all those lovely close friends from the 3+X program including Jixin Gong, Lanjun Yin, Ningjun Tong, Runqian Zhang, Shuzhen Wei, Xiaolu Guo, just to name a few. Thanks a lot for all their generous supports whenever and wherever I needed. I feel so blessed to have all of them in my life in the United States.

## TABLE OF CONTENTS

## LIST OF TABLES

## LIST OF FIGURES

## Introduction

Landfill, a commonly seen process that involves burying unwanted solid wastes in the ground and letting them consume by microorganisms in nature, has been used to dispose of cotton fabrics since the dawn of civilization. The historical record has been found suggesting the presence of primeval landfill sites in ancient Greeks as early as 300 BC.[1] Nowadays, landfilling has been an elementary source for solid waste treatment in the US. According to the statistics from EPA, there are over 2,000 active landfill sites in the US and nearly 66% of textile waste is landfilled in 2017.[2] Despite its wide coverage, the process of how landfill decomposes cotton fabrics is not fully studied and this research needs to overcome several challenges. First of all, landfilling is a macro-scale process that is controlled by a variety of parameters such as temperature and moisture. Second, the analyte of interest may be mixed with soil matrix and maybe only a trace amount of analyte is available for study. Thus, as my doctoral project, I would like to investigate the chemical changes that happened to cotton fabrics with auxiliaries (reactive dye or chemical finishing) during a simulated small-scale landfill process with qualitative and quantitative analytical methods. The outcome of this project could further our understanding of the landfill degradation process.

In the following literature review, first, the properties and the behavior of reactive dye and chemical finishing on cotton will be discussed. Then the composition of mass spectrometry and the working mechanism of each component will be introduced. After these two chapters, the third chapter will be focused on the chemical composition of soil and different matrix extraction techniques. Then in chapter 4, a published study about the detection of reactive dyes from dyed fabrics after soil degradation via QuEChERS extraction and mass spectrometry will be presented. In chapter 5, a quantitative tandem mass spectrometry study will be introduced featuring the measurement of the concentration of docusate antimicrobial agent in soil. Finally, in chapter 6 a

qualitative mass spectrometry study will be presented featuring the identification of two Reactive Blue 19 degradation products after aqueous degradation.

# CHAPTER 1

## Reactive dyes and cotton finishing

## 1.1 Reactive dyes

The invention of synthetic dyes by William Henry Perkin in 1856 has deeply reshaped the modern textile industry as the selection of color was no longer limited to natural colors.[3] Since then, considerable resources have been invested in the development of new synthetic dyes with better color fastness and more availability of colors. One representative of this kind of innovation is the invention of reactive dyes in the 1950s by Imperial Chemical Industries. In this section, the classification, composition, and the dyeing behavior of reactive dye will be discussed.

### 1.1.1 Structural composition of reactive dye

The structure of reactive dye could be represented by a descriptive model: S-D-B-RG, where S represents the solubilizing group like the sulfonate group, D represents the chromogen, B represents the bridging group, and RG represents the reactive group. All of these structural components have their unique contributions to the performance of the reactive dye. An example is provided in Figure 1, which shows the structural composition of C.I. Reactive Yellow 174. As a core of a synthetic dye, the chromogen provides a major contribution to the dye's hue as it usually contains a conjugation system that could selectively absorb a proportion of light from the visible electromagnetic spectrum. Then the introduction of the reactive group enables the dye to form a covalent bond with the hydroxyl group of the cellulose polymer chain, Additionally, the bridging group serves as the connection between the reactive group and chromogen and the solubilizing groups provide the dye with additional hydrophilicity so that the dye could perform better in an aqueous dyebath.[4,5]

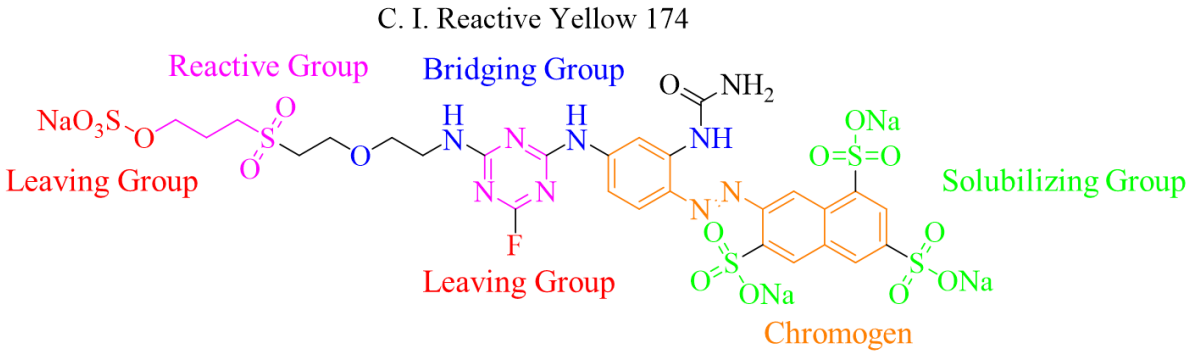


Figure 1: Structural composition of C.I. Reactive Yellow 174

### 1.1.2 Classification of reactive dyes

The family of reactive dyes could be classified or categorized in different ways such as by chromogen and by reactive groups. Depending on the chromogen used to construct its structure, the family of reactive dye could be classified into four categories: azo, anthraquinone, phthalocyanine, and formazan type. The difference in the selection of chromogen would result in the difference in the color of the dye. For example, for red, yellow, or orange colors, chromogens with one or two azo units will be preferred. For relatively darker colors such as blue, purple, and black, chromogens with metal complex based on phthalocyanine or anthraquinone derivatives will be preferred. [1, 2, 4]

The categorization of reactive dyes based on reactive groups include the triazine groups with one or multiple halogen atoms such as monochlorotriazine (MCT) and monofluorotriazine (MFT), vinyl sulfone reactive groups, and phosphorus-based reactive groups. Different reactive groups will have different reaction mechanisms and different stability against hydrolysis. For example, the reaction between the halogen-containing triazine reactive group and cellulose group is essentially an aromatic nucleophilic substitution reaction, where an ether bond is formed between the triazine ring and the hydroxy group of cellulose. The reaction between the vinyl sulfone reactive group and the hydroxyl group of cellulose is essentially a nucleophilic addition reaction.

Figure 2 shows the structures of four commercially available reactive dyes (C.I. Reactive Orange 35, C. I. Reactive Black 5, and C. I. Reactive Blue 19) with different types (monochlorotriazine or vinyl sulfone) and numbers of reactive groups (single or multiple).

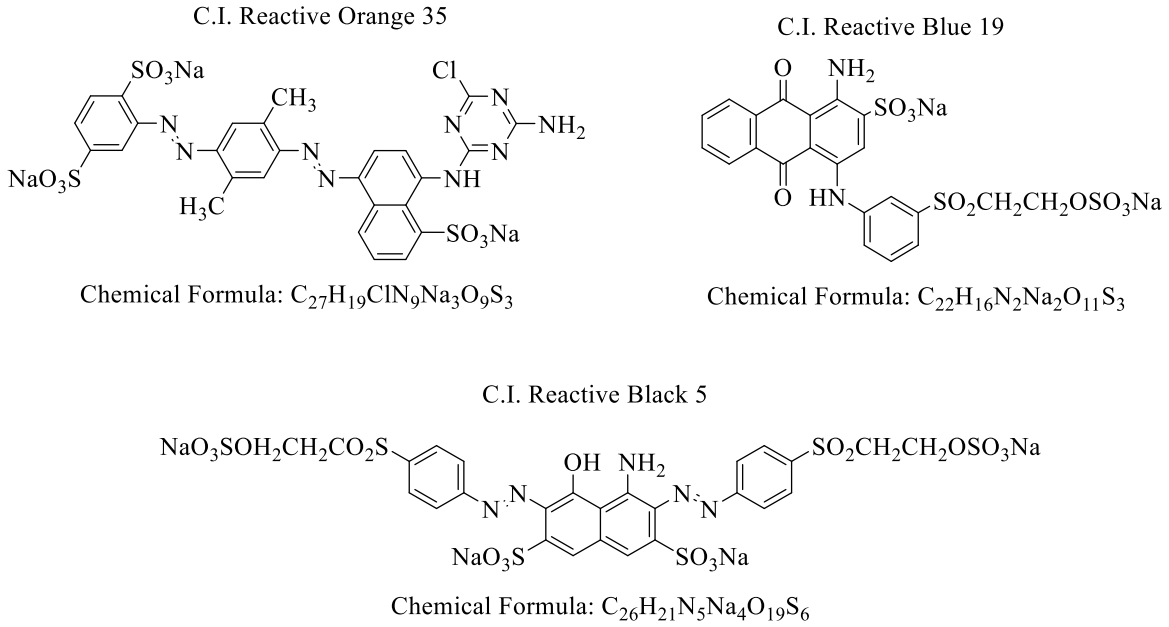


Figure 2: Chemical structures of C.I. Reactive Orange 35, C. I. Reactive Black 5 and C. I. Reactive Blue 19

### 1.1.3 Dyeing affinity of commonly used synthetic dye

To better illustrate the innovation of reactive dyes compared with other kinds of synthetic dyes, their interaction with different kinds of fibers will be discussed.

#### 1.1.3.1 Direct dyes

Direct dyes, or substantive dyes, are a kind of synthetic dyes that uses dipole-dipole interaction and hydrogen bonding to color cellulosic fiber without the aid of mordant agents. The family of direct dyes has grown rapidly since the discovery of Congo Red, or C.I. Direct Red 28, by Bottiger in 1884. The substantivity of direct dyes has a strong correlation with its chemical structure. Figure 3 showed the chemical structure of C.I. Direct Red 28 (DR28) in 2D shapes. Generally, the substantivity of direct dye is contributed by three structural factors: the linearity of

structure, coplanarity of structural components, and the ability to form hydrogen bonds with cellulose. All these features could be found and illustrated in Figure 3.[2, 3, 4, 5]

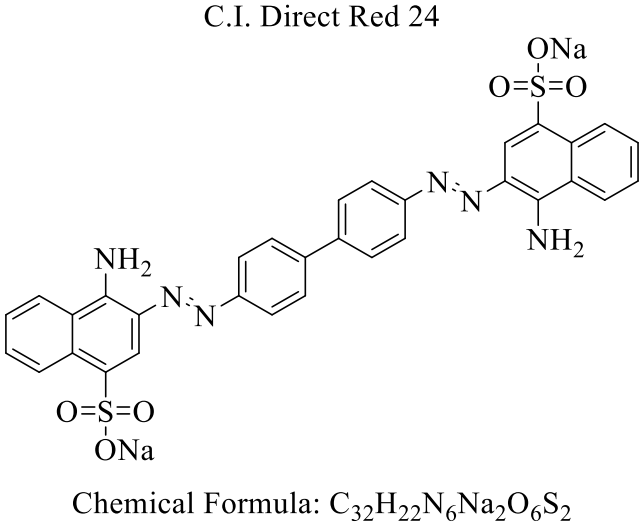


Figure 3: Chemical structure of C.I. Direct Yellow 28[3,4]

The structure of DR28 showed good linearity as the two trans-azo bonds result in linear molecular conformation. Then, the conjugation system made up of the biphenyl and azo provides the molecule with good coplanarity. These two geometric features could facilitate the dyeing process as the dye molecule could stick flatly onto the cellulose chain and aligns along the axial direction, maximizing the substantivity between the dye and cellulose molecule. The chemical structure of DR28 also contains two hydroxyl groups, which are capable of forming intermolecular hydrogen bonds with the hydroxyl group on the cellulose chain. This process is illustrated in Figure 4.

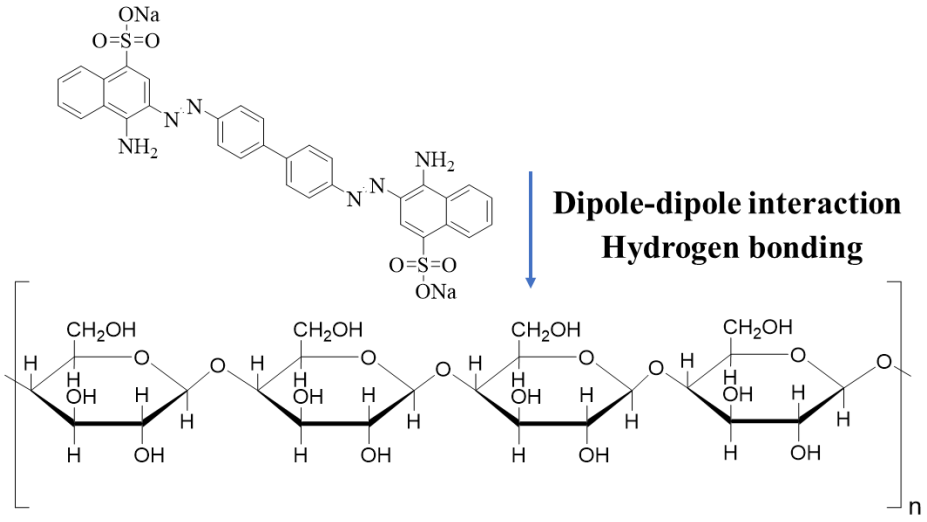


Figure 4: Diagram showing the affinity mechanism of direct dye towards cellulose

### 1.1.3.2 Vat dye

Vat dyes, which sometimes are also called reduced dyes because of their dyeing process, are another type of commonly used synthetic dye on cellulose fabrics. First used as a replacement for naturally derived indigo, synthetic vat dyes have made considerable growth in both quality and quantity since the discovery of indigo structure by Adolf von Baeyer and his team in 1883. The structure of C. I. Vat Blue 4Bis shown in Figure 5 and it could be noticed that this molecule would have poor solubility in water as it lacks solubilizing groups such as $-SO_3$ and -COOH. As a result, the original dye molecule could be used to color synthetic fibers like polyethylene terephthalate (PET) in certain circumstances but it only has a limited affinity towards cellulosic fiber like cotton. [4, 5]

C.I. Vat Blue 4B

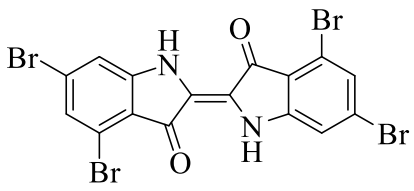


Chemical Formula: $C_{16}H_6Br_4N_2O_2$

Figure 5: Chemical Structure of C. I. Vat Blue 4B

The reason why vat dye could be used on cotton fiber is that it could obtain a higher affinity to cellulose is by changing its structure via a redox reaction. As is shown in Figure 6, under strong alkaline condition (usually using NaOH), the two ketone groups in the structure could be reduced to the salt form of leuco by sodium dithionite ($Na_2S_2O_4$), which provides the dye molecule with additional solubility in water and the ability to be adsorbed onto the cellulose polymer chain via mechanical entrapment. Following the adsorption of leuco salt, the molecule is then oxidized back to its original form where the -ONa group is first converted back to -OH by $CO_2$ and $H_2O$ in the air before being oxidized to ketone by the oxygen in the air. As a result, the dye could stay on the fabrics with good wash fastness. [1, 2, 4, 5]

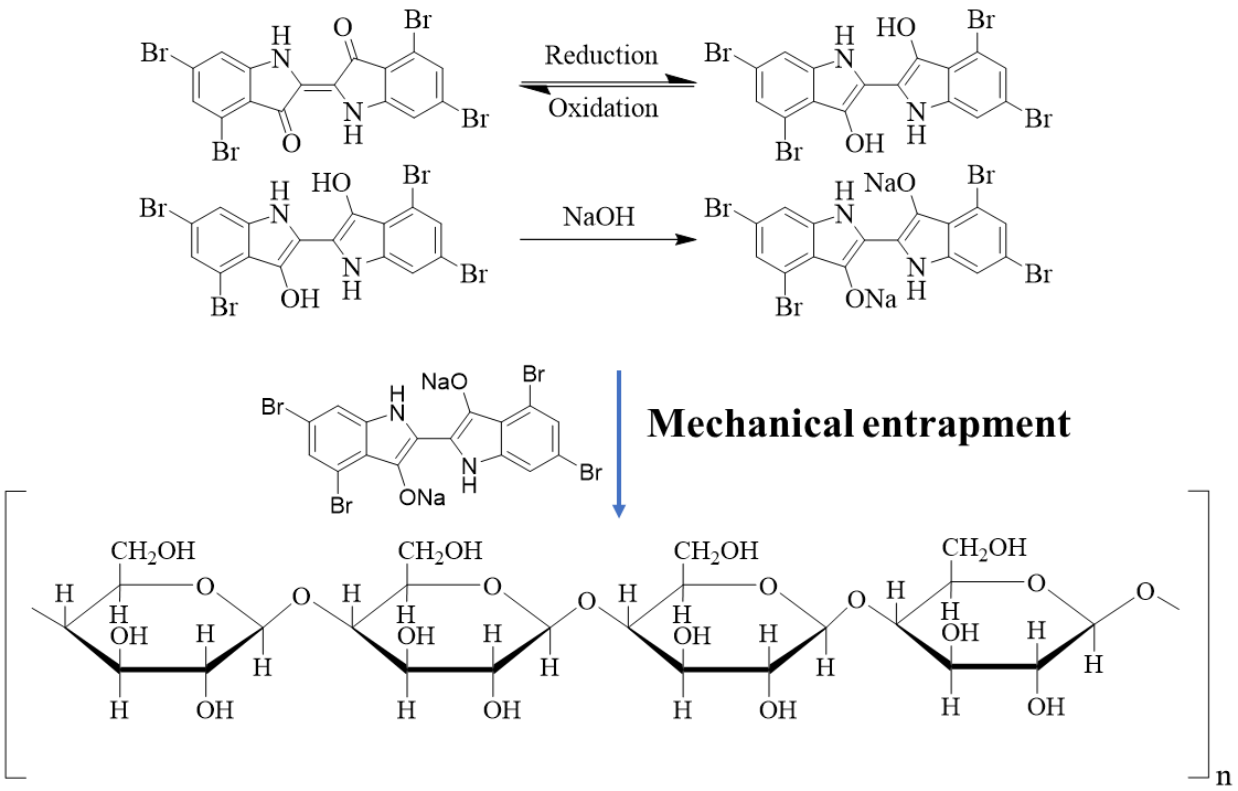


Figure 6: Diagram showing the reduction of C. I. Vat Blue 4B and its adsorption onto cellulose

### 1.1.3.3 Acid dyes

Besides Van der Waals interaction and hydrogen bonding, another type of non-covalent intermodular interaction used commonly by synthetic dyes is ionic interaction. One representative of this kind of interaction is an acid dye, which is commonly used to color natural protein fiber such as wool, silk, and synthetic fibers like nylon. Structures of two typical acid dyes, C.I. Acid Black 1 and C.I. Acid Blue 25, are shown in Figure 7.

C.I. Acid Black 1

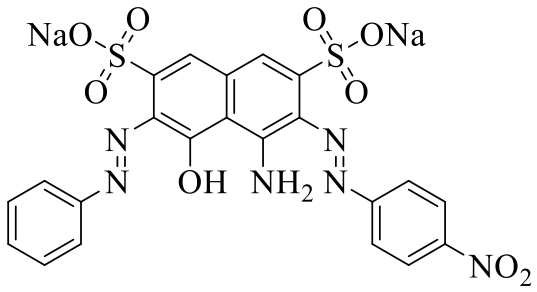

Chemical Formula: $C_{22}H_{15}N_6NaO_9S_2$

C.I. Acid Blue 25

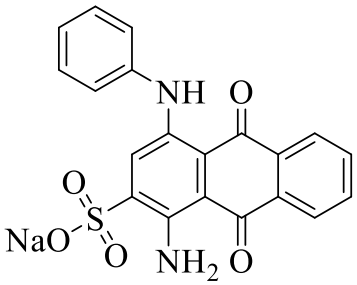

Chemical Formula: $C_{20}H_{13}N_2NaO_5S$

Figure 7: Chemical Structure of C. I. Acid Black 1 and C.I. Acid Blue 25

As is shown in these structures, acid dyes usually contain one or multiple sulfonate groups, which serve as both solubilizing groups and one part of the ionic interaction with fiber. Figure 8 shows the deprotonated sulfonate group ($SO_3^-$) is attracted by the protonated amine group ($NH_2^+$) due to electrostatic forces of attraction between anions and cations. To promote the deprotonation of the sulfonate group, usually, certain degrees of acidity is required in the dye bath and the exact pH condition required usually depends on the number of deprotonation groups in the structure. For acid dyes with multiple sulfonate groups generally need a strongly acidic environment (pH = 2.5 to 4) to deprotonate all of the sulfonate groups whereas acid dyes with one or a smaller number of sulfonate groups could operate under a milder pH condition (pH = 4 to 5). Although more commonly used for protein fiber and polyamide fibers, acid dyes can be used to color cationized cotton where cotton fabrics are treated with 3-chloro-2-hydroxypropyl-trimethyl-ammonium chloride (CHPTAC), and a quaternary amine cation is covalent-bonded to cellulose chain. As a result, anions from acid dye or direct dye could attach to the cellulose chain via ionic interaction.

6-8

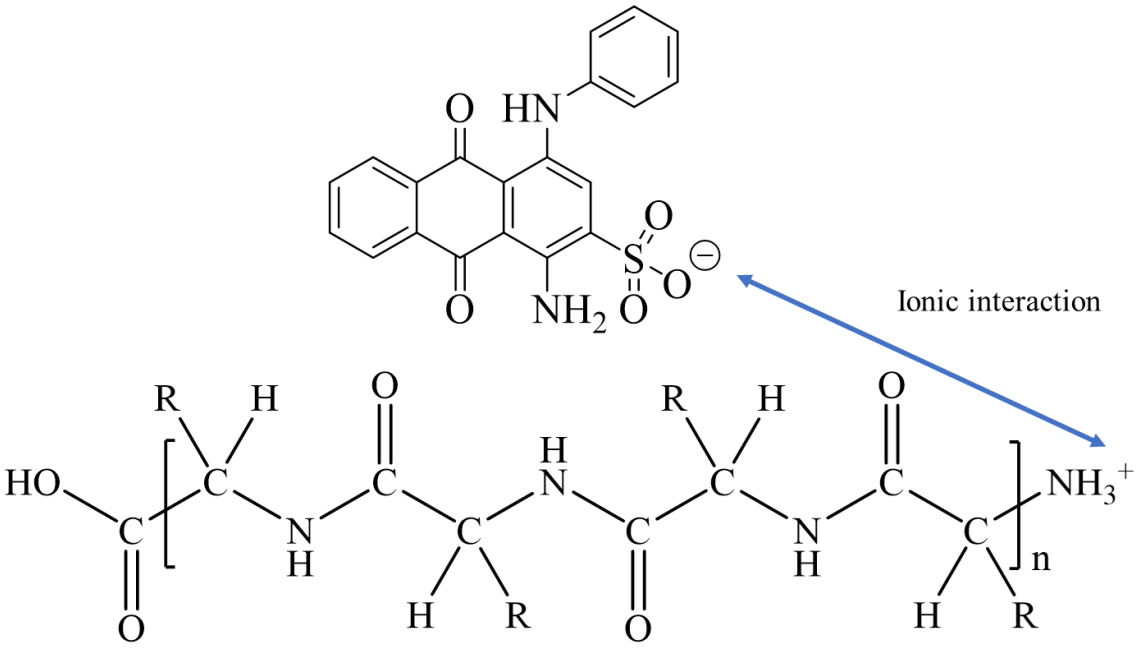


Figure 8: Diagram showing the affinity mechanism between an acid dye and protein fiber

### 1.1.3.4 Disperse dyes

Besides the affinity mechanism mentioned above, disperse dyes represent a different kind of dyeing mechanism, where the dispersed dye particle is adsorbed by the PET fiber and get diffused into the free volume of PET fiber under heat. Originally, disperse dyes were developed to color polyester fiber (PET) and acetate fiber because its structure has three special features that could meet the requirement of the polyester dyeing process. First, a disperse dye has a relatively simple structure and low molecular weight. Polyester fiber usually has a high degree of crystallinity and a high degree of orientation, which results in tight and highly ordered packing of the polymer chains. As a result, to diffuse into the fiber, the dye molecule has to be small and has a low molecular weight, specifically, the structure is usually limited to a single azo chromogen with benzene unit or simple anthraquinone chromogen without heterocyclic substructure. Then, the structure of disperse dye need to high hydrophobicity as polyester lacks hydrophilic groups such as -COOH or -$SO_3$ groups. Besides, the dye needs to be heat-resistant and has high fastness against

sublimation. In the polyester dyeing process, usually, the temperature of the dye bath will be higher than the glass transition temperature (75°C to 85°C depending on the crystallinity) of polyester to mobilize the polymer chain segment. Thus, the structure of the disperse dye needs to be stable enough and its sublimation temperature needs to be higher than the temperature of the dye bath so the dye could maintain its structure during the dyeing process. [1, 2, 4, 9, 10]

The dyeing of polyester fiber with disperse dye includes multiple processes. In this case, one typical disperse dye, C. I. Disperse Orange 1 whose structure is shown in Figure 9, will be used as an example. In a water-based dye bath, the insoluble dye will be dispersed into microparticles with the help of dispersing agents. At this point, a solubility equilibrium will be created between dye molecule in the dye bath and different forms of dispersed dye including microcrystal of dye, aggregate formed by multiple dye molecule, and dye molecules encapsulated in the micelle. Then, as the dye gets adsorbed onto the surface of the fiber (shown as PET fiber in Figure 8) and gets diffused inside the polymer's free volume. In this process, the affinity between polyester and dispersed dye is solely the contribution of hydrophobic interactions. Certain types of disperse dyes could have hydrogen bonding groups such as $-NH_2$ or -NH- group, which are capable of forming hydrogen bonds with the C=O group in the polyester structure. [1, 2, 4, 9, 10]

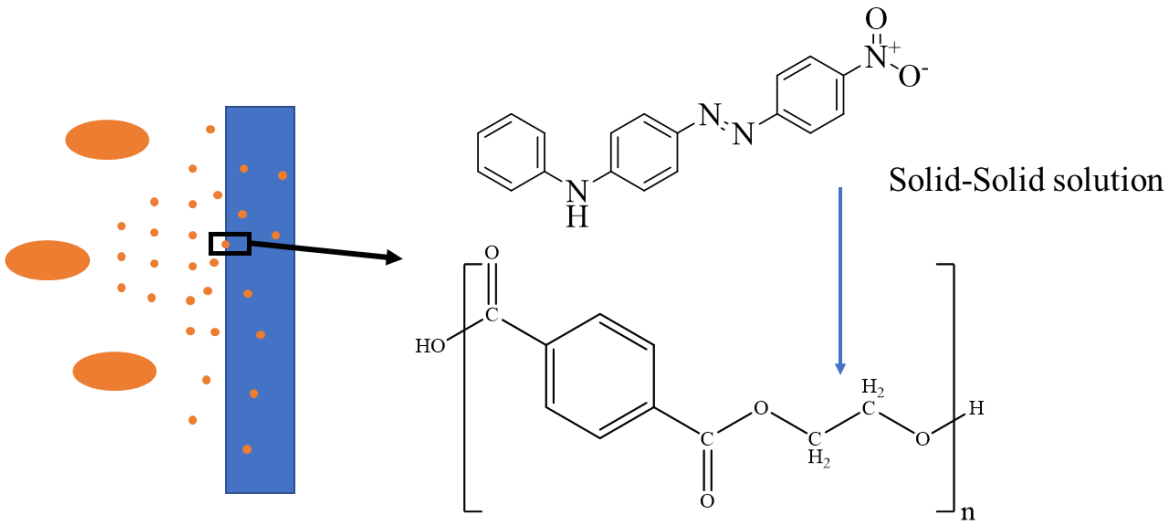


Figure 9: Diagram showing the interaction between a disperse dye and a polyester fiber via solid-solid solution

### 1.1.4 Chemical reactions between reactive dyes and cellulose

#### 1.1.4.1 Formation of the cellulose anion

In a nucleophilic reaction, generally, there will be a nucleophile and a reaction site to which the nucleophile will attack. In the case of reactive dye and cellulose, the reaction, which is often called the fixation of reactive dyes, begins with the deprotonation of the hydroxyl groups of cellulose (see Figure 10). Cellulose usually contains a great number of primary and second -OH groups and these -OH groups could be deprotonated under strongly alkaline conditions. Considering this process, theoretically, according to the Le Chatelier's principle, this reaction could be promoted by raising the pH and increase the concentration of $OH^-$ ion but this would also promote the reaction of the reactive dye with this ion, generating a side reaction product called the hydrolysis product. This is a problem because the reactive dye cannot react further with cellulose. For this reason, the pH is generally maintained below a value of 11. After deprotonation, depending on the type of reactive groups on the dye, the cellulose will participate in two different reactions that include nucleophilic aromatic substitution and nucleophilic Michael addition. [1, 2, 4, 5, 11]

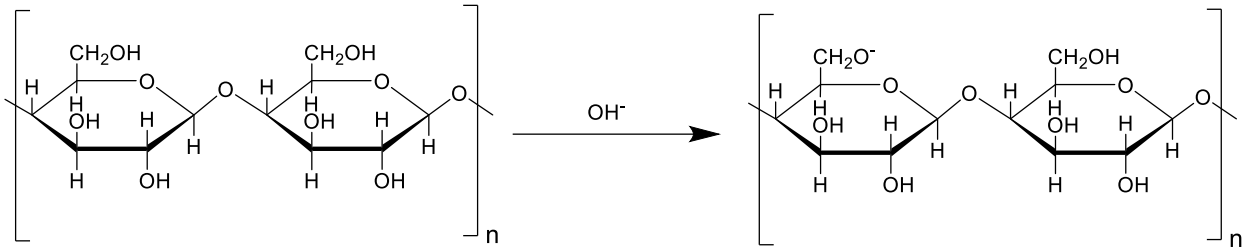


Figure 10: Diagram showing the deprotonation of cellulose under alkaline condition

### 1.1.4.2 Nucleophilic aromatic substitution

A diagram illustrating the reaction mechanism of nucleophilic aromatic substitution reaction is shown in Figure 11. The fixation reaction between cellulose anion and halogen triazine reactive group starts with the delocalization of the electron cloud on the triazine ring. Here the carbon bonded to the halogen atom is partially positively charged and can easily be attacked by a nucleophile. The cellulose anion will attack this positive site and create an ether-type covalent bond between the reactive group and cellulose fiber. In the meantime, halogen atom such as chlorine, a good leaving group, will cleave from the triazine ring to rearomatize the ring. The chloride will form hydrochloric acid, which is neutralized by the alkaline media of the dyebath. As the acid gets consumed by the alkaline solution, the progress of this reaction will also be promoted.

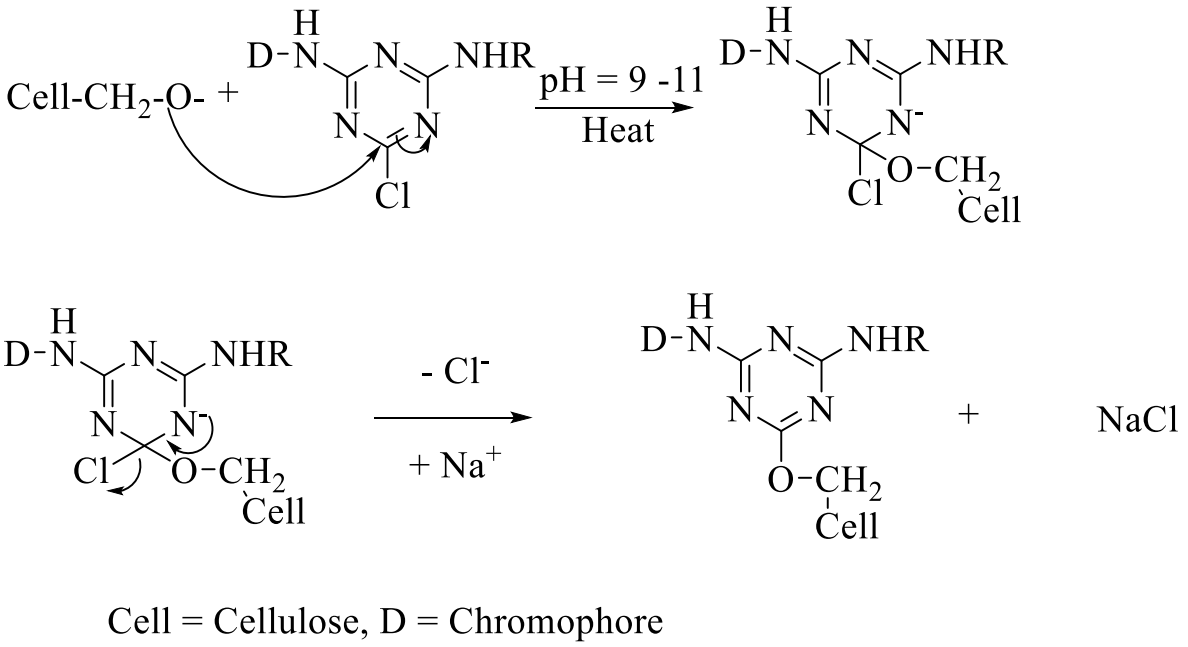


Figure 11: Diagram showing the mechanism of nucleophilic aromatic substitution reaction between monochlorotriazine and cellulose anion

In this reaction, the reactivity of the triazine ring could be altered by the inductive effects of the substituent group and the electronegativity of the halogen leaving group. As is shown in Figure 11, this nucleophilic substitution reaction relies on the partial positive charge on the carbon atom, which is brought by the reduction of electron density on this carbon atom via electron delocalization. So, by introducing additional substituent groups with different inductive effects onto the triazine ring, the reactivity of the triazine ring will be enhanced or reduced. For example, by introducing an additional chlorine atom into the system, which provides an electron-withdrawing inductive effect, the reactivity of the triazine ring could be enhanced as the electron cloud density is further reduced. On the contrary, if functional groups with an electron-donating inductive effect such as $-NH_2$ or $-OCH_3$ were introduced, the reactivity of the triazine reactive group will be suppressed. [11-13]

### 1.1.4.3 Nucleophilic addition

The reaction between cellulose anion and vinyl sulfone reactive dye is essentially a type of nucleophilic addition reaction, where the alkaline condition first aids the elimination of $NaHSO_4$ from sulfatoethylsulfone (SES) group, forming activated vinyl sulfone (VS) form, and cellulose anion then attacks the double bond on vinyl sulfone group, forming an ether type covalent bond. A diagram showing the mechanism of this reaction is provided in Figure 12. In the SES form, because of the influence from the electron-withdrawing inductive effects of $SO_2$, the higher electronegativity of the oxygen atom, and the introduction of extra hydroxide ion by basic conditions, the carbon-carbon single bond is converted into a double bond with the elimination of $NaHSO_4$. Then due to the electron-withdrawing inductive effect of $SO_2$, the electron cloud on β-carbon will be shifted towards the adjacent α-carbon, resulting in a partially positive site that could be attacked by cellulose anion. Then the negative charge on α-carbon is neutralized by protons in water. As a result, an ether type covalent bond is created between the vinyl sulfone reactive group and cellulose. [1, 3, 4, 11, 14]

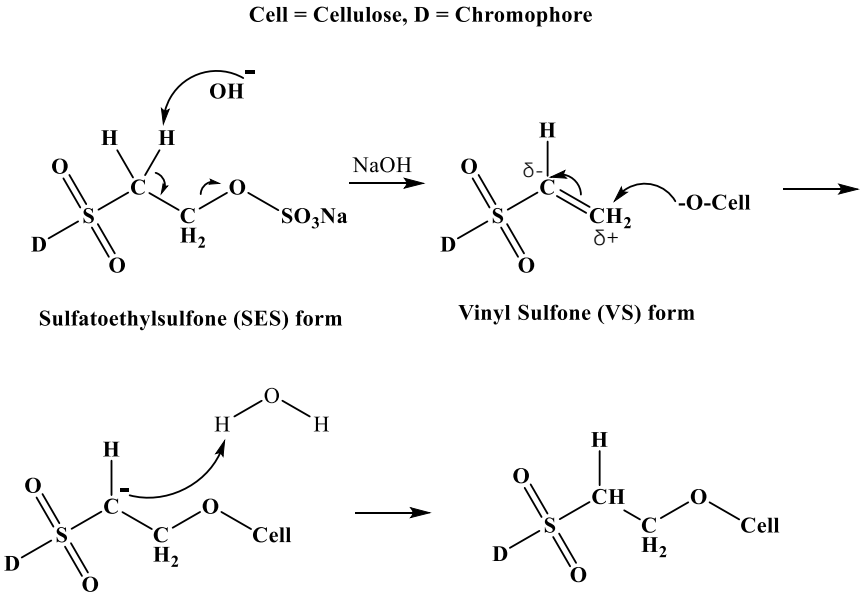


Figure 12: Diagram showing the reaction mechanism between vinyl sulfone reactive group and cellulose anion

### 1.1.4.4 Hydrolysis of reactive dyes

The hydrolysis of reactive dyes is a chemical reaction where the reactive dye reacts with the hydroxide anion and transformed into a hydrolyzed form of the dye. The reactive group is deactivated and could no longer create a covalent bond with cellulose. Depending on the reagent involved in the reaction, the hydrolysis of reactive dye could be divided into two sub-categories: the hydrolysis of unreacted reactive dye and the hydrolysis of bonded reactive dye. Two diagrams showing the mechanism of these reactions are shown in Figure 13 and Figure 14.

The hydrolysis of unreacted reactive dye happens mostly during the fixation process and it could be considered as the side reaction of fixation reaction as essentially the hydroxide anion is competing with the cellulose anion for reactive dye. After the reaction, the hydrolysis form of dye is formed and it could be adsorbed onto the fiber through non-covalent interaction such as Van der Waals force or hydrogen bonding, which would compromise the quality of the product as these unbonded dye could be washed off during laundering. It should be mentioned, however, that hydroxide ion is also participating in the fixation reaction so the hydrolysis of reactive dye during fixation is inevitable but it could be reduced to a point where a majority of reactive dye reacted with the cellulose anion by designing a dye with moderate reactivity through structural modification discussed previously in section 1.1.4.2 and controlling the reaction condition in the dye bath. [1, 3, 9]

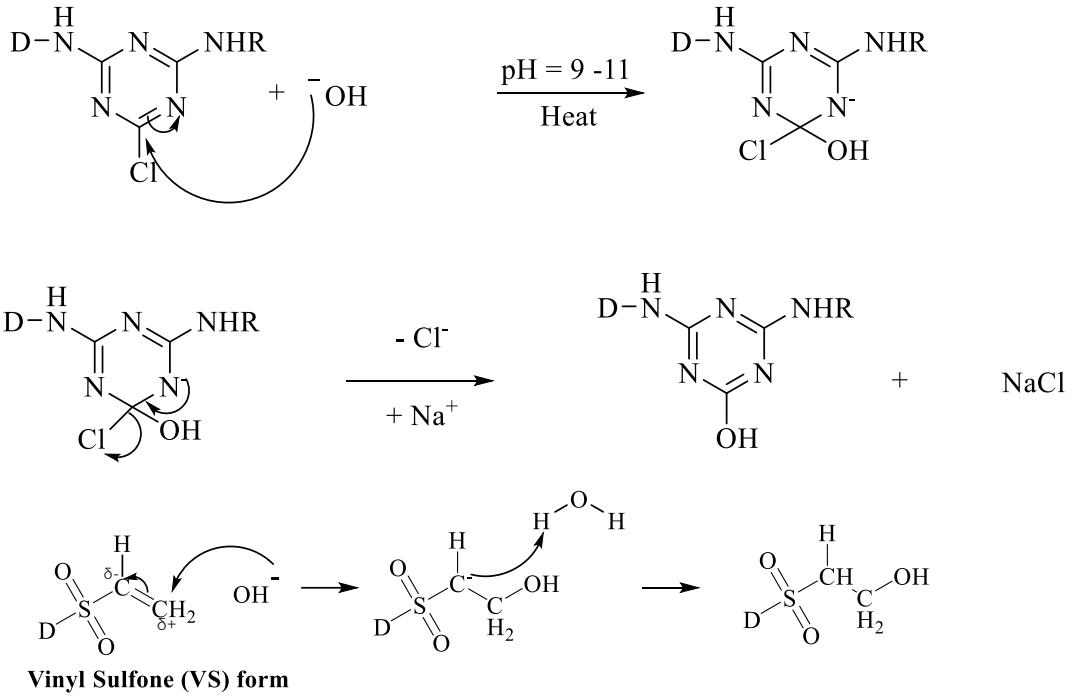


Cell = Cellulose, D = Chromophore

Figure 13: Diagram demonstrating the hydrolysis of monochlorotriazine reactive dye and vinyl sulfone reactive dye

Another case of reactive dye hydrolysis happens on bonded reactive dyes, which essentially depend on the stability of the covalent bond between reactive dye and cellulose. For triazine based reactive dye, studies have shown that the covalent bond between the triazine ring-based reactive group and cellulose is more vulnerable to hydrolysis under acidic conditions than in basic conditions. This vulnerability could bring a practical issue to fabrics with reactive dye as the combination of $CO_2$ and moisture in the air could lead to slow but inevitable hydrolysis of reactive dye. One practical way to address this issue is to use triazine reactive dyes that are less reactive. Because of their relatively low reactivity, they are less vulnerable to hydrolysis but catalyst such tertiary amine is usually used to enhance their reactivity during fixation. On the other hand, for vinyl sulfone based reactive dyes, the covalent bond with cellulose, which is essentially a type of ether bond, is more stable in acidic than in basic condition. [1, 3, 4, 15]

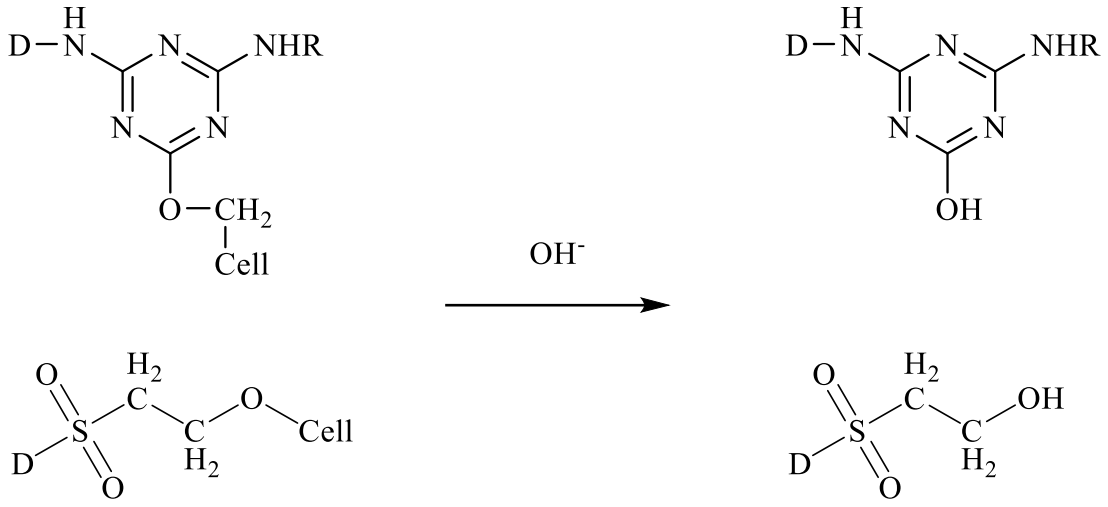


Figure 14: Hydrolysis of bonded reactive dye

To evaluate the performance of reactive dye against hydrolysis, a concept named rate of fixation is proposed, which generally describes the percentage of reactive dye that has bonded with cellulose. Because the fixation process is essentially a reaction, the rate of this reaction would be affected by factors from both the reagents and reaction conditions. In practice, the rate of fixation during the dyeing process could be increased by the alteration of dye structure and the optimization of reaction conditions, which includes reducing the reaction temperature to control the rate of the hydrolysis reaction, adding salts into the system to facilitate the adsorption of reactive dye, and using a smaller dye bath liquor ratios. Currently, according to the report from the manufacturer, certain types of reactive dye could be synthesized to have more than one reactive group (such as Cibacron C reactive dye with a monofluorotriazine and vinyl sulfone reactive group) and have a rate of fixation level as high as 80%.[1, 3, 5]

## 1.2 Cotton Chemical finishing

Cotton fabrics, which essentially is kind of cellulose fiber, have certain intrinsic properties that enable its application as one of the most common natural fiber. Despite these features, additional features were still demanded by the growing textile market such as wrinkle-free and anti-microbial properties. These properties do not belong to the intrinsic properties of cotton and have to be acquired from chemical finishing that is applied to the fabrics after dyeing. In this section, two types of chemical finishing, specifically wrinkle-free finishing (also known as anti-wrinkle finishing or durable press finishing), and antimicrobial finishing, will be discussed.

### 1.2.1 Wrinkle-free finishing

#### 1.2.1.1 Origin of cotton wrinkle

As a kind of semi-crystal fiber, the crystal structure of cotton contains both a crystalline region and an amorphous region. When the fiber is stretched under external stress, these two regions will exhibit different degrees of deformation. In the crystalline region, because of the tight packing of the polymer chain, the relative motion between the cellulose chain is restricted. In the amorphous region, because of a lack of tight packing, the stress would be able to break some of the original hydrogen bonds (1-1', 2-2' and 3-3'), forcing the cellulose chain to slide away from its original position and create new hydrogen bonding at a new location. These newly formed hydrogen bonds (2-1', 3 – 2') could prevent the fiber from recovering from this deformation, resulting in a long-lasting deformation of cotton fiber, which is observed as wrinkle or creeping on the macro scale. A diagram showing the origin of cotton wrinkling is shown in Figure 15. [16, 17]

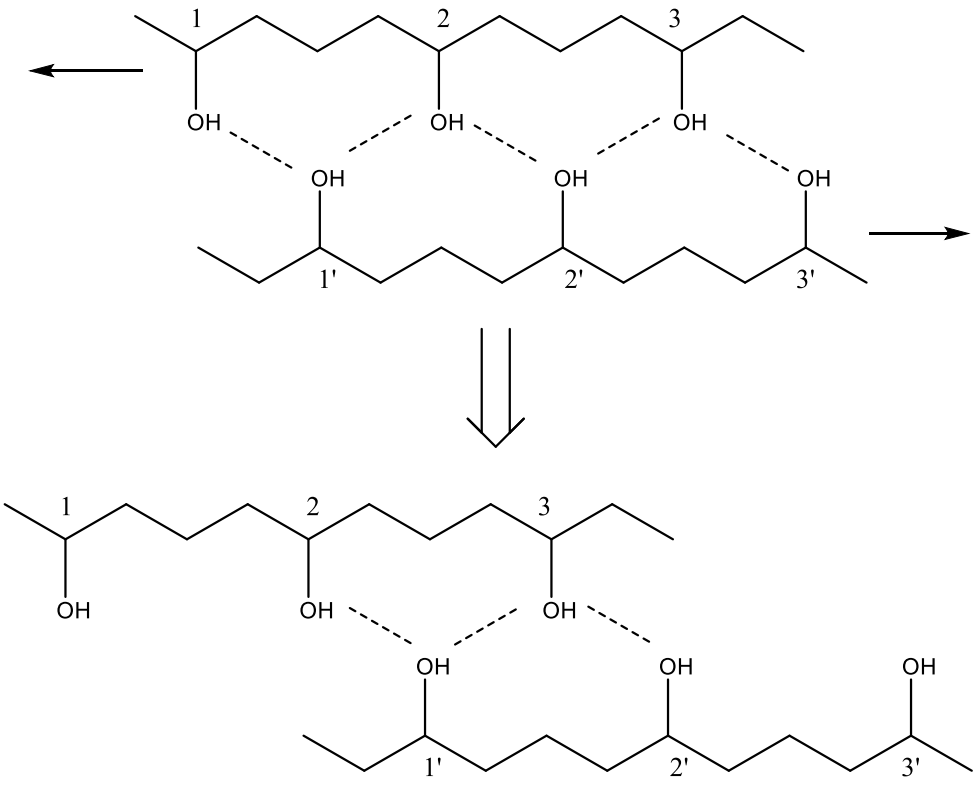


Figure 15: Diagram showing the origin of cotton wrinkling

### 1.2.1.2 Theories to counter cotton wrinkling

Considering the origin of cotton wrinkling, two theories with different mechanisms were proposed to counter cotton wrinkling, which includes resin condensation theory and resin crosslink theory. In resin condensation theory, urea-formaldehyde (U-F) or melamine – formaldehyde (M-F) based crosslinked resin system is being used to form a polymer network that could fill in the vacancy between cellulose chains and restrict the relative sliding between two adjacent cellulose chains. Cotton products produced based on this theory will have good anti-wrinkle performance but poor durability against washing as the crosslinked system is only adsorbed via non-covalent interaction such as Van der Waals force and hydrogen bonding. A diagram illustrating the working mechanism of resin condensation theory is shown in Figure 16. [9, 18-20]

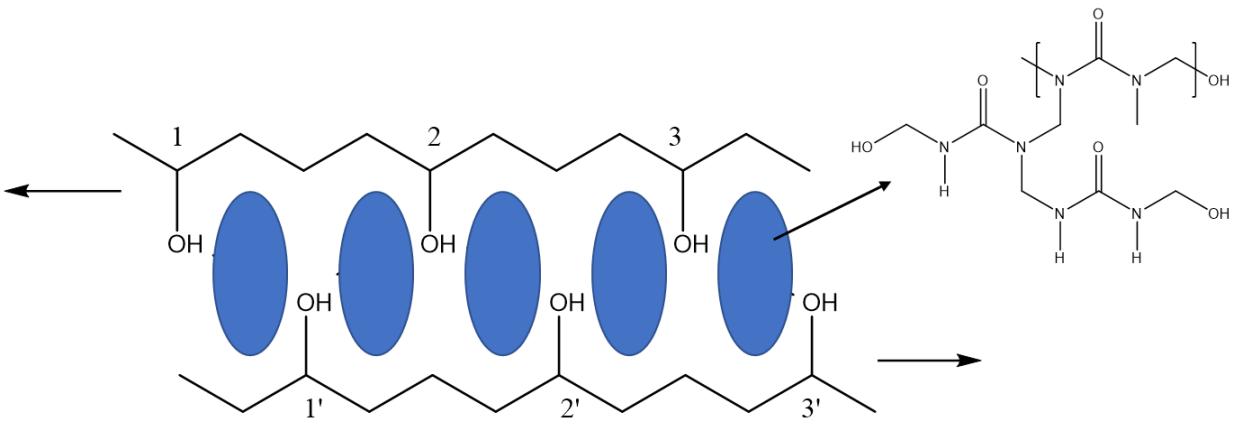


Figure 16: The working mechanism of resin condensation theory

To overcome the drawbacks of resin condensation theory, the theory of resin crosslinking is proposed. According to this theory, dimethylolethylene urea (DMEU) or dimethyloldihydroxyethylene urea (DMDHEU) based crosslinker is introduced into the system and react with hydroxy groups on cellulose via N- methylol (or N- hydroxymethyl) reaction. As a result, two adjacent cellulose chains will be linked together via covalent bonds and the crosslinker will be able to pull the chain back to the original position when the cellulose chain starts to slide away from its original position, preventing the fabrics from wrinkling. This process is illustrated in the diagram shown in Figure 17. Compared with resin condensation theory, the benefit of using this theory is that it provides a durable wrinkle-free effect against washing but brings problems like chlorine retention and formaldehyde release. [9, 18-20]

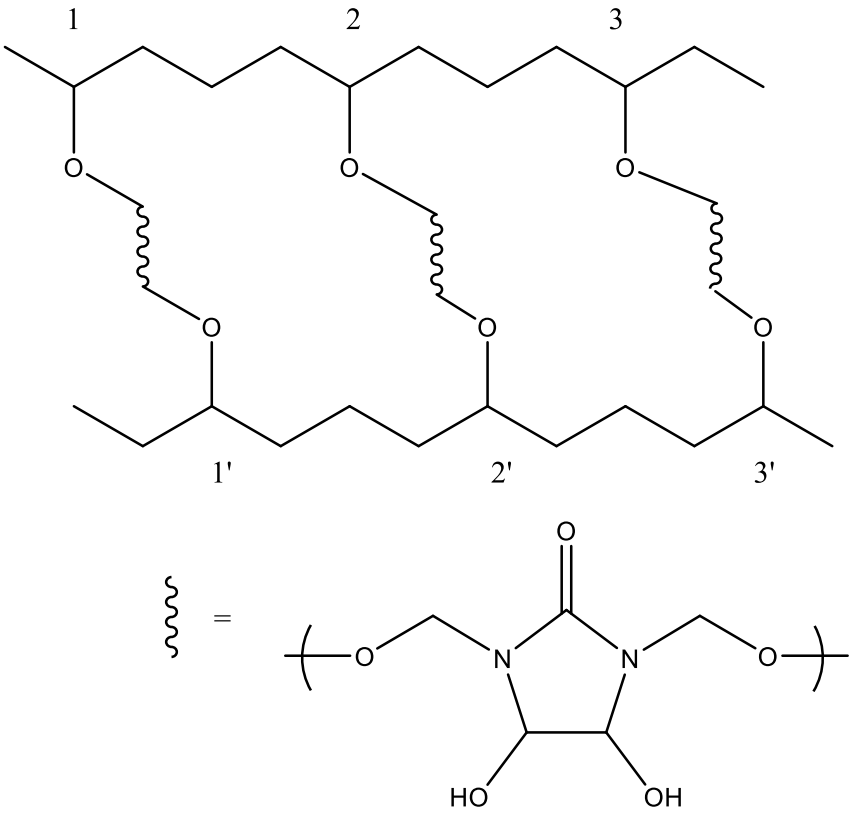


Figure 17: Diagram showing the working mechanism of resin crosslink theory

## 1.2.1.3 Mechanism of N-methylol reaction

### 1.2.1.3.1 Formation of N-methylol compound

Anti-wrinkle agents such as DMEU and DMDHEU are essentially a kind of N-methylol (or N- hydroxymethyl) compound, which is generally synthesized via an acid-catalyzed reaction between amide and formaldehyde. The general structure of the N-methylol compound is shown in Figure 18. In the electrophilic substitution reaction with cellulose, a carbon cation formed by N-methylol compound will be attacked by the hydroxy group of cellulose, and different inductive effect on the substituent groups (-R) would affect the reactivity of carbon cation differently. If R is a functional group with an electron-withdrawing inductive effect like -OH or -COOH, the electron-withdrawing inductive effect will consume the ion pair electron on the nitrogen and

destabilize the carbon cation, which results in a reduced reactivity of the crosslinker. On the other hand, if R represents a functional group with an electron-donating inductive effect such as $-CH_3$ or $-OCH_3$, the reactivity of the N-methylol crosslinker will be enhanced. After the formation of the N-methylol compound, it could then be used to react with cellulose and two theories explained this catalyzed reaction is proposed. One is the proton catalyst theory and the other is Lewis acid catalyst theory.[9, 16-18, 20]

**1.2.1.3.2 N-methylol reaction with proton as a catalyst**

The reaction between the N-methylol compound and cellulose could be divided into stages: the formation of carbon cation and the attachment of cellulose. The mechanism of this reaction is shown in Figure 18. First, protons provided by the acidic conditions will attack the hydroxyl group, forming an $H_2O$ leaving group. After the detachment of water, this carbon cation will then be attacked by the hydroxyl group on cellulose, forming an intermediate state with an extra proton. Finally, the proton will detach, creating a covalent bond between the N-methylol compound and cellulose. It should be noticed that to achieve a crosslinker effect, the crosslinker needs to be bonded with at least two different cellulose chains. As a result, N-methylol crosslinker used in anti-wrinkle treatment is usually designed to have at least two N-methylol groups. [9, 16-18, 20]

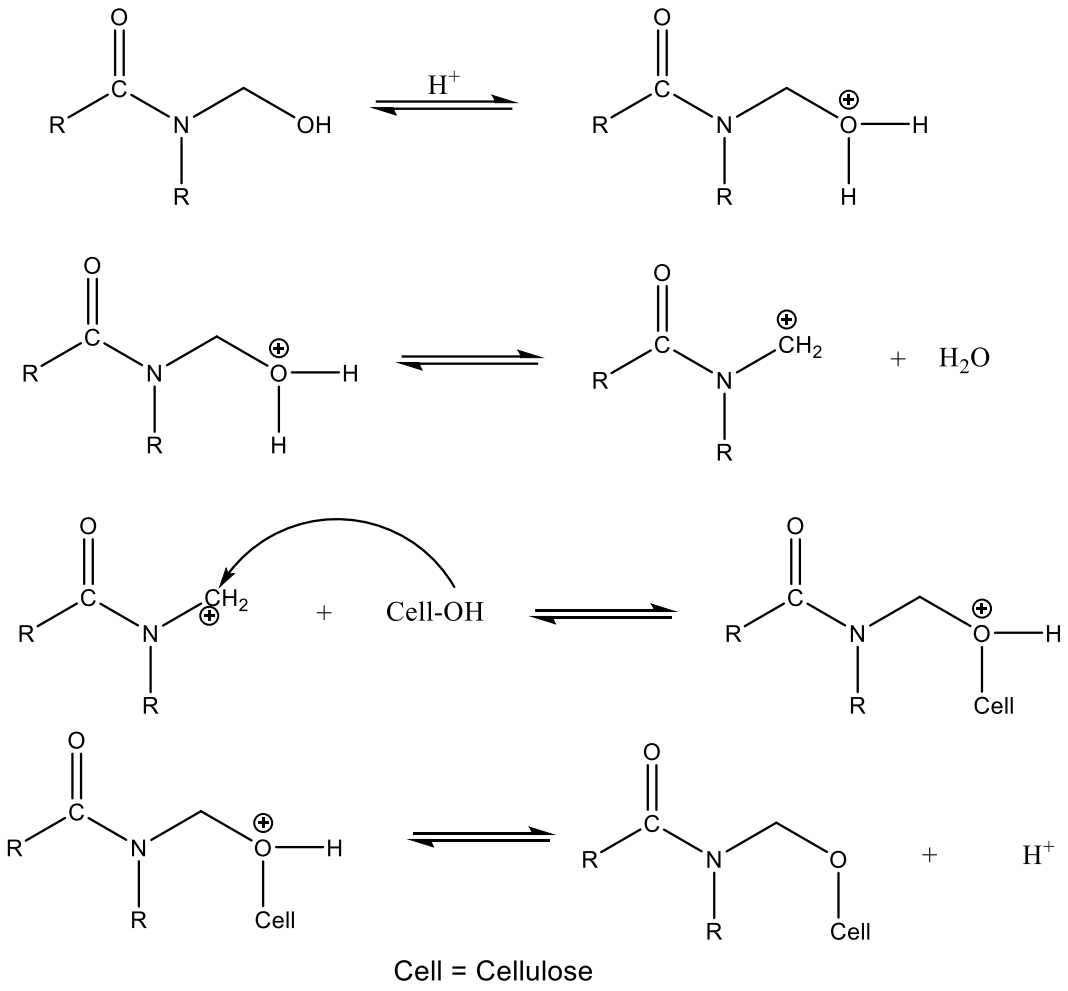


Figure 18: Reaction mechanism of proton catalyzed N-methylol reaction with cellulose

In this mechanism, because the proton catalyst is provided by the acidic condition, the selection of acid type and the concentration of acid is crucial to this process. The selection of acid type is usually determined by the reactivity of the crosslinker, for relatively more reactive crosslinker like DMU or DMEU, a weaker acid could be used but for crosslinker that is less reactive like DMDHEU or DMUG, a stronger acid is needed. Theoretically, a stronger acid such as HCl, $H_2SO_4$, and $HNO_3$, will result in a higher reaction rate as stronger acid will provide lower pH and a higher concentration of protons compared with a weak acid, but the problem of using stronger acids is that they could weaken or even damage the cotton fabric as the glycosidic bond

between glucose units is vulnerable to the hydrolysis under strong acid conditions. As a result, to avoid the damage of fabrics while maintaining a reasonable reaction rate, weak organic acid with buffer and latent acid could be used. [9, 16-18, 20]

**1.2.1.3.3 N-methylol reaction with Lewis acid as catalyst**

Another catalyst that could be used to promote N-methylol reaction is a Lewis acid, which specifically refers to metals ion with vacant orbital to accept electron pair. Traditionally, the criteria for acid and base is based on the Bronsted–Lowry acid-base theory, which distinguishes acid and base by whether a compound could accept or donate a proton. If compounds could accept a proton, it is defined as a base while compounds able to donate proton will be defined as acid. On the other hand, Lewis acid-base theory defines an acid as a compound that could accept an electron pair and a base as a compound that could donate an electron pair. In the case of N-methylol reaction, metal ions such as $Mg^{2+}$ and $Zn^{2+}$ would participate in the formation of carbon cation as Lewis acid. This process is demonstrated in a diagram shown in Figure 19. First, the metal ion will attack the hydroxy group and form an intermediate state where the vacant d-orbital on the metal will overlap with the filled p-orbital on the oxygen atom. Then an $M^{+}OH$ will detach from the intermedia state, creating a primary carbon cation that could then be attacked by the hydroxy group on the cellulose and form a covalent bond between the N-methylol crosslinker and the cellulose chain. After the formation of covalent bonding, the proton released from the N-methylol group will neutralize the $M^{+}OH$, forming an $M^{2+}$ ion that could be used again in the next cycle of reaction. Compared with proton catalyst, the metal catalyst could bring more benefits as it could avoid the damaging of fabrics by strong acid and enable the use of less reactive crosslinker like dimethylol-dihydroxy-ethylene urea (DMDHEU) and dimethylurea glyoxal (DMUG), which is also eco-friendlier as these crosslinkers usually have less formaldehyde release compared with DMU and DMEU. [9, 16-18, 20]

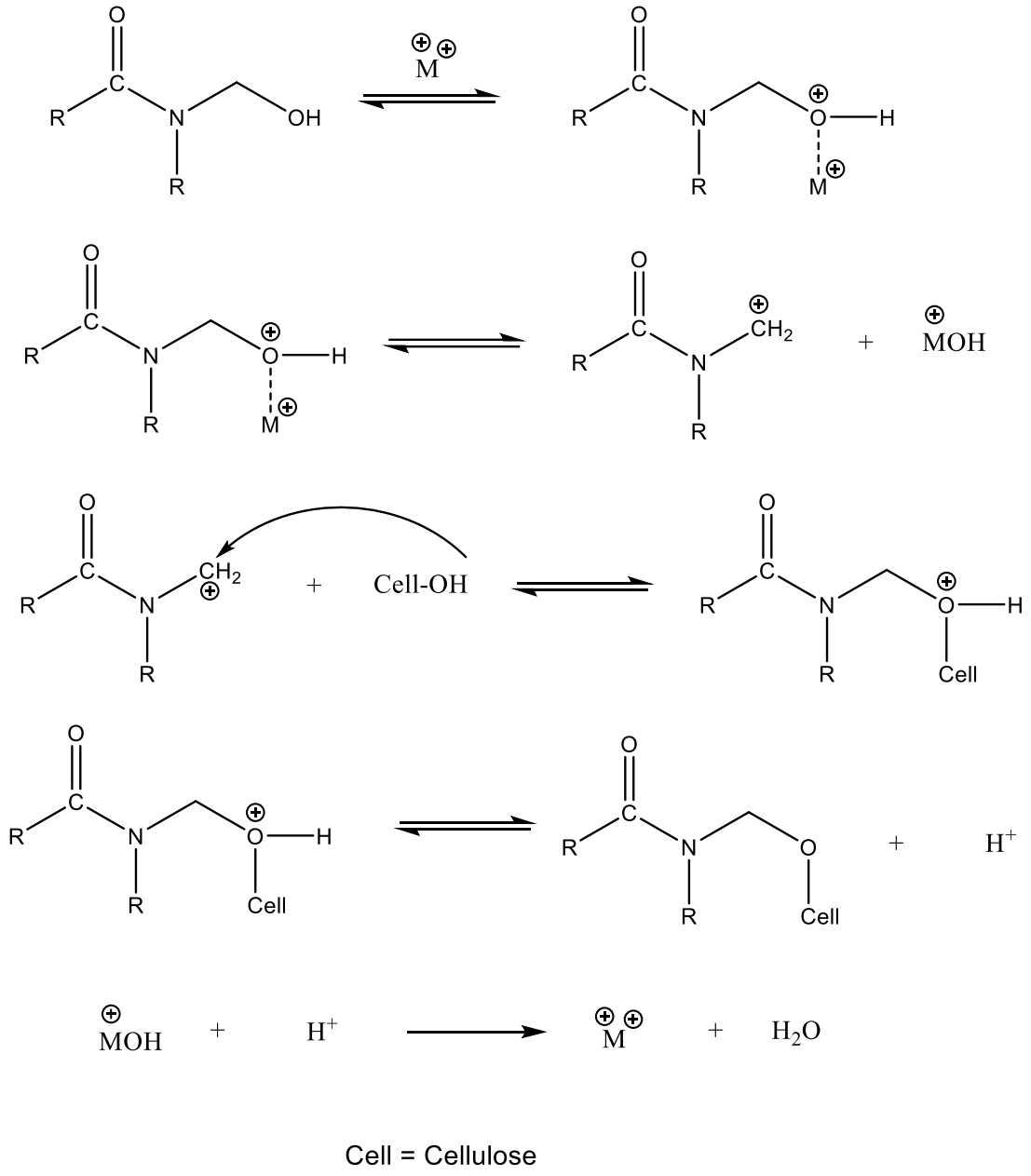


Figure 19: Reaction mechanism of a Lewis acid catalyzed N-methylol reaction with cellulose

## 1.2.1.4 Evolution of anti-wrinkle agents

### 1.2.1.4.1 Dimethylol Urea (DMU)

The selection of cellulose crosslinkers in anti-wrinkle finishing has been evolving since the beginning of the last century and a series of different N-methylol-based crosslinkers have been

developed to reduce or eliminate the drawbacks that were found in their previous generation. Figure 20 showed the structure of DMU, DMEU, DMDHEU, and DMUG.

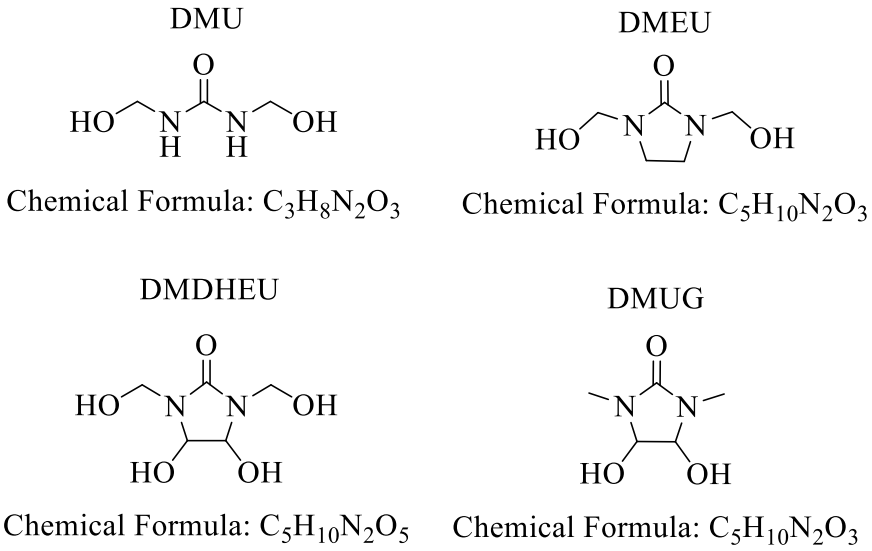


Figure 20: Structure of different cellulose crosslinkers

The development of novel cellulose crosslinkers starts from DMU, which belongs to some of the early attempts to make an anti-wrinkle agent. The structure of DMU contains two methylol groups that could create crosslinks between two different cellulose chains. As a cellulose crosslinker, DMU is easy to cure and has good anti-wrinkle performance and excellent recovery against creasing. Despite its good performance, early developed N-methylol crosslinker is so reactive that it has some major drawbacks such as poor durability against washing, short "pot life" during the application, self-crosslinking between crosslinker, and the loss of fabrics strength caused by chlorine retention. [9, 16-18, 20]

#### 1.2.1.4.2 N, N'-Dimethylol Ethylene Urea (DMEU)

To overcome or eliminate the drawbacks of DMU, a series of N-methylol based crosslinkers were developed in the 1950s. The first variant is N, N'-Dimethylol Ethylene Urea (DMEU), which is synthesized by reacting ethylene urea with formaldehyde and widely used as a wrinkle-free

agent before the 1960s. Compared with DMU, DMEU also delivers a good wrinkle-free performance with longer pad life and softer hand feeling, which is majorly contributed by the reduction of reactivity. Another improvement of DMEU over DMU is the elimination of self-crosslink, which is accomplished by replacing urea with ethylene urea and reducing the number of reactive sites from four to two. By eliminating the loss from self- crosslink, DMEU would have higher efficiency compared with DMU but it still suffered from the loss of strength brought by chlorine retention and poor durability against washing. [9, 16-18]

#### 1.2.1.4.3 N, N'- Dimethylol-Dihydroxy-Ethylene Urea (DMDHEU)

DMEU is an effective crosslinker but it suffers from the hydrolysis of the crosslinked bond. To overcome this issue, further modification of structure is introduced where the ethylene urea is replaced by dihydroxy-ethylene urea to react with formaldehyde, resulting in a less reactive but more stable crosslinker. As is shown in Figure 20, the structure of DMDHEU contains two reactive sites that could perform N-methylol reaction with cellulose. Compared with DMEU, because two additional -OH provides an electron-withdrawing inductive effect that destabilizes the carbocation, DMDHEU is less reactive, which brings a series of improvements to the anti-wrinkling process including longer pad bath life, less chlorine retention, and better laundry durability. Because of these improvements in both performance and stability, DMDHEU has become the most popular choice for wrinkle-free finishing and the concept of wrinkle-free has become one of the common requirements for formal or business casual clothing. [9, 16-18, 20]

#### 1.2.1.4.4 Wrinkle-free finishing with low or no formaldehyde release

Starting from DMU to DMEU and then to DMDHEU, the performance of wrinkle-free agents has been noticeably improved in terms of both stability and durability. It is found out later, however, that crosslinks made by these N-methylol based compounds could release formaldehyde,

a naturally available compound that has been found to be carcinogenic under accumulated or concentrated conditions, via hydrolysis of crosslinkers and crosslinked bond. As is shown in Figure 21, formaldehyde released from fabrics with wrinkle-free finishing could come from three major sources: absorption of formaldehyde from the atmosphere, releasing of formaldehyde from unreacted or partially reacted crosslinker, and the hydrolysis of crosslinks. Among these sources, it is believed that formaldehyde release from unreacted or partially reacted crosslinker contributes the most. To effectively control the release of formaldehyde, the stability of the crosslinker should be enhanced. However, even on improved crosslinkers such as DMDHEU, the release of formaldehyde is around 1000 ppm (parts-per-million). Thus, in order to further reduce the level of formaldehyde release, modified DMDHEU, and other formaldehyde-free crosslinkers, were developed. [18]

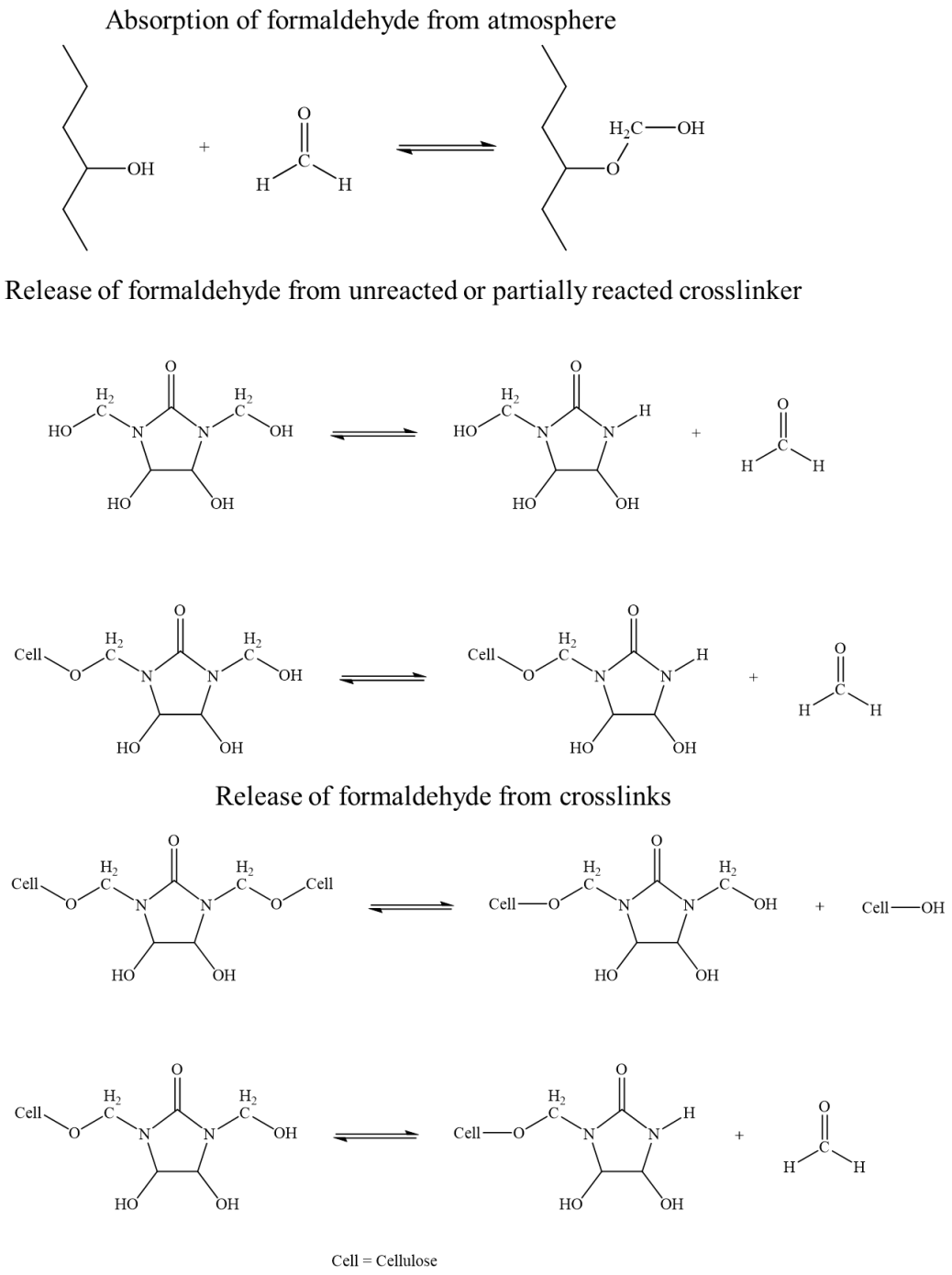


Figure 21: Source of formaldehyde on fabrics with wrinkle-free finishing

To reduce the formaldehyde release of DMDHEU, an alkyl group such as $CH_3$ could be introduced to replace the “free hydrogen” on N-methylol groups. By fully methylating all of the four alcohol groups on DMDHEU, the formaldehyde release could be reduced to a level of around

300 ppm. Another route to modify the structure of DMDHEU is to introduce diethylene glycol ($HOCH_2CH_2OCH_2CH_2OH$) into the structure of DMDHEU. Some of the commercial wrinkle-free products like PermaFresh 600 are manufactured based on this reaction, where the product liquid will contain a mixture of mono or di-substituted DMDHEU, unreacted DMDHEU, and unreacted diethylene glycol. By introducing diethylene glycol into the structure of DMDHEU, the release of formaldehyde could be reduced to a level around 50 ppm, but the release of formaldehyde is still inevitable as the hydrolysis site ($N\text{-}CH_2\text{-}O\text{-}R$) is still present. Thus, to eliminate the release of formaldehyde, the hydrolysis site has to be removed from the crosslinker. As a result, a new kind of cotton crosslinker, dimethyl urea glyoxal (DMUG) is developed, which could be synthesized by reacting dimethyl urea with glyoxal. The most apparent benefit of DMUG is the elimination of formaldehyde release as there is no available hydrolysis site ($N\text{-}CH_2\text{-}O\text{-}R$) present in the structure but this benefit comes at a cost that includes higher pricing than DMDHEU and reduced anti-wrinkle performance. [9, 18, 20, 21]

### 1.2.2 Anti-microbial finishing

Like other carbohydrate compounds such as glucose and cellobiose, cellulosic fiber is an ideal environment for the growth of microorganisms including bacteria and fungi as it serves as an excellent source of nutrients. With an ambient external condition such as proper degree of moisture, suitable temperature, and the supply of oxygen in the air, the reproduction of these microorganisms will be promoted, and the colony of microorganisms will expand. As a result, the affected textile product will have deteriorated structural properties including reduced tensile strength, damaged appearance, and unpleasant odor brought by the respiration effect of the microorganism. Thus, to limit the growth of microorganisms, anti-microbial finishing with different working mechanism could be applied to cotton fabrics.[18, 21]

### 1.2.2.1 Classification of anti-microbial finishing

Depending on their working mechanism, anti-microbial finishing could be divided into two categories: biocide and biostatic. Among them, biocide is defined as toxic materials that could kill the microorganism via internal biochemical reactions, and these substances were usually derived from antibiotics. Conventionally, these poison-based anti-microbial agents replied on pharmaceutical effects to interfere with microbe's internal processes and they are very effective during the initial treatment but the accumulation of mutation response from microbes against these compounds could eventually lead to resistant strains, where the anti-microbial agent is no longer effective against this kind of microbe. One better approach regarding the selection of anti-microbial agents on textiles is to select biostatic agents that could control the growth of the microbe colony by disrupting their cell walls, which is less likely to cause mutation accumulation and resistant strains. Another consideration during the selection of biocide anti-microbial finishing is the restriction from the government administration. According to the regulation from Environment Protection Agency (EPA), any anti-microbial product advertising public health claims should register with EPA and prove the quality of this product in terms of efficacy and environmental risks. On the other hand, if an anti-microbial product is advertising non-public health claims such as resisting odor or inhibiting microorganisms, it prevents the registration requirements at EPA. Thus, in practice, many manufacturers will choose biostatic anti-microbial finishing to avoid administration costs. [9, 18, 21]

Besides their working mechanism, another way to categorize the anti-microbial finishing is by their attachment mode. This describes how the finishing is attached to the fiber. The first type of releasing mode of anti-microbial finishing is the leaching mode in which the antimicrobial agents were adsorbed onto the surface of the fabrics and as the fabrics get exposed during usage,

the anti-microbial agents will be released from the fabrics. Because of this releasing mode, the performance of anti-microbial finishing will be maximized during the initial time of usage but as the fabrics being worn or washed, the performance of this kind of finishing will reduce and some active ingredients will be released into the environment as the available agents on fabrics get worn off. One example of this type of finishing is sliver docusate, which is the active ingredient in Polygiene AT300 finishing. The structure of sliver docusate is shown in Figure 22. [9, 18]

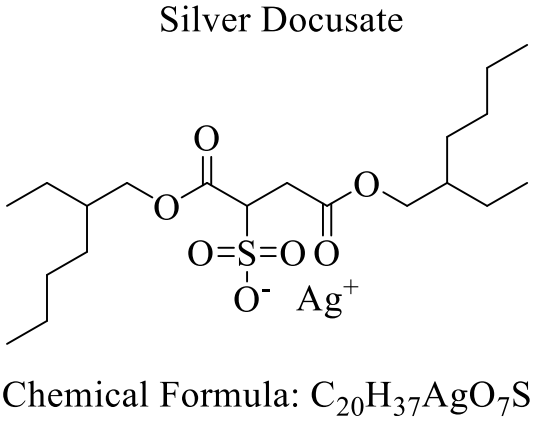


Figure 22: Structure of Silver docusate

In addition to the leaching mode, another activity mode of anti-microbial finishing is the bound mode in which the anti-microbial agent is attached to the fiber via intermolecular interaction like Van der Waals force and hydrogen bonding. The chemical structure of this type of finishing usually contains a polymerizable site and the bioactive site. As is shown in Figure 23, the polymerizable site is usually made by silicone monomer that could polymerize on the fabric surface and the anti-microbial site would have bio-active groups such as quaternary amine in order to create a biocidal or biostatic effect. Compared with leaching mode, bound mode anti-microbial finishing is generally less likely to cause environment issue as the affinity between fiber and finishing agent is stronger than the affinity in leaching mode but anti-microbial finishing relying

on this mode could suffer from a reduction of performance brought by the deactivation of the active site during usages. [9, 18]

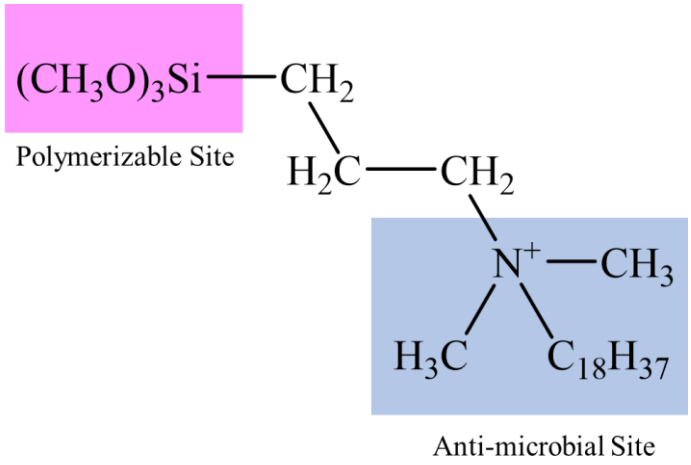


Figure 23: Example of bound mode anti-microbial finishing

# CHAPTER 2

## Mass spectrometry (MS)

From the first discovery of the electron by Joseph John Thomson in 1897 to the announcement of the first commercialized orbitrap mass spectrometer by Thermo Scientific in 2005,[22, 23] mass spectrometry (MS) has been progressing dramatically in capabilities and applications.

Nowadays, mass spectrometry or any specific analysis conducted on a mass spectrometer has become a major contributor to the analytical chemistry field. Thus, in this chapter of the literature review, some concepts associated with MS will be discussed. Then the hardware and working mechanisms of modern mass spectrometer systems will be introduced.

## 2.1 Basic concepts in mass spectrometry

### 2.1.1 Exact mass

MS works by ionizing, separating, and detected charged particles, called ions, from a molecule. Each ion can be associated with and specific mass but there are more multiple ways to define the mass of an ion. The simplest way to represent the mass of a certain molecule is by its nominal mass. The nominal mass of a molecule is defined as an integer linear combination of each elements' most abundant stable isotopic mass.[24, 25] Nominal mass is generally intuitive and easy to understand but in order to accurately describe the isotropic distribution of different molecules, the system of exact mass is proposed which is calculated based on the linear combination of the lightest stable isotope in the molecule.[26] In addition, the exact mass could provide more information regarding the isotropic distribution of molecules when coupled with a mass spectrometer that has high resolving power. For example, carbon monoxide (CO) and nitrogen gas ($N_2$) have different elemental composition but the same nominal mass of 28, if we account that the mass of carbon, oxygen, and nitrogen is 12, 16, and 14 Daltons (Da), respectively. It will be

difficult to differentiate these two molecules with nominal mass. In the case of exact mass, however, their exact masses are different (27.9949 Da vs. 28.0061 Da) because their isotopic composition is different, which enabled the discrimination and detection of different molecules by exact mass. By calculating and measuring the exact mass of different molecules, the concept of exact mass establishes a connection between molecular formula and instrumental observation.

### 2.1.2 Mass accuracy and ppm error

Like any other analytical instrument, the exact mass measured by mass spectrometer always has a certain degree of error, which essentially represents the deviation between measured mass and theoretical mass, and this error would usually be express as mass accuracy. Most of the current high-resolution mass spectrometers such as the Quadrupole Time-Of-Flight (QTOF), the Fourier-Transform Ion Cyclotron Resonance (FT-ICR), and the Orbitrap could provide a measurement of exact mass with up to four or even five decimal places. In order to clearly describe the mass accuracy of high-resolution instruments, mass accuracy in parts-per-million (**ppm error**) is used. The equation to calculate ppm error is shown in Equation (1).[26] By calculating the relative error between measured exact mass and theoretical exact mass, the accuracy of the formula generation, and the performance of the instrument, could be evaluated. Usually, a single TOF instrument will have a ppm error within 10 ppm, QTOF will have a ppm error within 5 ppm, and ultra-high-resolution instruments such as FT-ICR and Orbitrap could have an even lower ppm error usually within 1 ppm or less.

$$ppm\ error = \frac{Mass_{exp} - Mass_{theo}}{Mass_{theo}} \times 10^6 \quad (1)$$

### 2.1.3 Mass resolution and mass resolving power

Like other analytical instruments such as FT-IR and Raman, mass spectrometers also use the concept of resolution to describe the instruments' ability to separate adjacent peaks. Higher resolution would result in the illustration of more peaks and provide more detailed information on the spectrum. In mass spectrometry, mass resolution is defined as the mass-to-charge ratio (m/z) difference, Δm, that exists between two adjacent peaks in a specific mass spectrum that has an equal abundance and Gaussian shape with a specified amount of overlap (10% valley or Full-Width Half Maximum (FWHM)).[27-29] It should be noticed, however, that mass resolution is specific to a certain spectrum in which two peaks need to be compared with each other. In the case of evaluating the performance of the instrument, mass resolving power should be used. As is shown in Figure 24 and Equation (2), mass resolving power describes the ratio between the corresponding m/z value of the peak and m/z width of the peak. Compared with mass resolution, the concept of mass resolving power is more applicable as it is not specific to a certain spectrum and it makes it possible to compare the performance of different types of mass spectrometers. For instance, on low resolving power instruments such as quadrupole and ion trap, the resolving power is at the level of several hundred while in high-end instruments such as orbitrap and FT-ICR, the resolving power could be at the level of one million. Although it is obvious that mass spectrometers with higher resolving power could provide more spectral information, these instruments usually cost more than other low resolving power instruments.

$$Mass\ resolving\ power = \frac{m}{\Delta m} \qquad (2)$$

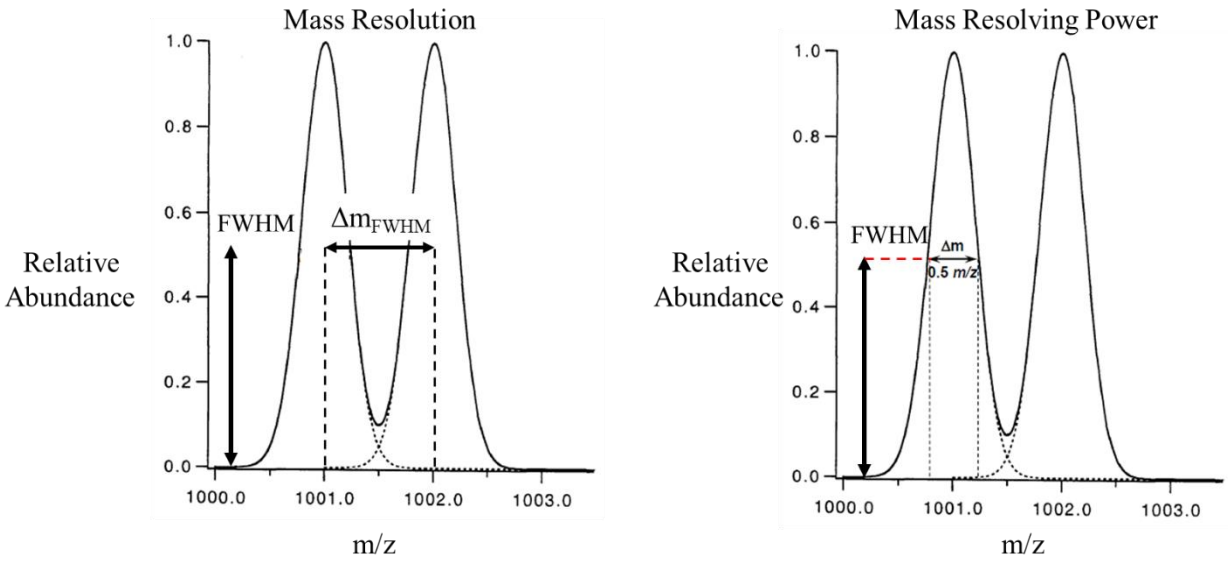


Figure 24: Comparison between mass resolution and mass resolving power[28]

## 2.2 Configuration of modern mass spectrometers

Although a mass spectrometer usually is considered as a single piece of instrument, it is actually made up of a series of different essential components, which perform different duties in the measurement of exact mass. As is shown in Figure 25, a modern mass spectrometer system usually consists of five functional components: sample inlet, ionization source, high-performance mass analyzer, detection system, and data system. [27, 28] In this section, the operation mechanisms of some of the major techniques used in this study will be discussed, including High-Performance Liquid chromatography (HPLC), Electrospray Ionization (ESI), quadrupole mass analyzer, and Time-Of-Flight mass analyzer (TOF).

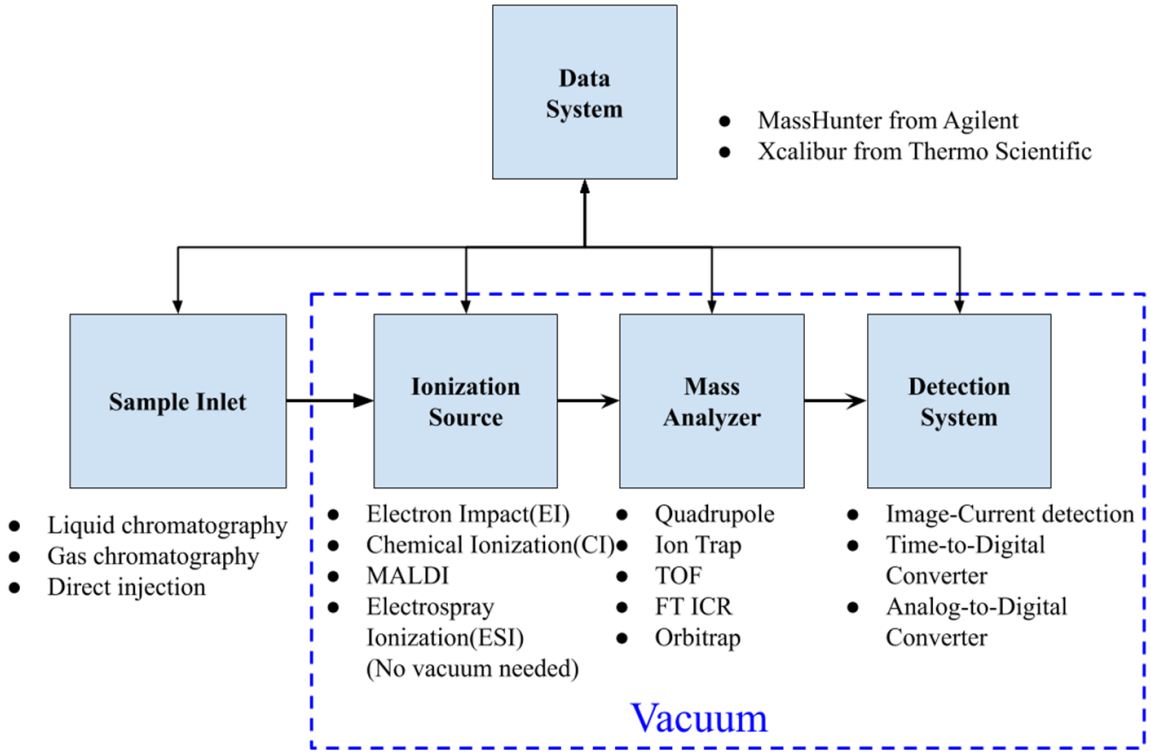


Figure 25: Components of a typical modern mass spectrometer

### 2.2.1 High-Performance Liquid chromatography (HPLC)

There are multiple ways to introduce liquid samples into a mass spectrometer including direct injection, gas chromatography, and liquid chromatography. Direct injection is often used when the sample composition is not complex and gas chromatography requires the sample to have certain degrees of volitivity. In most cases, liquid samples usually have to be introduced via High-Performance Liquid chromatography (HPLC). Like any other chromatography techniques, HPLC works by separating the liquid sample into multiple components depending on their affinity (e.g. polarity, ionic interaction,) towards the solid stationary phase. Most of the current HPLC systems are based on the theory of reverse phase chromatography where the stationary phase is non-polar, and the mobile phase is polar. As is shown in Figure 26, as the mobile phase carries the sample into the column, initially component A, B, and mobile phase (M) have the same speed V but as the sample moves through the stationary phase (S), component A and B are slowed down to a

different speed ($V_a < V$, $V_b < V$). Because component B has a higher affinity towards the mobile phase, it would travel faster than component A ($V_b > V_a$). As a result, the mobile phase will reach the detector first, and then component B following by component A. This dragging effect provided by the stationary phase enables the separation of a complex matrix and the purification of the sample. [30, 31]

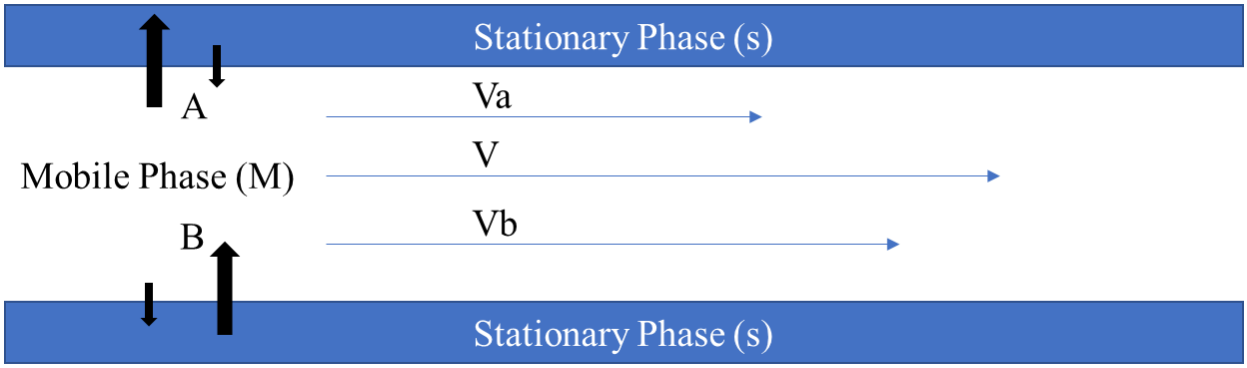


Figure 26 Separation mechanism of liquid chromatography

A number of different parameters could impact the quality of separation including the composition of the stationary phase and mobile phase, the column temperature, the flow rate, the injection volume, and the total run time. In order to precisely control these parameters, currently, HPLC systems are usually made up of a series of well-designed modules. A diagram illustrating the composition of a modern HPLC system is shown in Figure 27. Before entering the flow loop, each solvent first passes through a vacuum-based degasser to remove any air bubbles that may be in the line. Then one or multiple types of solvent will be mixed to form the mobile phase at a solvent pump, where either quaternary or binary pump could be used depending on different designs from different vendors. By changing the solvent ratio during the sample run, a gradient elution could be established, which may result in better separation than isocratic elution. After mixing, the mobile phase enters the autosampler where a liquid sample is injected into the flow system and mixed with the mobile phase. Depending on the purpose of analysis, the injection

volume at the autosampler could be adjusted. After injection, the mobile phase carrying the sample will enter the column compartment where the HPLC column is installed and maintained at an established temperature. After being separated in the column, each component in the sample reaches the detector, where different types of instrumental responses like UV-Vis absorption, refractive index, and mass-to-charge ratio are generated. Finally, for most detectors other than MS, the mobile phase, and sample excess, will be collected by a waste bottle. To systematically monitor and control these modules, most HPLC vendors will provide a software platform where different HPLC parameters for different types of analysis could be controlled independently. [28, 30-33]

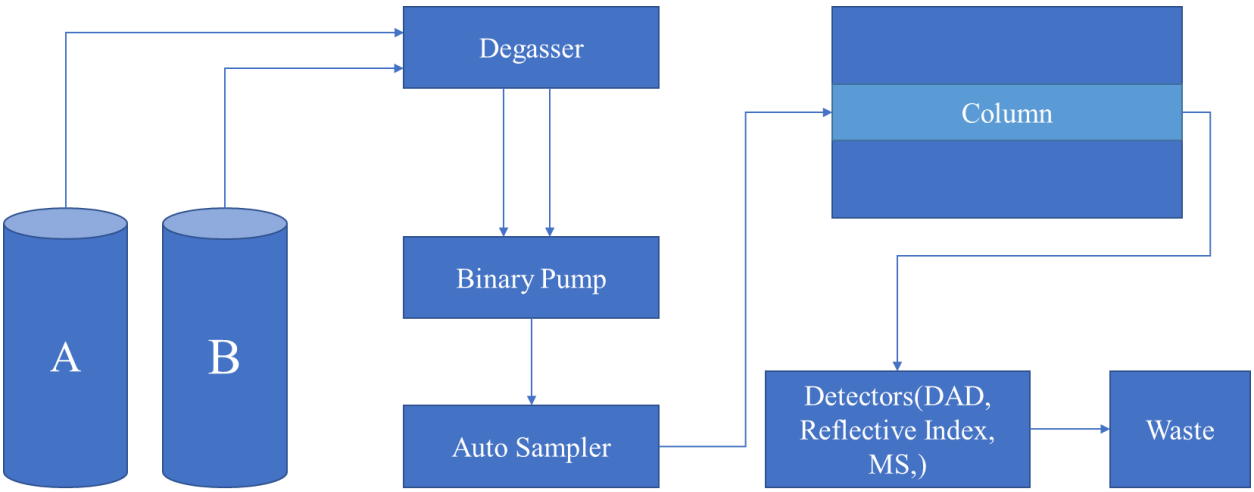


Figure 27: Composition of modern HPLC system

## 2.2.2 Electrospray Ionization (ESI)

Following the introduction of the sample is the ionization source where the sample is ionized and gained a certain amount of charge. Ionization is an essential step in mass spectrometry analysis because mass analyzer relies on electric and magnetic fields to manipulate the ions. Depending on different properties of different analytes, different types of ionization sources could be selected including Electron Impact Ionization (EI), Atmosphere Pressure Chemical Ionization (APCI), Matrix-Assisted Laser Desorption Ionization (MALDI), and Electrospray Ionization (ESI).

Compared with other ionization techniques like APCI or MALDI, ESI is known for its more softness, in which the analytes experience minimum fragmentation and the chemical structure of analyte could be almost perfectly maintained after ionization. Another benefit of ESI is the ability to form multiple-charged ions, which not only increases the dynamic range of the mass analyzer but also reduce mass measurement error by a factor of 1/z, where z represents the number of charges.[28] This ability of ESI to ionize polar compound combining with its ability to form multiple charged ions, promotes its application in the analysis of synthetic dyes, especially acid and reactive dye because these dyes have multiple sulfonate solubilizing groups that could be deprotonated and detected as multiple charged negative ion. This increases the range of detection of dyes with high molecular weight. In this section, the operational mechanism of ESI, and the different models explaining the formation of ions during ESI, will be introduced.

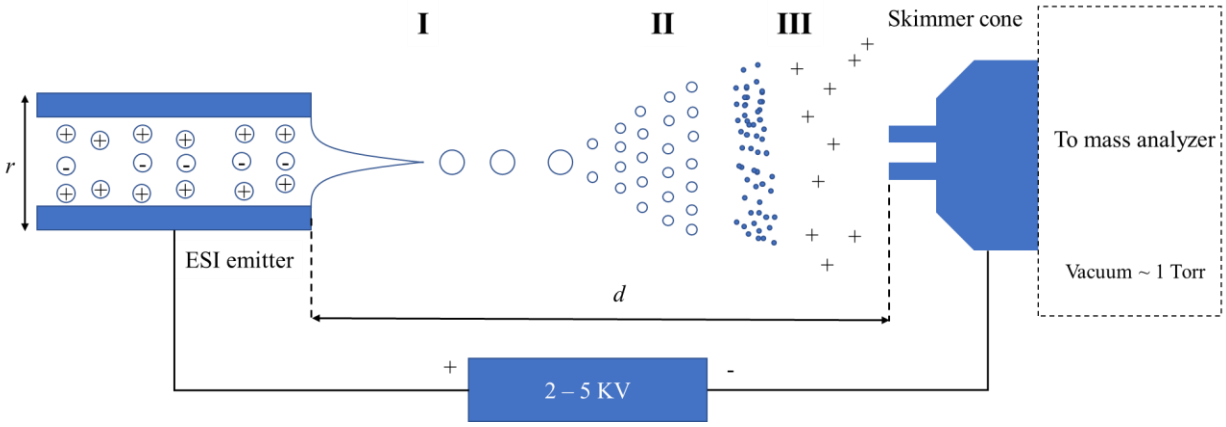


Figure 28: Conceptual diagram of Electrospray Ionization (ESI)

A diagram showing the setup of ESI is shown in Figure 28. A metal needle and skimmer cone are placed inside a closed chamber and connected with a power supply which creates an electrical field between them. [34] As the solvent travels out from the emitter, charged droplets are generated from electrically distorted meniscus and those charged droplets are then dragged towards the skimmer cone connected with the mass spectrometer by the electric field between the needle and

skimmer cone and vacuum. During this process, due to the evaporation of the solvent, the size of charged droplets gradually reduced to a point when the coulombic force on the surface exceeds the surface tension of the droplet, and large parent droplets dissociated into small droplets. This process continues until charged ions are formed from offspring droplets in the gas phase.[28, 34] This process of forming charged ions could be better illustrated by dividing the event into three-time phases.

At phase **I**, under an applied external voltage, the accumulation of electric charge at the ESI emitter creates a drag force, which starts to deform the solvent flow. When this drag force exceeds the surface tension of the solvent, a Tylor Cone is formed and charged droplets are emitted from this solvent cone. This process could be mathematically described by Equation (3). $V_{on}$ represents the onset voltage required to initiate the emission of charged droplets, $r$ represents the diameter of the ESI emitter, $d$ represents the distance between the emitter and the skimmer cone and $\gamma$ represents the surface tension of the spray solvent. To generate a Taylor cone and produce charged droplets, the electric dragging force offered by the power supply has to be able to overcome the surface tension of the solvent. If the voltage V is much smaller than $V_{on}$, the drops from the solvent are spherical. As the voltage starts to match with $V_{on}$, the drops get elongated due to pressure from the accumulation of charges on the tip. At $V_{on}$ electric dragging force starts exceeding the surface tension of solvent flow and a Taylor cone is formed. Usually for more aqueous spray solvent like water requires more voltage than organic solvents like methanol. For example, the surface tension of methanol is 22.55 mN/m and the surface tension of water is 72.8 mN/m. So the ratio between their offset voltage is equal to the square root of their surface tension ratio, which is around 1:2. This suggested that it requires only half of the voltage to spray methanol compared with spraying water.

$$V_{On} = 2 \times 10^5 \times \sqrt{\gamma \times r} \times \ln \frac{4d}{r} \quad (3)$$

At phase **II**, these charged droplets got dragged towards further towards the skimmer cone. At this time because of the evaporation of solvent and collisions with gas molecules, these parent droplets started to shrink. As the surface area of the droplets decreases, the charges on the surface become closer to each other, resulting in a columbic fission which caused the disintegration of the parent droplet into offspring droplets. To quantitively describe this process, the equation for the Rayleigh limit is used and this equation is shown in Equation (4). According to this equation, for a charged droplet to be stable, the columbic force from the charges on the surface has to be equal to the surface tension of the droplet. But as the surface area of the droplets reduces, the balance could only be maintained by the disintegration of the parent droplet into offspring droplets as smaller offspring droplets will have a greater overall surface area than the bigger parent droplets.

$$q_r = \sqrt{64\pi^2 \varepsilon_0 \gamma r} \quad (4)$$

At phase **III**, due to the further evaporation of the solvent, offspring droplets are significantly reduced in their radius and charged ions are formed in the gas phase. Here two different models have been proposed explaining the origin of charged ion from offspring droplets. Figure 29 shows a diagram illustrating these two models. The **Charge Residue Model (CRM)** by Dole, proposed that offspring droplets generated in phase II will then undergo further solvent evaporation and experience further columbic fissions. This process continues until there is on average one analyte molecule per droplet with some charge. The remaining solvent then evaporates leaving the charge deposited on the molecule.[34-36] Another model is the **Ion Evaporation Model (IEM)** by Iribarne and Thomson, which claims that after the production of offspring droplets form parent droplets, these offspring droplets, rather than continuing to undergo further columbic fission, will be

affected by the external electric field on the surface. As a result, gas-phase ions are ejected from the droplet and different physicochemical properties of different analyte could result in different rates of emission and ion abundance.[34, 36, 37] Debates are still active on these two models and both two models have their strengths and weaknesses. Charge Residue Model works better on bigger molecules like proteins and peptides, especially polymer molecules because each droplet can only hold one single molecule. On the other hand, Ion Evaporation Model provides a good explanation about ion formation selectivity but mostly on small molecules. Recently progresses in Molecular Dynamic (MD) simulations have provided some new insights regarding the generation of gas-phase ions from offspring droplets as calculated "molecular films" in the scales of nanosecond could illustrate how small molecules like $Na^+$ gets ejected from the droplets and how residue charges get deposited onto the remaining larger molecule. [38-40]

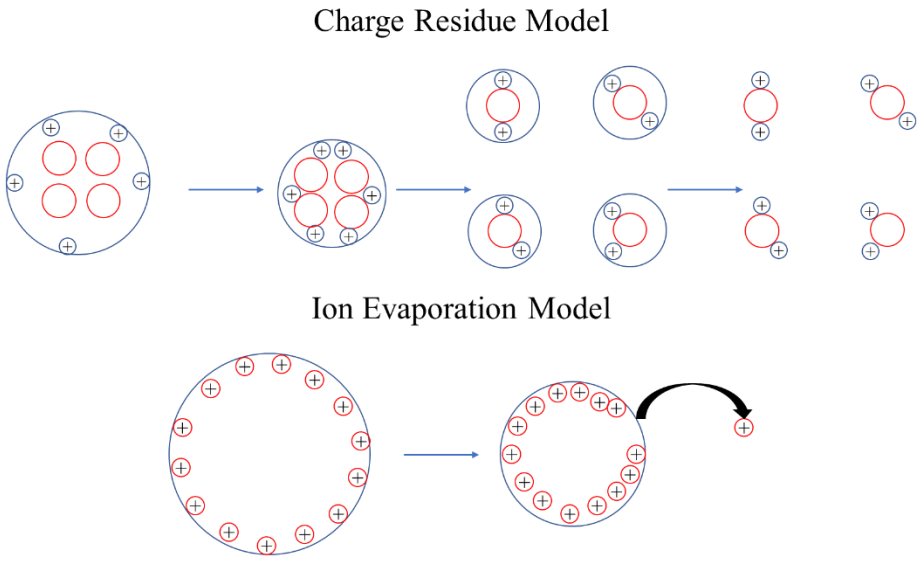


Figure 29: Diagram illustrating Charge Residue Model and Ion Evaporation Model during ESI

### 2.2.3 Quadrupole mass analyzer

After ionization, different ions generated from the ionization source are sent to the mass analyzers through focusing lenses where the ions with different mass-to-charge ratios are separated

according to their responses to different electric or magnetic fields. A great variety of mass analyzers are available for different types of mass spectrometry researches today including quadrupole, ion trap, Time-Of-Flight (TOF), Orbitrap, and FTICR. Among them, one of the most basic mass analyzers is the quadrupole mass analyzer, which could also be referred to as quadrupole.

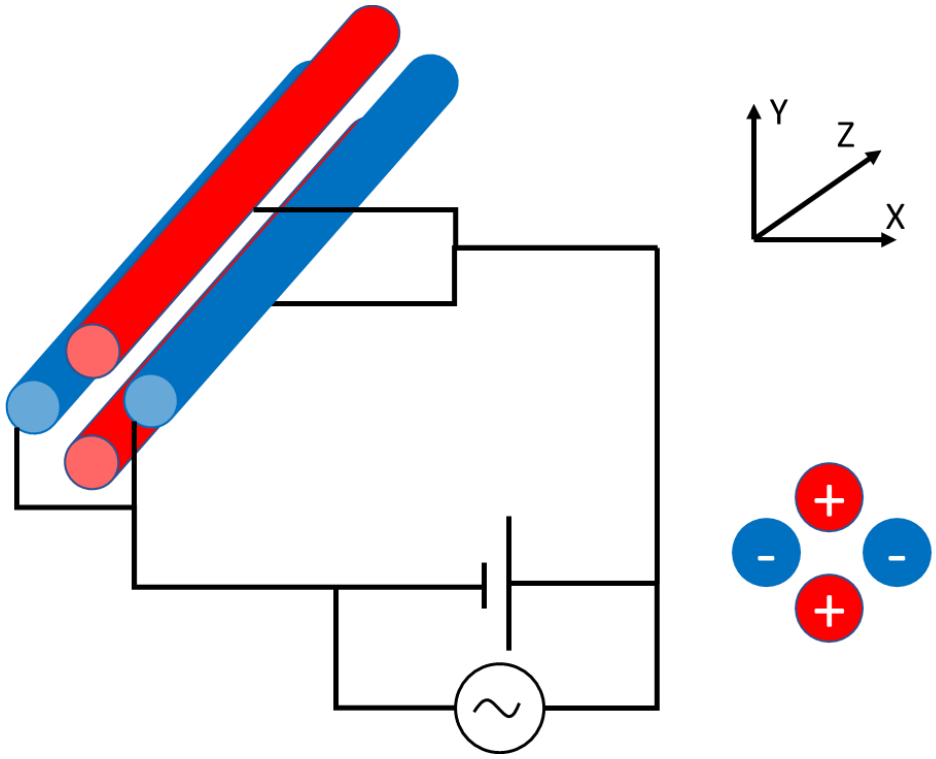


Figure 30: Cross-section of a quadrupole with cylindrical approximation

As is shown in Figure 30, a quadrupole is usually made up of two pairs of hyperbolically shaped metal rods that are connected with two poles of the power supply. In this way, an electric field is created within the four rods which could filter through ions with different m/z by alternating their motion in the XY plane. When ions entered the quadrupole along the z-axis direction, their motion in radius plain would be affected by an electric field made up of a combination of DC (Direct Current) voltage U and RF (Radio Frequency) voltage V. As is shown in Figure 31, in the field of positive-charged rods, only ions whose m/z is higher than the threshold could pass through

and the in the field of negatively charged rods, only ions whose m/z is lower than the threshold could pass through. As a result, at a specific time point, only a small range of ions with a specific range of m/z could pass through the quadrupole and reach the detectors.[28, 29, 41]

Mathematically, this process is described in Equation (5), where the threshold of each pair of rods is determined by a DC-related parameter ***a*** and an RF (Radio Frequency) related parameter ***q***. For a specific ion with a specific m/z, only a finite number of ***a*** and ***q*** could result in a stable motion inside the quadrupole and this range of ***a*** and ***q*** combination could be represented by a certain area in Mathieu Stability Diagram (see Figure 32). As a result, different ions would have different stability ranges (shown as m1, m2, m3 in Figure 32) and an operation line (purple line in Figure 32) represents the voltage condition applied on quadrupole. Usually, as quadrupole scans through a range of mass, the value of U and V changes but the ratio between ***a*** and ***q*** stays constant. As a result, under an optimal condition, this scanning line will pass through different ion stability region, gradually allowing ions with corresponding m/z to pass through the quadrupole and reach the detector. In this way, one m/z window at a time, a quadrupole mass analyzer could scan over a wide range of m/z values. [28, 29, 42]

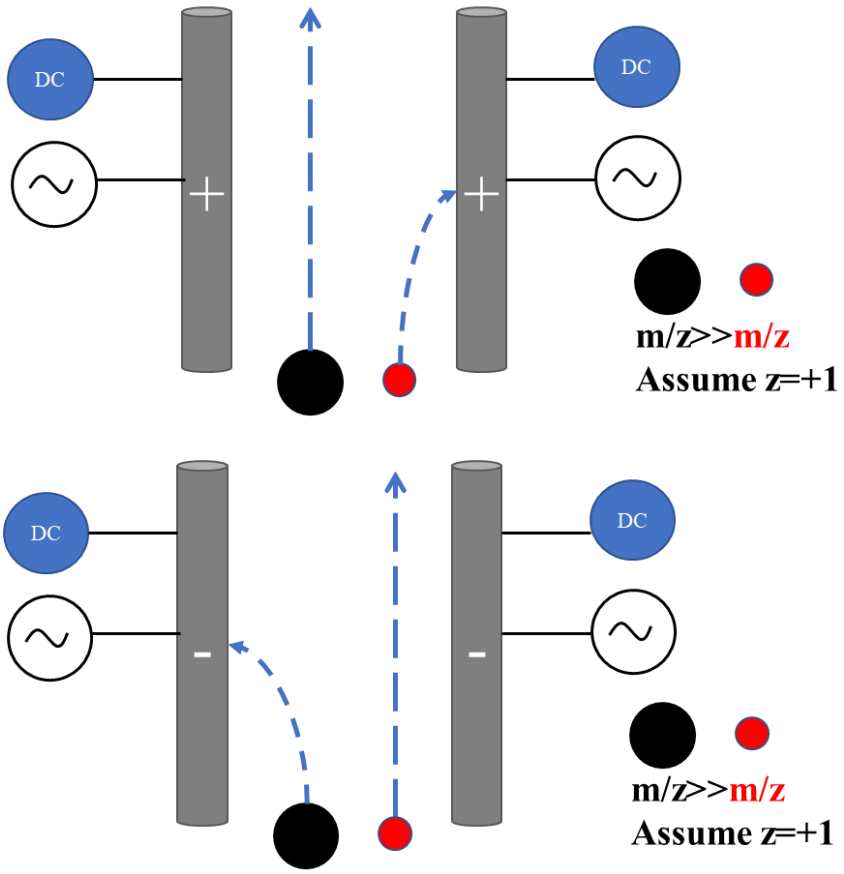


Figure 31: Diagram demonstrating how quadrupole mass analyzer filter ions

$$a = \frac{8eU}{(m/z)\omega^2 r_0^2} \, q = \frac{4eV}{(m/z)\omega^2 r_0^2} \tag{5}$$

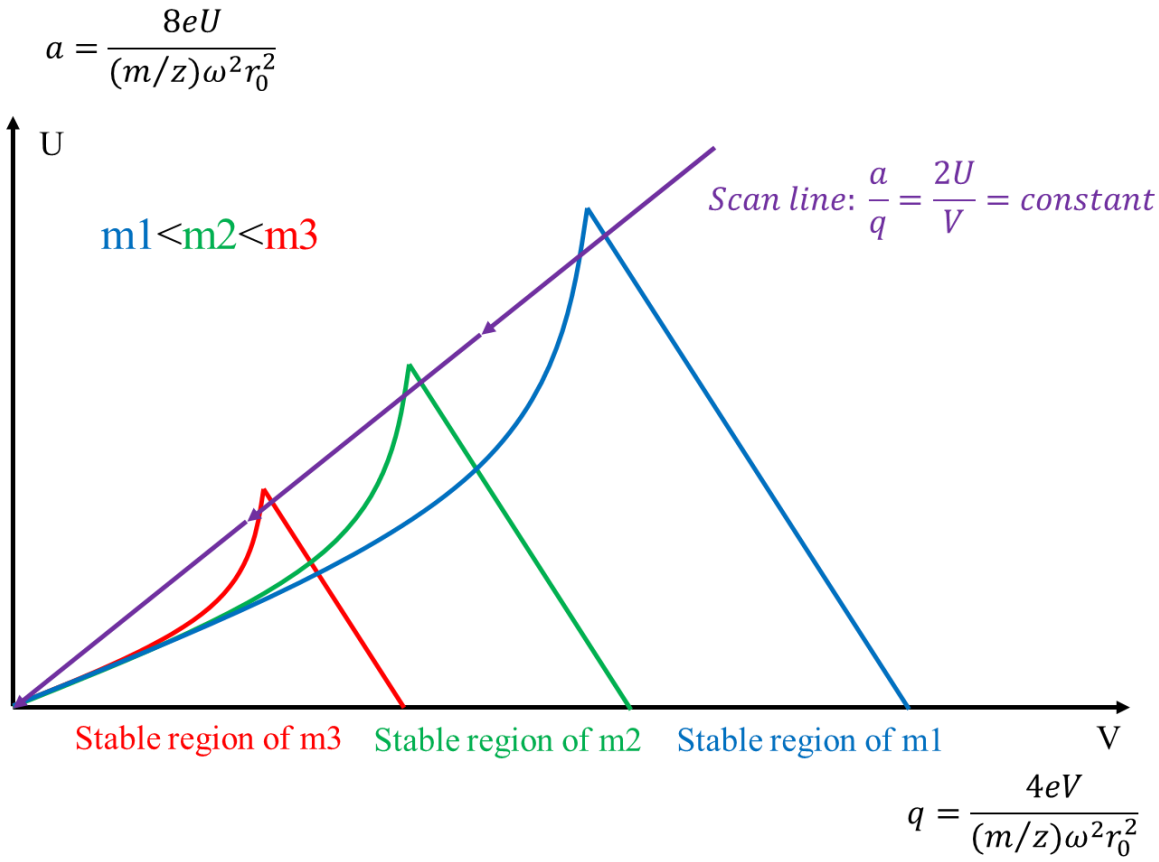


Figure 32: Diagram demonstrating the scanning of quadrupole

Besides filtering ions with different m/z, another function of quadrupole is to regulate the motion of ion beams. By turning off the DC resolving voltage while keeping the RF voltage on, the quadrupole would not be able to filter ions. Instead, it could be used as an ion guide where the RF electric field would confine all ions to travel along the centerline of the quadrupole, reducing the spread of kinetic energy. This process is also called "collisional cooling" as the excess kinetic energy of different ions are reduced by colliding with other ions.[28]

### 2.2.4 Time-Of-Flight mass analyzer (TOF)

Another type of mass analyzer commonly used today is the Time-Of-Flight, which essentially separates the ions with different m/z by measuring their flight time over a certain distance.[28] The theories behind TOF is summarized in Equations (6) to (8):

$$Kinetic\ Energy(KE) = zeU_{ex} = \frac{1}{2}mv^2 = \frac{1}{2}m(\frac{dx}{dt})^2 \quad (6)$$

$$m/z = 2eU_{ex}\frac{\Delta t^2}{\Delta x^2} \quad (7)$$

$$\Delta t = t_{arrival} - t_0 = \Delta x\sqrt{\frac{m}{2zeU_{ex}}} \quad (8)$$

When a package of charged ions is accelerated by a given electric field and travels over a certain distance, the flight time of each ion is proportional to the square root of its mass-to-charge ratio. Thus, by precisely measuring the arrival time of each ion, a detailed mass-to-charge ratio profile of this package of ions could be obtained simultaneously. Based on this theory, the first commercial linear TOF mass analyzer is developed by Wiley & McLaren in 1953 but by that time, TOF only has limited resolving power (lower than Quadrupole at that time) due to a spread of initial kinetic energy caused by linear motion of ions. Then during the 1970s, the improvement in electronics and the invention of reflectron by Mamyrin in 1973 greatly enhanced the resolving power of TOF. [24, 27, 43] The function of a reflectron could be considered as an "ion mirror", where the trajectory of ions is bent by a series of single-layer electric fields. A diagram showing the working mechanism of reflectron is shown in Figure 33. In linear TOF, due to the initial spread of kinetic energy, ions with the same mass-to-charge ratio could have different flight times, which results in a broadening of the signal peak and a reduction of resolving power. By implementing a reflectron, ions with higher KE will have to travel an extra distance in the reflection, which in the end balances the difference in KE and makes them arrive at the same time. Another technique used to deal with initial kinetic energy distribution is delayed ion extraction, which is also called time-lag focus or pulsed ion extraction. The principle of it is shown in Figure 34. Without delayed ion extraction, the ions get accelerated by the electrical field as soon as they are produced from the ionization source so there will be a considerable kinetic energy spread. By delaying the time of the

extraction, the ions get “cooled down” by the collision cooling effect brought the delayed voltage. In the meantime, ions are also separated out from each other to reduce the chance of hitting each other. [29, 44, 45] Using this enhanced resolving power, a rapid quality control (QC) identification of textile dyes would be possible as the isotopic distribution and exact mass measured by TOF mass analyzer could be used to confirm the formula of a commercial dye sample. For example, for reactive dyes with MCT reactive group such as C. I. Reactive Red 198, an abundance ratio of 3:1 between monoisotopic peak (M) and M+2 peak is expected whereas disperse dye with bromine atom (e.g. C. I. Disperse Violet 93) will produce a ratio of 1:1.

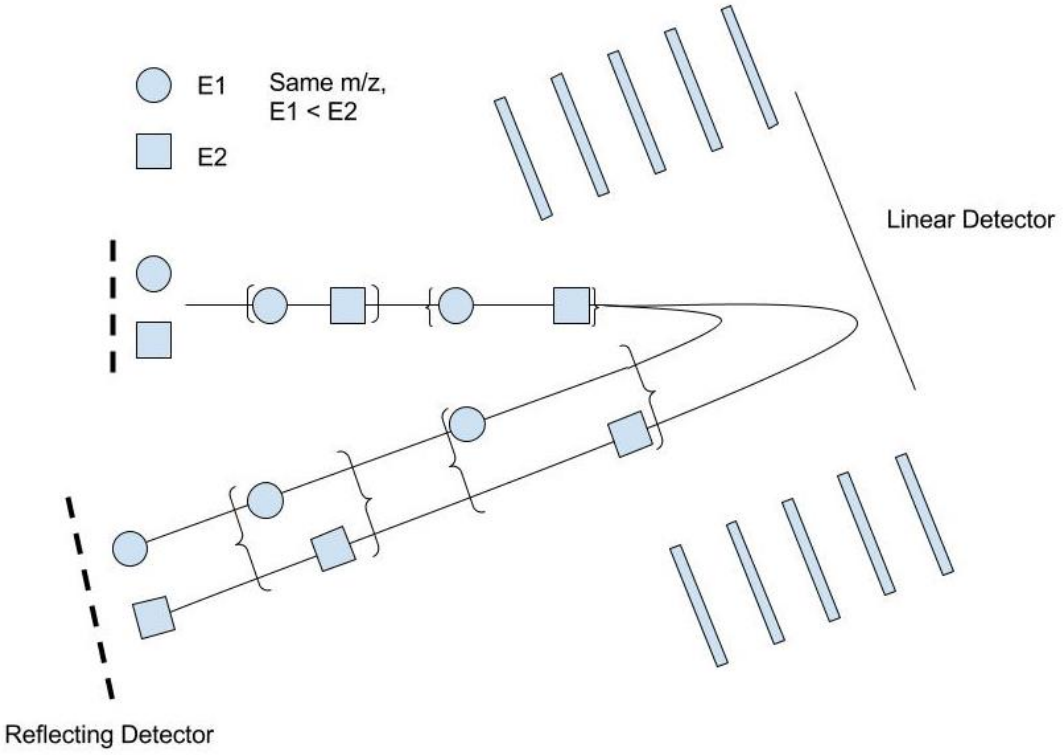


Figure 33: Working mechanism of the reflectron

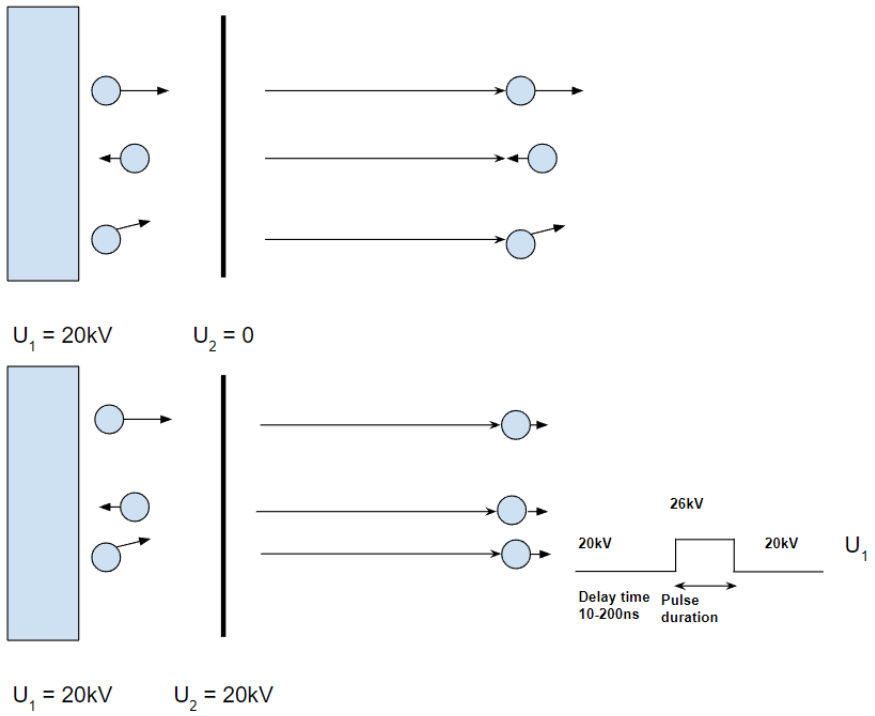


Figure 34: Principle of using a delayed ion extraction to reduce kinetic energy distribution

## 2.3 Tandem mass spectrometry (MS/MS)

Although single-stage mass spectrometry is already a very powerful analytical tool for absolute molecular specificity as it is capable of providing accurate exact mass measurement, in some cases, it is not enough to generate a confident structural identification. A perfect example of this is the problem of isomers, where a group of molecules has the same exact mass but different structures. As a result, single-stage mass spectrometry would not be able to differentiate those ions by exact mass. To overcome this challenge, instruments with MS/MS, or tandem MS capability have been developed over the years. Tandem mass spectrometry generally describes a process where more than one mass analyzer is coupled together (tandem in space) or a single mass analyzer is used to perform multiple stages of analysis (tandem in time).[28, 31] In a tandem-in-space capable instrument such as Quadrupole Time-Of-Flight (QTOF) and triple quadrupole (QqQ). There is a limitation on how many times the ion could be fragmented, while in theory, no limits for tandem-

in-time exists. For example, in a triple quadrupole MS, the target ion is selected in the first quadrupole, then fragmented in the second quadrupole (collision cell), and fragmented ions are guided through the third quadrupole and then detected. If there is a need for another level of fragmentation, two additional quadrupoles have to be installed. Figure 35 shows the diagram of one stage tandem MS in space and two-stage tandem MS in space. Q represents the quadrupole that is assigned to select and separate the ions and q represents the dissociation chamber. By coupling multiple mass analyzers together, the structural elucidation of targeted ion could be achieved by breaking up this ion by different dissociation techniques, which includes including Collision-Induced Dissociation (CID), higher-energy collisional dissociation (HCD), Surface Induced Dissociation, and Electron Transfer Dissociation (ETD). After dissociation, a structural specific fragmentation pattern could be obtained and could then be used for identification and quantification purposes. In this section, the working mechanism, and the theory behind CID and MS/MS quantification, will be introduced.

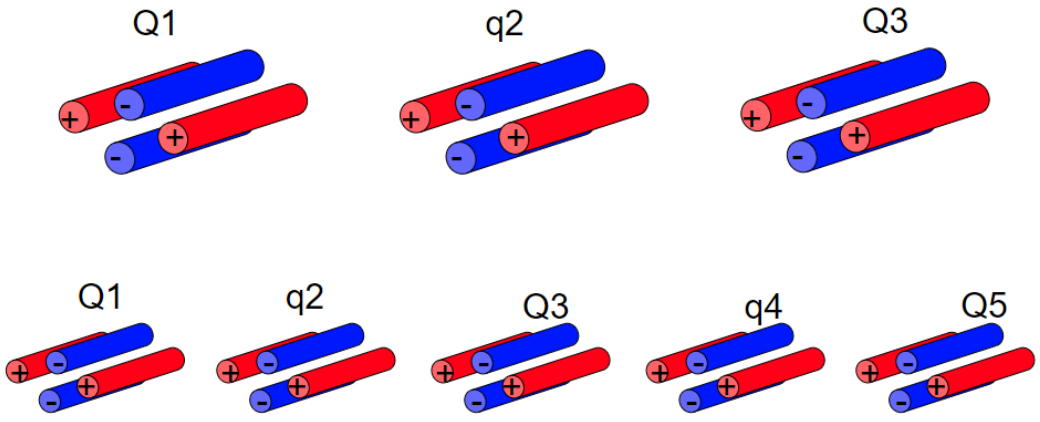


Figure 35: Diagram of one (top) and two (bottom) staged tandem in space MS

### 2.3.1 Collision-Induced Dissociation (CID)

CID, which is also called Collision-Activated Dissociation (CAD) is a commonly used dissociation technique in tandem mass spectrometry. In theory, it involves the inelastic collision between a target molecule ion and neutral gas molecules. Regarding the mechanism of CID, the revised Rice–Ramsperger–Kassel–Marcus (RRKM) theory is proposed to describe this process.[46, 47] Figure 36 shows a diagram explaining this theory. As the target ion (precursor ion) perform inelastic collision with neutral gas molecules, a proportion of the kinetic energy ($\mathbf{E_{Tr}}$) could be transferred into the internal energy of the precursor ion ($\mathbf{E_{cm}}$). This proportion could be calculated by an equation shown in Equation (9) where the amount of transferred kinetic energy is determined by the mass of precursor ion ($\mathbf{m_i}$), gas molecule ($\mathbf{m_t}$), and the initial kinetic energy carried by precursor ion. After a short excitation time, additional internal energy soon gets redistributed among all the vibration modes of the molecule, which also raises the level of total potential energy in the system. As soon as the potential energy reaches a threshold, the molecule starts to undergo unimolecular dissociation and produce product ions via a series of competitive and consecutive reactions. Regarding the efficiency of CID, as is shown in equation (9), the product ion yield would increase as the kinetic energy and target mass increase. To achieve the same level of energy transfer, an ion with higher molecular weight would require higher kinetic energy than the ion with lower molecular weight. Because the process of unimolecular dissociation is largely dependent on the structure of precursor ion, different molecules will result in different fragmentation patterns, which would greatly facilitate the identification of unknown molecules.[28] Considering the process of CID, this technique could be further used in the quality control of textile dye where an unknown dye sample could be fragmented by CID and its structural-specific fragmentation pattern could be compared against CID patterns from a group of known analytical standards as a kind of "molecular

fingerprint". If the pattern from the unknown sample is the same compared to the standard, the structure of this unknown dye could be confirmed.

$$E_{cm} = E_{TR} \times \frac{m_t}{m_t + m_i} \tag{9}$$

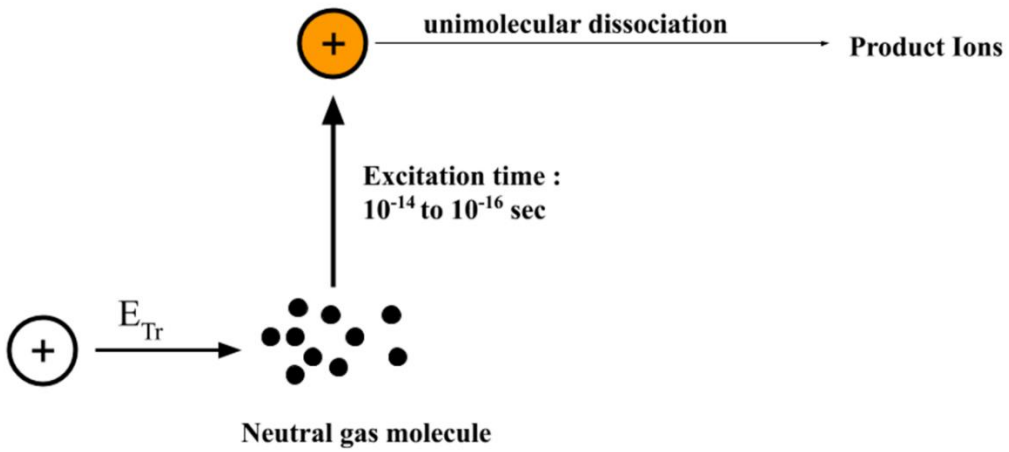


Figure 36: Diagram of Collision Induced Dissociation

### 2.3.2 Tandem mass spectrometry and quantification

A common misunderstanding regarding mass spectrometry is that the abundance in mass spectra represents the quantity sample. It should be mentioned, however, that in most cases, mass spectrometry is not a quantitative method as some ions could be less efficiently ionized due to ionization suppression. The mechanism behind ionization suppression is shown in Figure 37. In an ideal scenario, there are infinite amounts of charges available at the ionization source and all molecules in the sample could be fully ionized. In that case, the peak height (abundance) in a mass spectrum is determined solely by the concentration of this molecule in solution. Thus, in an ideal case, a calibration curve between peak height and sample concentration could be established. In the real-world scenario, however, because of the limitation of the ionization source, this amount

of charge available is not unlimited. Thus, during ionization, there will be competition for charges between different molecules according to their ability to be ionized and in the case of ESI, this competition is determined by the analyte's basicity. As a result, some molecules could be ionized better than other molecules, creating a higher peak height than others while the abundance of other molecules gets reduced. This competition in the ionization process is often referred to as ionization suppression and it is a critical factor to consider during mass spectrometry analysis. [31, 35]

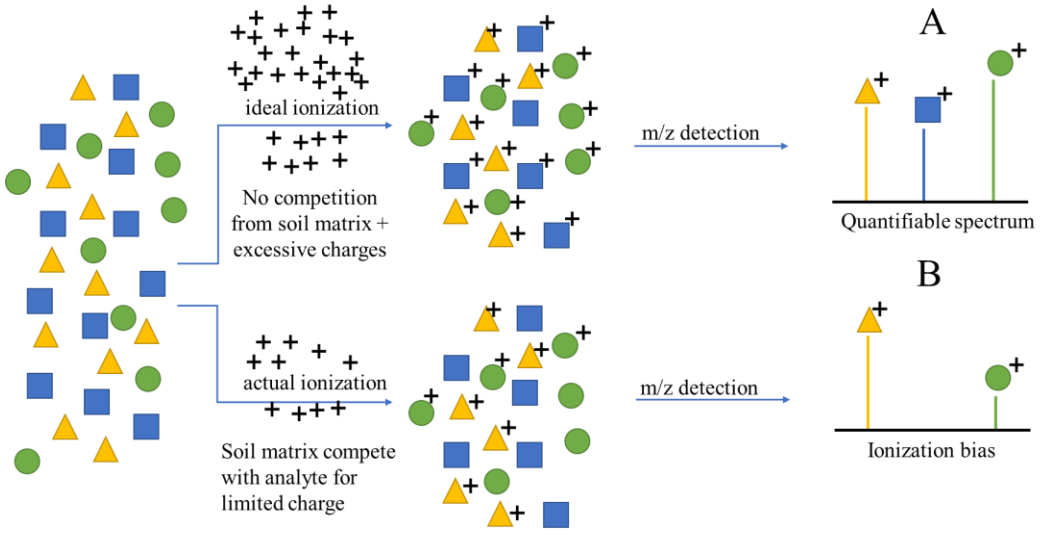


Figure 37: Diagram explaining the cause of ionization suppression

To overcome the error and inconsistency brought by ionization suppression during electrospray ionization, a methodology of quantification with an isotopically labeled internal standard is used. The theory behind this method is illustrated in Figure 38. In this method, the same amount of internal standard solution is introduced into each point in the calibration system. As a result, under a certain tandem mass spectrometry condition (e.g. isolation width, collision energy, and collision gas), the abundance ratio between analyte fragment ion and internal standard fragment ion should be proportional to the concentration of the analyte. Thus, despite the alteration of abundance brought by the fluctuation of instrument condition or insufficient ionization, the

abundance ratio between the analyte and internal standard stays the same, which strengthens the quality of the calibration curve. [25, 48, 49]

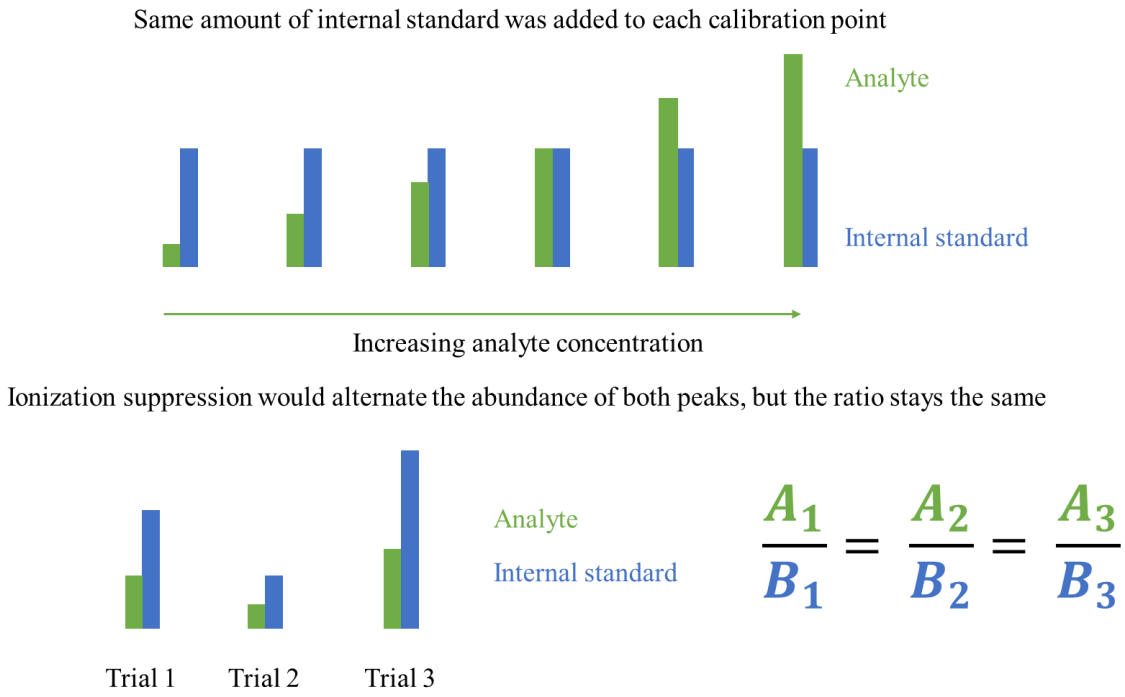


Figure 38: Diagram showing mechanism of quantification with internal standard

Considering the benefit of quantification with an internal standard, the selection of internal standards is crucial to the success of quantification. Ideally, the internal standard for tandem mass spectrometry quantification should have the same chemical structure as the analyte but different exact masses so they could separate by the mass analyzer and produce a similar fragmentation pattern. An ideal case for this kind of internal standard will be the isotopically labeled analyte like anthracene and D10-anthracene shown in Figure 39. They have exactly the same chemical structure and the only difference is their exact mass, which is brought by the replacement of hydrogen with deuterium.

In terms of textile dye, conventionally, the quantification of textile dyes has been based on Beer-Lambert law where a calibration curve between concentration and spectral absorption at

maximum absorption is established and used to quantify the concentration of the analyte.[50] With MS/MS quantification and isotopically labeled internal standard, the same analyte could be quantified with higher sensitivity as the detection limit of the mass spectrometer is lower than that of the diode array detector.[63]

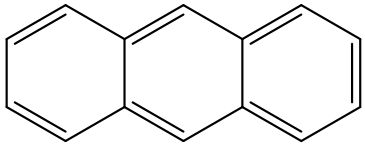

anthracene
Chemical Formula: $C_{14}H_{10}$
Exact Mass: 178.0783

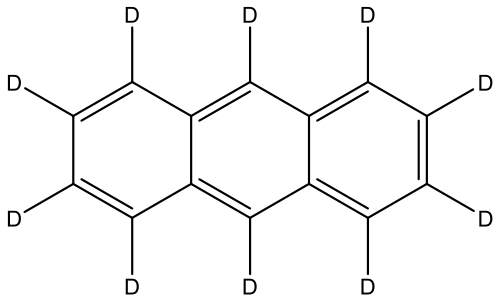


anthracene-$d_{10}$
Chemical Formula: $C_{14}D_{10}$
Exact Mass: 188.1410

Figure 39: Structure of anthracene and anthracene-$d_{10}$

# CHAPTER 3

## Soil and QuEChERS extraction

An important task of my doctoral project is to investigate the chemical change of cotton auxiliaries, dyes, and finishing, after degradation in soil. This chapter discusses important aspects of soil and the analytical methods that can help the extraction of analytes of interest from the soil.

## 3.1 Chemical composition of soil

Usually, when people think of soil, it is considered as a single-phase system as it looks homogeneous in terms of color and hand-feeling. In fact, in the view of chemists, soil is a heterogeneous system made up of two phases: soil solids and soil solutions, and three active environmental compartments: atmosphere, biosphere, and hydrosphere. Their interaction could be illustrated by the diagram shown in Figure 40. [50-52]

Soil solid is the most observable part in a soil system as in most cases it could be visually assessed and physically touched. Soil solids could be divided into organic and inorganic. Organic solids usually contain plant and animal residues after decomposition, cells, and tissues of soil microorganisms (bacteria or fungus), and substances synthesized by these microorganism's populations. Inorganic soil solids are made up largely of two major components: abundant primary minerals like quartz ($SiO_2$) and feldspars ($MAlSi_3O_8$, M is a combination of $Na^+$, $K^+$, $Ca^{2+}$); secondary minerals such as layers of silicates, aluminum ($Al(OH)_3$), iron hydroxides ($Fe(OH)_3$), carbonates ($CaCO_3$) and sulfur-containing compounds. Although quantitatively, the proportion of organic solids is smaller compared with inorganic solid, they make a larger impact on the properties of soil because of their relatively higher reactivity. [50-52]

Besides soil solids, another important component of this system is its soil solution. The role of soil solution in the whole soil system is to serve as the interface between soil solid and three

other compartments, as the materials could circulate the whole system. Unlike other conventional solutions where the interaction with other phases (such as air or other types of immiscible solvent) relies on a contacting surface. The interaction between soil solid and soil solution is extensive as the interaction happens on all interfaces available. Because of this reason, the boundary between soil solid and soil solution is considered as diffuse as the interface is extensive throughout all available contacting area. [50-52]

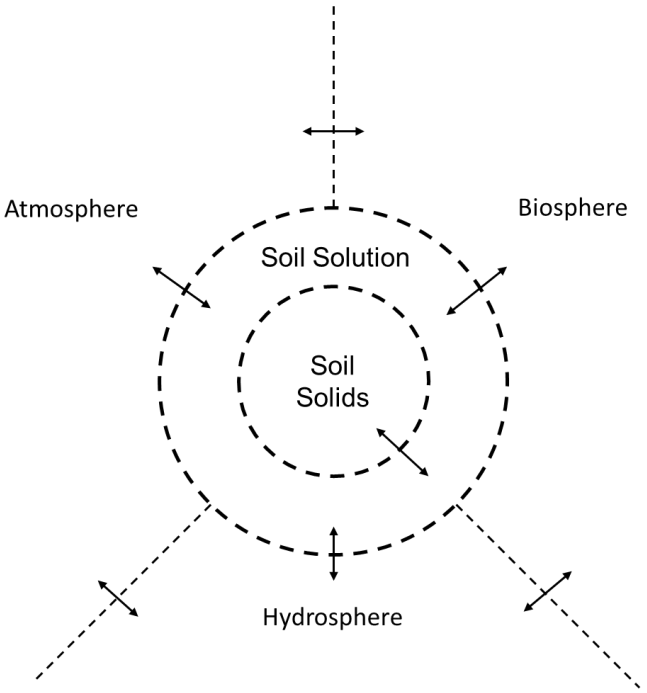


Figure 40: Interaction between different soil compartments and soil solution from birds eye view[50]

Besides serving as an internal interface within the soil system, this interaction between soil solid and soil solution is also crucial to the degradation of cotton fabrics with reactive dyes or finishings in soil, as it could provide an environment that facilitates biodegradation and a channel to dispense potential degradation products way from the contacting region. Thus, it would be reasonable to expect that if there could be a method to extract those degradation products out of the soil and detect them via an analytical instrument. The chemical changes that occurred on cotton fabrics with reactive dye or textile finishing during the compost degradation process could be

explored to have a better understanding of this process. We can think that dyes and finishing are an extra layer that can have a significant role in the decomposition of the cotton fabric.

## 3.2 Different extraction methods for potential soil pollutants

As is discussed in the last section, to investigate the chemical changes that occurred on cotton fabrics with reactive dye or textile finishing during the compost biodegradation process, an extraction process is needed. Currently, a variety of different extraction methods are available such as Solid Phase Extraction (SPE) and Quick, Easy, Cheap, Effective, Rugged, and Safe (QuEChERS).[58] However, for this project, because of the difference in the target analyte, the theoretical feasibility of these methods may need to be evaluated. In the section, three extraction methods will be discussed including Solvent extraction, Solid Phase Extraction (SPE), and QuEChERS extraction method.

### 3.2.1 Solvent extraction

Extraction and separation of a mixture by organic solvents is a very common purification technique used in both the academic and industrial fields. In academia, solvent extraction is commonly used to extract and concentrate synthesis products from the liquid mixture after reactions. One classic example is the separation of phenol from benzene, which is illustrated by a diagram shown in Figure 41. By adding sodium hydroxide (NaOH) solution into a mixture of phenol and benzene, phenol could react with NaOH, forming sodium phenoxide (reaction **1**). As a salt, sodium phenoxide is more soluble in water than in benzene, so as the mixture is separated into two layers: an organic layer and an aqueous layer. After that, phenol impurities could be removed from benzene by using a separatory funnel. Then if the collection of extracted phenol is needed, carbon dioxide ($CO_2$) gas could be blown into the aqueous layer containing sodium

phenoxide (reaction 2 in Figure 41) and sodium phenoxide will react with carbonic acid ($H_2CO_3$), forming phenol and sodium hydrogen carbonate as the pKa of phenol (around 9.9) is higher than that of carbonic acid (pKa = 6.4) but lower than hydrogen carbonate anion (pKa = 10.3 ). Then as phenol is only slightly soluble in water at room temperature and the density of phenol is greater than water, the aqueous layer could be separated again from the organic layer by using a separatory funnel. As a result, phenol impurities in benzene could be removed and collected using solubility difference and the rule of acidity.[33, 53] Another example from the food industry is the decaffeination of coffee beans. Dry weight coffee bean contains around 2.5 % of caffeine, a simulating compound that is favored by many people but also disliked by others. To accommodate the demand for caffeine-free coffee, caffeine needs to be extracted out of the coffee bean. Caffeine is soluble in hot water, but this extraction comes with a cost as hot water could also remove certain flavorful oil, which would potentially undermine the commercial value of decaffeinated coffee beans. Thus, food industries often use non-polar solvents such as dichloromethane to specifically extract caffeine and the extracted caffeine could then be used to produce caffeinated soft drinks like Coca-Cola. [54]

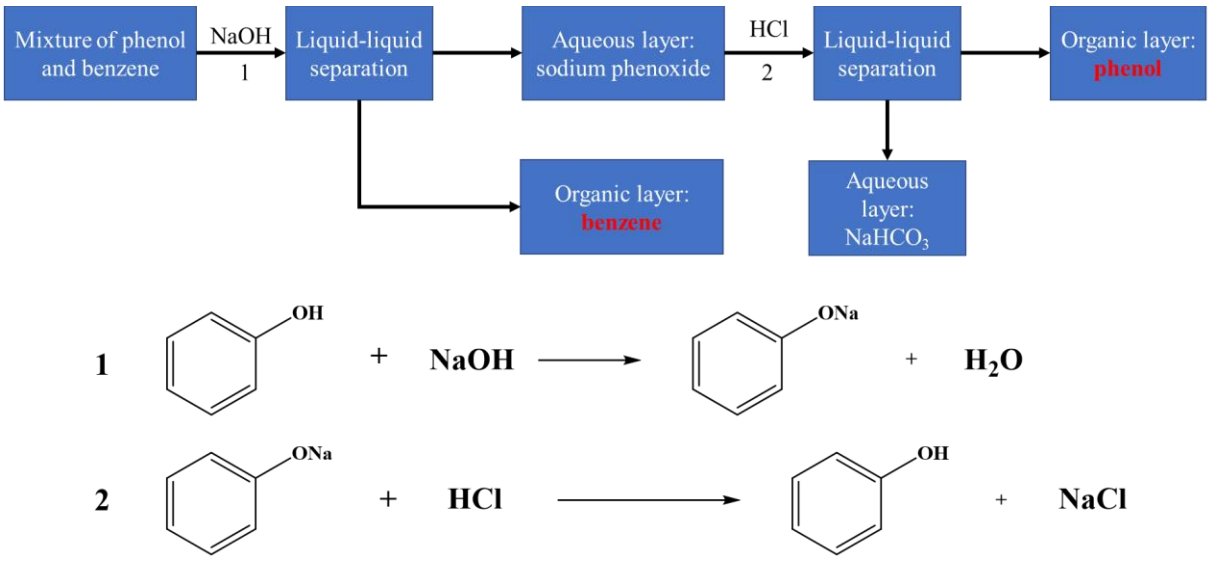


Figure 41: Separation of phenol from benzene by solvent extraction and liquid-liquid phase separation

From the example of benzene purification and caffeine extraction, it could be noticed that finding a suitable solvent is key in designing a solvent extraction process. Overall, the most important criterion in the selection of solvent is the solubility of the target compound in this solvent. Generally, a rule-of-thumb would be "like dissolves like" as polar compounds (like potassium permanganate $KMnO_4$) tend to be more soluble in polar solvents like water while nonpolar substances like iodine ($I_2$) tend to be more soluble in nonpolar solvents like tetrachloride ($CCl_4$).[53] Now, in the case of extraction of potential reactive dye degradation products from soil after compost degradation, the solubility of reactive dye should be evaluated. Although reactive dyes usually are synthesized based on organic chromogens like anthraquinone or azo (already discussed in Chapter 1). These dyes are designed to have multiple hydrophilic functional groups such as sulfonate groups to facilitate the aqueous dying purposes and increase their polarity. It seems that water could be used to extract potential reactive dye degradation products from soil after compost degradation. However, as is discussed in section 3.1 soil solution contains serval types of inorganic mineral salt that is also soluble in water, so the extracted solution will be a mixture of reactive dye degradation products and a variety of different salts, which will negatively affect the analysis of MS when ESI is used as the ionization mechanism. [34, 55] For this reason, solvent extraction may not be a suitable technique for the extraction of reactive dye degradation products from soil after compost degradation.

### 3.2.2 Solid-Phase Extraction (SPE)

Solid-phase extraction is defined as a sample reparation technique in which a solid particle, usually chromatographic packing material made from silica gel, is used to separate different components in a mixture according to their affinity. This technique is very similar to the separation principle of the HPLC (see Chapter 2). SPE is sometimes nicknamed as "manual HPLC in a tube"

as it requires manual injection of the sample and gravity to move the mobile phase through the stationary phase. Like HPLC, SPE could bring several benefits to mixture analysis including simplification of the mixture along with the reduction of ion suppression due to concentrated analytes and separation of the mixture. Regarding the application of SPE in solid sample extraction, one example could be the extraction of food dyes from commercial drinking power (like Kool-Aid). From its ingredients list, the inclusion of two food dyes (C.I. Food Red 17 and C.I. Food Blue 2, structures shown in Figure 42) could be found and SPE extraction could be used to separate these two dyes. The procedure is illustrated in Figure 42. Before extraction, Kool-Aid powder needs to be dissolved in deionized water and the cartridge needs to be primed by 70 % isopropyl alcohol (IPA) in water. The primed cartridge is first loaded with a dissolved Kool-Aid solution. Then by flowing 5% IPA solution through the cartridge, sugars, and other polar components such as flavor additives are extracted from the mixture. Then 25% IPA is introduced into the cartridge and C.I. Food Red 17 will be taken out from the mixture as it is less polar than sugar but more polar than C.I. Food Blue 2. Finally, the remaining nonpolar component, and the blue dyes, will be eluted by 70% IPA. Thus, these two kinds of food dyes are extracted from the mixture liquid due to their difference in polarity and their affinities towards different mobile phase compositions.[48, 56]

From the example of Kool-Aid extraction, it could be noticed that although the extraction is performed on a solid sample, the sample has to be dissolved before separated by SPE. In the case of extracting reactive dye or textile finishing degradation products from soil after compost degradation, it would be difficult to push the entire soil system through the cartridge considering the separation mechanism of SPE. Similar to HPLC, advantages of the SPE process include

simplification of the complex mixture in which a great proportion of matrix material is separated from the analyte, reducing matrix effects, and enhancing the ionization of analyte for MS analysis.

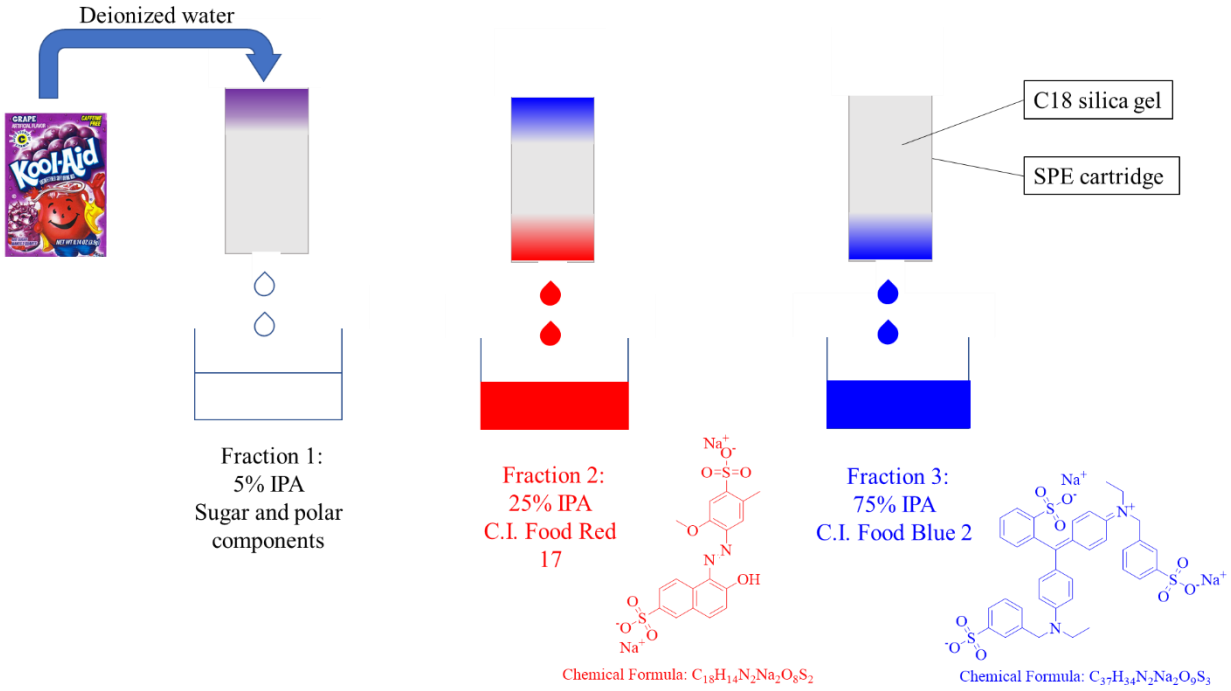


Figure 42: Extraction of food dyes from Kool-Aid powder by Solid Phase Extraction

### 3.2.3 Quick, Easy, Cheap, Effective, Rugged and Safe (QuEChERS) method

#### 3.2.3.1 Origin of QuEChERS extraction method

QuEChERS extraction method is originally developed by a group of European scientists in 2002 and its popularity in the analytical field has grown dramatically since its first publication on the Pesticide Residue Workshop (EPRW) 2002 in Rome.[57] According to a quick search of the QuEChERS in the middle of 2019, there are a total of 4520 references found from *Scifinder*, 2777 results from *Web of Science*, and 30,100 results from *Google Scholar*. According to one review article, the intention behind the initial development of QuEChERS is to replace the old " Luke method", where large quantities of organic solvents such as petroleum ether and dichloromethane

are used, and create a method that is quick, easy, cheap, effective, rugged and safe. Thus, this novel extraction method is named as QuEChERS. [58]

### 3.2.3.2 Evolution of QuEChERS extraction method

According to the original publication, the QuEChERS method includes two steps: extraction or partition and dispersive Solid Phase Extraction (dSPE). In the first steps, 10 g of well-chopped sample (fruits, vegetables, or meats) are extracted by 10 mL of acetonitrile (ACN) and mixed by vortex mixer. Then 4 g of magnesium sulfate ($MgSO_4$) and 1 g of NaCl are added to the system and mixed well by vortex mixer. Follow by the addition of 50 μL of triphenyl phosphate (TPP) as an internal standard for recovery rate tests. The system is then mixed for 30 seconds and centrifuged for 5 minutes at 5000 rotations per minute (rpm).

In the second step, an aliquot of 1 mL of the upper layer is transferred to another centrifuge tube and added with 25 mg of N-propyl ethylenediamine as SPE sorbent and 150 mg of $MgSO_4$. Then the system is mixed for 30 seconds by vortex mixer and centrifuged for 1 minute at 6000 rpm before prepared for Gas-Chromatography Mass spectrometry (GC-MS) analysis. [57]

From this detailed procedure, the improvement of the QuEChERS method could be found as it uses less solvent (10g sample with 10 ml ACN vs. 15 g sample with 20mL petroleum ether and 10 mL dichloromethane in Luke method), a safer solvent (acetonitrile vs. petroleum ether and dichloromethane), and in a shorter time (no evaporation needed vs. solvent need to be evaporated). Besides these apparent benefits, another advantage of the QuEChERS method is that it is a customizable method. Based on the original QuEChERS method, a series of improvements could be made including changing separation salts, changing solvents, changing clean-up materials, changing of agitation mode, and the introduction of pH buffer systems. A detailed list of available options in customizing the QuEChERS method is shown in Figure 43. Regarding the extraction

solvent, in the original method, acetonitrile is used but other solvent selection could also be found from literature including methanol, chloroform, ethyl acetate, hexane, and a mixture of different solvents. Salts used during the partition step is initially a mixture of NaCl and $MgSO_4$ at a ratio of 1: 4 as it gives better peak shape in chromatography but other options such as $MgSO_4$, $CH_3COONa$, $CH_3COONH_4$, and $NaHCO_3$ are also available. In the original QuEChERS method, following the initial separation step is the clean-up by primary and secondary amine exchange material (PSA) and $MgSO_4$ solid mixture. In recent years to achieve a better cleanup effect, SPE cartridge with different materials such as C18 silica, aluminum oxide, and chitosan are also used depending on the complexity of the matrix. The clean-up step could also be removed from the procedure to simplify the procedure. Mechanical agitation via vortex mixer or sonication could also be introduced to replace the manual agitation. In addition, buffer systems could be added to maintain the pH condition during the extraction process and preserve pH-sensitive analytes. [58-60]

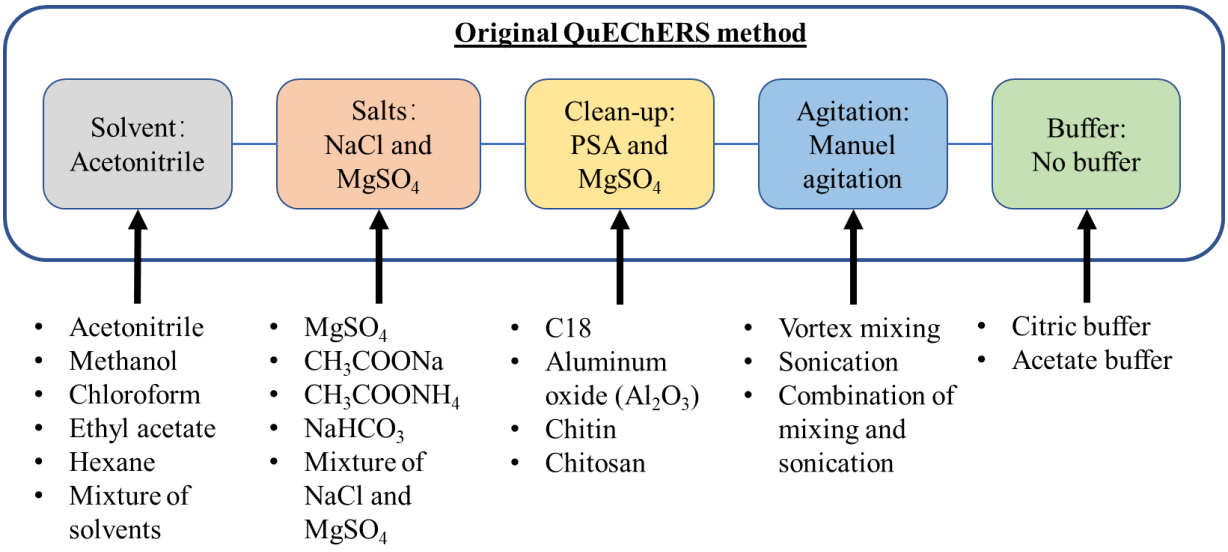


Figure 43: Improvement options based on original QuEChERS method

### 3.2.3.3 QuEChERS extraction on reactive dye and antimicrobial finishing

As is discussed in section 3.2.3.2, customization of QuEChERS extraction for a specific extraction scenario could be employed in five different compartments: solvent, salts, clean-up, agitation, and buffer system. During the customization of QuEChERS extraction method, one important factor that should be taken into consideration is the polarity difference between the analyte being extract and its environment. In the case of extracting reactive dye degradation products from soil. This would be a problem as reactive dyes have very different chemical properties compared to pesticide or veterinarian drugs. To facilitate the fixation of reactive dye in an aqueous dyeing bath, the structure of reactive dyes contains multiple hydrophilic groups such as sulfonate groups, so direct separation by acetonitrile and salts may have a limited effect on reactive dye in soil. For this reason, before performing extraction on soils after simulated compost degradation, preliminary tests should be employed to investigate the feasibility of using QuEChERS methodology to extract native reactive dye from water solution and later from blank soil spiked with reactive dye.

An important part of my research project is the development of an extraction method via QuEChERS to enhance the recovery of reactive dyes and their derivatives after biodegradation from soil. This can be divided into three phases:

- Phase 1: Qualitative study on the degradation of reactive dyed cotton fabrics in soil
    - Extraction of reactive dyes from spiking solution with QuEChERS method
    - Extraction of reactive dyes from blank soil spiked with reactive dyes with conventional QuEChERS method
    - Extraction of reactive dye degradation product from soil using a modified QuEChERS method

- Phase 2: Qualitative analysis on the degradation of antimicrobial finishing in soil
    - Extraction of antimicrobial finishing agent from its water solution via QuEChERS extraction method
    - Optimization of QuEChERS extraction on an antimicrobial agent by isotopically labeled internal standard
- Phase 3: Quantitative analysis of on the degradation of antimicrobial finishing in soil
    - Establishment of the calibration curve
    - Validation of the quantification method (Precision, Accuracy)
    - Extraction of degradation product from soil containing cotton fabrics with antimicrobial finishing using a modified QuEChERS method

## REFERENCES


1. Chandrappa, R.; Das, D. B. (. *Solid Waste Management: Principles and Practice;* Heidelberg: Springer, 2012]: 2012; .
2. Facts and Figures about Materials, Waste and Recycling; *https://www.epa.gov/facts-and-figures-about-materials-waste-and-recycling/textiles-material-specific-data* (accessed December 26, 2019).
3. Zollinger, H., 1919-2005 *Color chemistry: syntheses, properties, and applications of organic dyes and pigments;* Zu¨rich: Verlag Helvetica Chimica Acta; Weinheim: Wiley-VCH, 2003]: 2003;
4. Hunger, K. *Industrial dyes: chemistry, properties, applications;* Weinheim: Wiley-VCH, 2003]: 2003.
5. Gu¨rses, A. *Dyes and pigments;* Cham, Switzerland: Springer, 2016: 2016.
6. Christie, R. M. *Color chemistry;* Cambridge, England: Royal Society of Chemistry, 2015: 2015.
7. Pellew, C. E., author. *Dyes and dyeing;* Abhishek Publications: Chandigarh, 2007.
8. Kanik, M.; Hauser, P. J. Printing Cationized Cotton with Direct Dyes. *Textile Research Journal* **2004**, *74*, 43-50.
9. Hauser, P. J.; Tabba, A. H. Improving the environmental and economic aspects of cotton dyeing using a cationized cotton. *Coloration Technology* **2001**, *117*, 282-288.
10. Hashem, M.; Hauser, P.; Smith, B. Reaction Efficiency for Cellulose Cationization Using 3-Chloro-2- Hydroxypropyl Trimethyl Ammonium Chloride. *Textile Research Journal* **2003**, *73*, 1017-1023.

11. Shore, J.; Society of Dyers, and Colorists *Colorants and auxiliaries: organic chemistry and application properties;* Bradford, West Yorkshire, England: Society of Dyers and Colorists, 2002: 2002.

12. *Handbook of textile and industrial dyeing. Volume 1, Principles, processes, and types of dyes electronic resource];* Woodhead Publishing: Cambridge, England], 2011.

13. Stamm, O. A. Mechanisms of Reaction of Reactive Dyes with Cellulosic and other Fibres. *Journal of the Society of Dyers and Colorists* **1964**, *80*, 416-422.

14. Dawson, T. L. The Reaction Mechanism and Fixation of Monochloro-s-triazine Dyes on Cellulose Using Tertiary Amine Catalysts. *Journal of the Society of Dyers and Colorists* **1964**, *80*, 134-143.

15. Stead, C. V. Halogenated heterocycles in reactive dyes. *Dyes and Pigments* **1982**, *3*, 161-171.

16. Upadhyay, S. K. *Chemical kinetics and reaction dynamics;* Springer; Anamaya: New York; New Delhi, India, 2006.

17. Gorenšek, M. Dye–fiber bond stabilities of some reactive dyes on cotton. *Dyes and Pigments* **1999**, *40*, 225-233.

18. Olson, E. S. *Textile wet processes;* Noyes Publications: Park Ridge, N.J., U.S.A., 1983.

19. Heywood, D.; Society of Dyers, and Colourists *Textile finishing;* Bradford, West Yorkshire: Society of Dyers and Colourists, 2003: 2003.

20. Almeida, L. *Functional finishes for textiles: improving comfort, performance and protection;* Cambridge, England]: Woodhead Publishing, 2015: 2015.

21. Mather, R. R.; Wardman, R. H. *The chemistry of textile fibers;* Cambridge: Royal Society of Chemistry, 2015]: 2015.

22. Schindler, W. D.; Hauser, P. J.; Textile Institute (Manchester), E. *Chemical finishing of textiles;* Boca Raton: CRC; Cambridge, England: Woodhead, 2004: 2004.

23. Bechtold, T.; Pham, T. *Textile Chemistry;* Berlin; Boston: De Gruyter, 2019]: 2019.

24. Thomson, J. J. (. *Recollections and reflections;* New York, Macmillan, 1937: 1937.

25. Makarov, A. Electrostatic axially harmonic orbital trapping: A high-performance technique of mass analysis. *Anal. Chem.* **2000**, *72*, 1156-1162.

26. Grayson, M. A. *Measuring mass: from positive rays to proteins;* Philadelphia, PA: Chemical Heritage Press, 2002]: 2002.

27. Hamilton, L. F. (. F., 1893-; Simpson, S. G., 1894- *Quantitative chemical analysis;* New York: Macmillan, 1958]: 1958.

28. Watson, J. T. *Introduction to mass spectrometry: instrumentation, applications and strategies for data interpretation;* John Wiley & Sons: Chichester, England; Hoboken, NJ, 2007.

29. Dass, C. *Fundamentals of contemporary mass spectrometry;* Wiley-Interscience: Hoboken, N.J., 2007.

30. Watson, J. T.; Sparkman, O. D. *Introduction to mass spectrometry: instrumentation, applications and strategies for data interpretation;* Chichester, England; Hoboken, NJ: John Wiley & Sons, 2007]: 2007.

31. Chernushevich, I. V.; Loboda, A. V.; Thomson, B. A. An introduction to quadrupole–time-of-flight mass spectrometry. *Journal of Mass Spectrometry* **2001**, *36*, 849-865.

32. Snyder, L. R.; Kirkland, J. J. (.; Dolan, J. W. *Introduction to modern liquid chromatography;* Hoboken, N.J.: Wiley, 2010]: 2010;

33. Skoog, D. A.; Holler, F. J.; Crouch, S. R. *Principles of instrumental analysis;* Belmont, CA: Thomson Brooks/Cole, 2007]: 2007.

34. McMaster, M. C. *HPLC, a practical user's guide;* Wiley-Interscience: Hoboken, N.J., 2007.

35. Dean, J. A. (. A., 1921-2001 *Chemical separation methods;* New York: Van Nostrand Reinhold Co., 1969]: 1969.

36. Kebarle, P.; Verkerk, U. H. Electrospray: From ions in solution to ions in the gas phase, what we know now. *Mass Spectrometry Reviews* **2009**, *28*, 898-917.

37. Cole, R. B. *Electrospray and MALDI mass spectrometry;* Wiley: 2010.

38. Fenn, J. B. Ion formation from charged droplets: roles of geometry, energy, and time. *J. Am. Soc. Mass Spectrom.* **1993**, *4*, 524-535.

39. Cech, N. B.; Enke, C. G. Practical implications of some recent studies in electrospray ionization fundamentals. *Mass Spectrom. Rev.* **2001**, *20*, 362-387.

40. Ahadi, E.; Konermann, L. Ejection of Solvated Ions from Electrosprayed Methanol/Water Nanodroplets Studied by Molecular Dynamics Simulations. *Journal of the American Chemical Society* **2011**, *133*, 9354-9363.

41. Konermann, L.; Ahadi, E.; Rodriguez, A. D.; Vahidi, S. Unraveling the Mechanism of Electrospray Ionization. *Analytical chemistry* **2013**, *85*, 2-9.

42. Konermann, L.; Metwally, H.; McAllister, R. G.; Popa, V. How to run molecular dynamics simulations on electrospray droplets and gas phase proteins: Basic guidelines and selected applications. *Methods* **2018**, *144*, 104-112.

43. *Quadrupole mass spectrometry and its applications;* American Institute of Physics: New York, 1995.

44. Jonscher, K. R.; Yates, J. R. The Quadrupole Ion Trap Mass Spectrometer—A Small Solution to a Big Challenge. *Analytical Biochemistry* **1997**, *244*, 1-15.

45. Griffiths, J. A brief history of mass spectrometry. *Anal. Chem.* **2008**, *80*, 5678-5683.

46. Schlag, E. W. *Time-of-flight mass spectrometry and its applications;* Elsevier: Amsterdam [u.a.], 1994.

47. Guilhaus, M. Special feature: Tutorial. Principles and instrumentation in time-of-flight mass spectrometry. Physical and instrumental concepts. *Journal of Mass Spectrometry* **1995**, *30*, 1519-1532.

48. de Hoffmann, E. Tandem mass spectrometry: A primer. *Journal of Mass Spectrometry* **1996**, *31*, 129-137.

49. Baer, T.; Mayer, P. M. Statistical Rice-Ramsperger-Kassel-Marcus quasiequilibrium theory calculations in mass spectrometry. *J Am Soc Mass Spectrum* **1997**, *8*, 103-115.

50. Boyd, R. K.; Basic, C.; Bethem, R. A. *Trace quantitative analysis by mass spectrometry;* John Wiley & Sons: 2008.

51. Lavagnini, I. *Quantitative applications of mass spectrometry;* Chichester, England; Hoboken, NJ: John Wiley, 2006]: 2006.

52. Bohn, H. L., 1934-; McNeal, B. L., 1938-; O'Connor, G. A., 1944- *Soil chemistry;* New York: Wiley, 2001: 2001.

53. Strawn, D.; Bohn, H. L., 1934-; O'Connor, G. A., 1944- *Soil chemistry;* Chichester, West Sussex, UK; Hoboken, NJ, USA: Wiley Blackwell, 2015: 2015.

54. Sposito, G., 1939- *The chemistry of soils;* New York, NY: Oxford University Press, 2016: 2016.

55. Clayden, J.; Greeves, N.; Warren, S. G. *Organic chemistry;* Oxford; New York: Oxford University Press, c2012: 2012.

56. Ramalakshmi, K.; Raghavan, B. Caffeine in Coffee: Its Removal. Why and How? *Critical Reviews in Food Science and Nutrition* **1999**, *39*, 441-456.

57. Metwally, H.; McAllister, R. G.; Konermann, L. Exploring the Mechanism of Salt-Induced Signal Suppression in Protein Electrospray Mass Spectrometry Using Experiments and Molecular Dynamics Simulations. *Anal. Chem.* **2015**, *87*, 2434-2442.

58. Thurman, E. M. (.; Mills, M. S. *Solid-phase extraction: principles and practice;* New York: Wiley, 1998]: 1998.

59. Anastassiades, M.; Lehotay, S. J.; Stajnbaher, D.; Schenck, F. J. Fast and easy multiresidue method employing acetonitrile extraction/partitioning and "dispersive solid-phase extraction" for the determination of pesticide residues in produce. *Journal of AOAC International* **2003**, *86*, 412-431.

60. Perestrelo, R.; Silva, C.; Silva, P.; Porto-Figueira, P.; Pereira, J. A. M.; Medina, S.; Câmara, J. S. QuEChERS - Fundamentals, relevant improvements, applications, and future trends. *Analytica Chimica Acta* **2019**, *1070*, 1-28.

61. Vera, J.; Correia-S, L.; Paga, P.; Bragana, I.; Fernandes, V. C.; Domingues, V. F.; Delerue-Matos, C. QuEChERS, and soil analysis. An Overview. *Sample Preparation* **2013**, *1*, 54-77.

62. Santana-Mayor, Á; Socas-Rodríguez, B.; Herrera-Herrera, A. V.; Rodríguez-Delgado, M. Á Current trends in QuEChERS method. A versatile procedure for food, environmental and biological analysis. *Trends in Analytical Chemistry* **2019**, *116*, 214-235.

63. Verdu, C. F.; Gatto, J.; Freuze, I.; Richomme, P.; Laurens, F.; Guilet, D. Comparison of Two Methods, UHPLC-UV and UHPLC-MS/MS, for the Quantification of Polyphenols in Cider Apple Juices. Molecules (Basel, Switzerland) 2013, 18, 10213-10227.

**CHAPTER 4**

**Detection of Reactive Dyes from Dyed Fabrics after soil degradation via QuEChERS extraction and Mass Spectrometry**

(The following chapter was published in *Analytical Method* (X. Sui, C. Feng, Y. Chen, N. Sultana, M. Ankeny, and N. R. Vinueza, *Anal. Methods*, 2020, 12, 179) and has been adapted for this dissertation with permission from The Royal Society of Chemistry.

# 4.1 Introduction

As is has been discussed in Chapter 1. The introduction of reactive dye could greatly enhance the colorfastness of cotton fabrics thanks to its unique ability to form covalent bonding with cellulose polymer but because of the yield of this reaction, a certain amount of unreacted dye and hydrolysis product remain on fabric even after washing and scouring. As a result, when is disposed in a compost decomposition process, these molecules have the potential to degrade and leach out into soil.[1-3] Thus, following the plan proposed at the end of Chapter 3, the first part of my Ph.D. research project will be focused on a qualitative study of the degradation of reactive-dyed cotton fabric in soil after a simulated compost process via a combination of high-resolution mass spectrometry and QuEChERS extraction.

Current studies regarding soil degradation have been focused only on evaluating and predicting the efficiency of landfill sites during the decomposition process.[4-9] A recent study of the textile decomposition by Mazibuko *et. al.* shows that different fabrics, like silk, cotton, and denim will degrade at a different rate under controlled conditions using a soil burial test and the ASTM D 5988-03 method.[10] However, there are no studies that focus on the degradation of reactive dyes in cotton fabrics under compost conditions that can give a better idea of what happens to the dye during this process. The majority of degradation studies of reactive dyes are performed in aqueous conditions due to the presence of these dyes in wastewaters. [11-16]

One of the prerequisites for a successful analysis is the extraction and detection of waste substances from its matrixes such as water or soil. QuEChERS (QUick, Easy, Cheap, Effective, Rugged, and Safe) method developed by M. Anastassiades et al in 2003[17, 18] has been successful in the extraction of pesticides residues from fruit and vegetables, as well of pesticides or veterinarian drugs from the soil.[19-24] In the case of dyes, QuEChERS extraction has been performed on triphenylmethane dyes (malachite green (MG), leuco malachite green (LMG), brilliant green (BG), crystal violet (CV), and leuco crystal violet (LCV)) from fish tissue.[25] This showed the effectiveness of QuEChERS method in the extraction of dyes within the same family. However, compared to reactive dyes used in this study (Figure 44), triphenylmethane dyes have a series of differences that include lower polarity, higher hydrophobicity, and abilities to form hydrogen bonding.[25, 26] Thus, despite its wide-spread applications, QuEChERS has not been used on reactive dyes due to the differences in chemical structure between pesticides or veterinarian drugs and reactive dyes. One of the main differences is that reactive dyes have several solubilizing groups (Figure 44) that make these molecules extremely polar and water-soluble. These properties are very important for industrial dyeing processes but not ideal for the extraction with organic solvents.

Here-in a study was performed that focuses on the degradation of reactive dyes on dyed jersey-knit cotton fabrics under the ASTM D5988-03 method, to have a better understanding of how these dyes decompose and what chemical changes on the dye structure can be elucidated from the knitted fabric. In addition, we will determine what derivatives of reactive dyes are leached to the surrounding soil by using QuEChERS and Quadrupole Time-of-Flight mass spectrometry (QTOF-MS). The use of QTOF-MS has proven to ideal in the characterization of reactive dyes having multiple reactive and solubilizing groups. [27, 28]

## 4.2 Experimental

### 4.2.1 Materials

#### 4.2.1.1 Solvents

ACS grade acetonitrile (ACN) and methanol (MeOH) for QuEChERS extraction were purchased from Sigma-Aldrich (Sigma-Aldrich, MO, USA) and used without any further purification. HPLC grade water was acquired from a Pure Lab Ultra water purification system from ELGA Lab Water (ELGA Lab Water, High Wycombe, UK). LC-MS Grade acetonitrile was purchased from VWR Analytical (VWR International, PA, USA).

#### 4.2.1.2 Reactive Dyes

Four commonly commercial reactive dyes, C.I. Reactive Orange 35 (RO35), C.I. Reactive Blue 49 (RB49), C.I. Reactive Black 5 (Rblk 5), and C.I. Reactive Blue 19 (RB19) were provided by Cotton Incorporated and used with further purification. These reactive dyes were selected due to their common utilization in the textile industry. Their structures are shown in Figure 44.

**Reactive Orange 35**

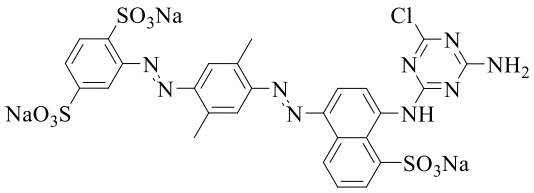

Chemical Formula: $C_{27}H_{19}ClN_9Na_3O_9S_3$
Exact Mass: 812.9849

**Reactive Blue 49**

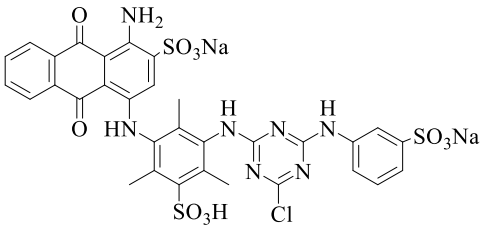

Chemical Formula: $C_{32}H_{24}ClN_7Na_2O_{11}S_3$
Exact Mass: 859.0180

**Reactive Black 5 - SES form**

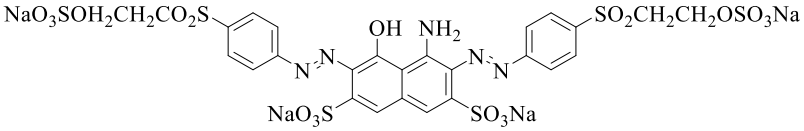

Chemical Formula: $C_{26}H_{21}N_5Na_4O_{19}S_6$
Exact Mass: 990.8746

**Reactive Blue 19 - SES form**

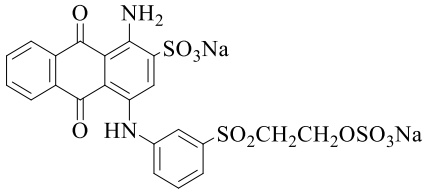

Chemical Formula: $C_{22}H_{16}N_2Na_2O_{11}S_3$
Exact Mass: 625.9712

**Reactive Black 5 - VS form**

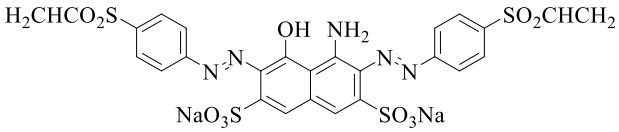

Chemical Formula: $C_{26}H_{19}N_5Na_2O_{11}S_4$
Exact Mass: 750.9759

**Reactive Blue 19 - VS form**

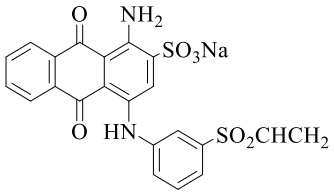

Chemical Formula: $C_{22}H_{15}N_2NaO_7S_2$
Exact Mass: 506.0218

Figure 44: Structure of Reactive dyes: Orange 35, Blue 49, Black 5, and Blue 19

### 4.2.1.3 Soil

The blank soil used for the spike test and simulated compost degradation process was provided by Cotton Incorporated. The same soil was used in the decomposition of reactive dye colored cotton fabrics. The decomposition process was carried out according to ASTM Standard D5988-03. The compost soil was purchased from Lowes and contained a blend of composted manure, wood compost, and sand. The soil was sieved to less than 2 mm particle size and stored at 4°C for 7 days to achieve a homogenous condition before use. Additionally, preliminary tests such as pH, moisture content, as well as the elemental composition was conducted to ensure an

appropriate composition. The degraded soil samples used in this study was also provided by Cotton Incorporated and they were taken from the same container used to decompose cotton fabrics that were dyed with reactive dyes.

#### 4.2.1.4 Chemicals

ACS grade magnesium sulfate ($MgSO_4$) powder and sodium chloride (NaCl) powder were purchased from Sigma-Aldrich (Sigma-Aldrich, MO, USA) and used without further purification.

#### 4.2.1.5 Other Supplies

Disposable Luer-slip plastic syringes (1 mL) were purchased from Sigma-Aldrich. Phenex™-PTFE 4mm 0.2 µm Non-Sterile Syringe Filters were purchased from Phenomenex. 15 x 45 mm, Fisherbrand™ Snap-Cap™ Flat-Top Graduated Microcentrifuge Tubes were purchased from Fisher Scientific. (Fisher Scientific, PA, USA) 2 mL Amber Glass Screw Vials for HPLC with 300 µL Fused Insert & Marking Spot was purchased for Analytical (Analytical Sales and Services Inc., NJ, USA).

### 4.2.2 Methods

### 4.2.2.1 Simulated compost degradation of reactive dye-dyed fabrics

Simulated compost degradation process with reactive dye-dyed fabrics was conducted by Cornell University and Cotton Incorporated. These single knit jersey clothes were made from 100% cotton. They were then bleached and dyed with the selected reactive dye at the Dyeing and Finishing Application Laboratory at Cotton Inc., USA. For each type of reactive dye used in this study, a 2 cm by 2 cm fabrics pieces were mixed with blank soil prepared in section 2.1.3 and stored at the bottom of a desiccator. A beaker with KOH solution was placed on a perforated plate above the soil in the dedicator to control the humidity as well as to absorb carbon dioxide. The laboratory conditions were controlled according to standard ASTM D 5988-03.[29] The room

temperature during degradation was controlled between 20°C and 21.1°C. The degradation time was 45 and 90 days. These time stages were chosen based on the observations in the previous study regarding the biodegradation of cotton.[30] After degradation, the fabrics and soil were collected and placed in different containers before analysis. A photograph of cotton fabrics collected after simulated compost degradation is shown in Figure 45.

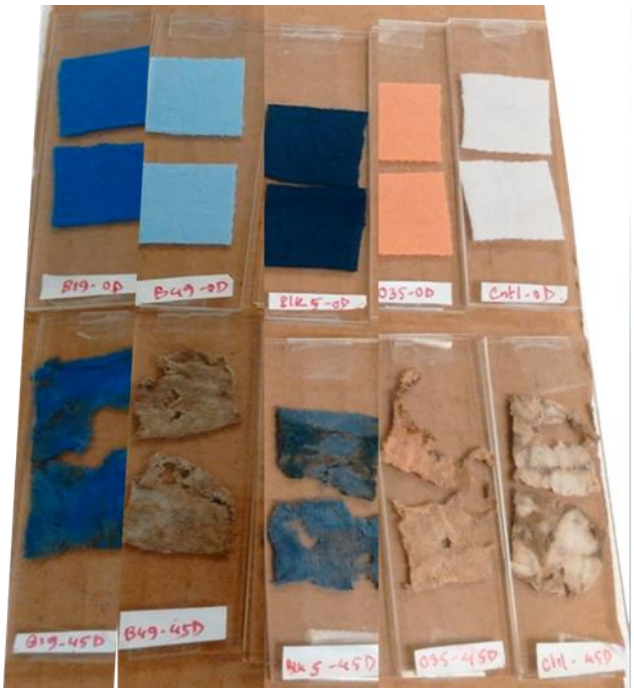


Figure 45: Picture of cotton fabrics after simulated compost degradation

### 4.2.2.2 Preparation of stock solution and spiked solutions

Four 1000 ppm stock solutions of each reactive dye shown in Figure 44 were prepared by dissolving 100 mg of commercial dye powder in a 100-mL volumetric flask with HPLC water. Then the spike solutions for each reactive dye, which will then be spiked into blank soil, were prepared by diluting each stock solution to a final concentration of 50 ppm. This concentration was selected based on the concentration of dye on fabrics. After considering doses of dye, owg (on-weight of goods), as well as the average weight of 2cm by 2cm fabrics (60.0 ± 1.1 mg), a concentration level of 1000 ppm was obtained. Thus, the spiking solution was diluted to 50 ppm

to represent a 5% leaching out from the fabrics. According to existing and industrial practice, the chemical structure of reactive dye is stable at room temperature (25 °C) but hydrolysis of the reactive group (vinyl sulfone or chlorotriazine group) may happen, which can affect the dyeing process since there no reactive site is available for the reaction with cellulose. Thus, to minimize hydrolysis and prevent the loss of active reactive sites, all spike solutions were prepared freshly every day before extraction tests, and stock solutions were stored in a refrigerator at 5 °C. LC-MS experiments were used to detect any hydrolysis product of the stock solutions prior to spiked experiments.

### 4.2.2.3 Extraction of reactive dye from spiking reactive dye solutions

The QuEChERS method was selected for the extraction of reactive dyes on the dye spiked solutions prepared in section 4.2.2.2. For this purpose, a 500 μL of acetonitrile, 80 mg of magnesium sulfate powder, and 20 mg of sodium chloride powder were added to a centrifuge tube loaded previously with 50 μL of the selected reactive dye solution. The centrifuge tube was then stirred by a VWR vortex mixer at 2500 rpm for 15 seconds before being centrifuged by a VWR® Mini Centrifuge at 8500 rpm for 5 minutes. The supernatant liquid was taken and filtered by a syringe filter before analyzed by an Agilent 1260 High-Performance Liquid Chromatography (HPLC) system coupled with Agilent 6520B Quadrupole Time-Of-Flight (QTOF) mass spectrometer.

### 4.2.2.4 Extraction of reactive dye from spiked soils

In order to know the best way to extract potential reactive dye degradation products from soil after a simulated compost degradation process, three different extraction methods were applied onto soils that were spiked with the reactive dye solution. First, extraction by solvent only with acetonitrile. Second, an original QuEChERS method (QuEChERS A) obtained directly from

existing literature and a modified QuEChERS method based on QuEChERS A method with additional sonication steps (QuEChERS B).[17] The spiked soil used in preliminary tests were prepared by adding 50 μL of 50 ppm reactive dye solution into a 2-ml microcentrifuge tube loaded with 100 mg of blank soil. The difference between these methods is shown in Table 1.

Table 1: Composition of different extraction methods used in preliminary tests

| Method | Salt | Solvent | Vortex mixing | Sonication | Centrifuge |
|---|---|---|---|---|---|
| Solvent Only | NI | I | I | NI | I |
| QuEChERS A | I | I | I | NI | I |
| QuEChERS B | I | I | I | I | I |

Note: I = Included, NI = Not included

A diagram showing the procedure of these three extraction methods is shown in Figure 46. In the solvent-only extraction, 500 μL of HPLC grade acetonitrile was added to the microcentrifuge tube loaded with the spiked soil and the tube was stirred by a VWR vortex mixer at 2500 rpm for 15 seconds. Then the tube was centrifuged by a VWR® Mini Centrifuge at 8500 rpm for 5 minutes and filtered by using a syringe filter before being analyzed by HPLC-MS. In QuEChERS A method, the procedure of vortex mixing, centrifuge, and HPLC-MS analysis were the same as solvent extractions except that 500 μL QuEChERS extraction solvent made up of 80% acetonitrile and 20% methanol, 80 mg of magnesium sulfate powder, and 20 mg of sodium chloride powder were added to the centrifuge tube and stirred by the VWR vortex mixer at 2500 rpm for 15 seconds. In QuEChERS B methods, all the procedure is the same as the QuEChERS A method except that two extra sonication steps were added after vortex mixing, where the centrifuge tube was sonicated by a Branson 2210 sonicator for 10 minutes. The mass-to-charge ratio (m/z) obtained from QTOF was used determine the presence of reactive dye or degradation product after extraction, spectral absorbance area at the $\lambda_{max}$ of each reactive dye obtained from Diode Array

Detector (DAD) was used to calculate percentage recovery, and the areas of extracted ion chromatogram (EIC) were used to determine matrix effect (ME).

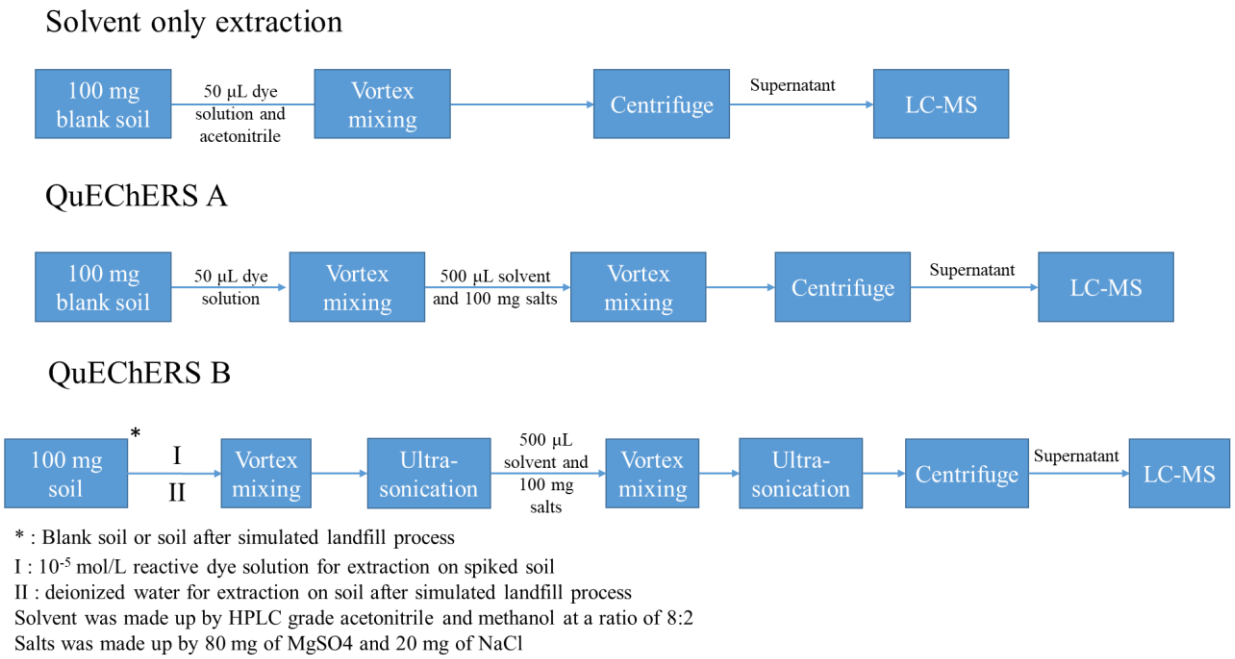


Figure 46: Diagram showing the procedure of different extraction methods on spiked soil

### 4.2.2.5 Cheminformatics calculation via KNIME

To help explaining results from extractions on soil spiked with reactive dye, a series of molecular descriptors were calculated, which include hydrogen bond donor, hydrogen bond acceptor, topological polar surface area, and XLogP. These descriptors were calculated on KNIME.[31] These descriptors were chosen because they were related to certain properties of reactive dyes such as hydrogen bonding ability and hydrophobicity. KNIME, which was also called Konstanz Information Miner, is a free and open-source data analytics and mining platform developed by a team of software engineers at the University of Konstanz in 2004.[31] Compared with other data mining software such as SPSS (Statistical Package for the Social Sciences) and SAS (Statistical Analysis System), KNIME was chosen in the study for its user-friendliness as well as its versatility. The calculations were performed via a workflow shown in Figure 47. SDF

(Spatial Data File) file containing digital structures of four reactive dyes used was first read by SDF reader node and curated by molecule to CDK node, where the digital structures were reformatted to be readable by other nodes. Then in the molecular properties node, selected molecular descriptors were calculated and the results were output as an Excel file.

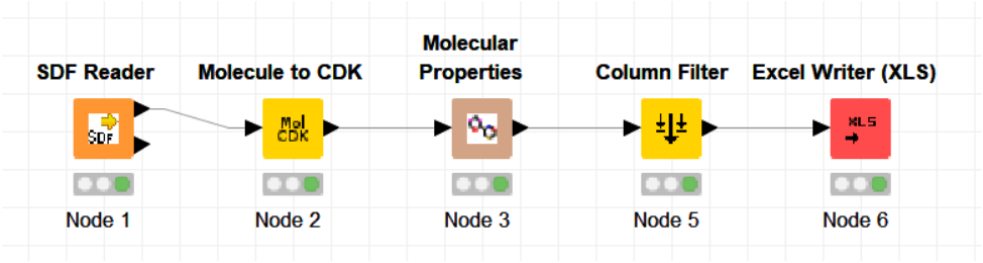


Figure 47: Design of workflow used to calculate molecular descriptors in section 4.2.2.5

### 4.2.2.6 Extraction of reactive dyes from decomposition soil

The procedure for the extraction of soil from simulated compost degradation process is shown in Figure 46. An aliquot of 100 µL of deionized water was added into a 2-ml microcentrifuge tube previously loaded with 100 mg of soil. Then the tube was ultra-sonicated before added with 400 µL of acetonitrile and 80 mg of $MgSO_4$ and 20 mg of NaCl. These substances were added to facilitate the extraction of reactive dye or their derivatives by decreasing the solubility of the reactive dye in water. The extraction of the soil after the degradation process was repeated three times to ensure reproducibility.

### 4.2.2.7 QuEChERS extraction by random sampling

The purpose of this experiment is to test the distribution of leach out of the dye into the soil from the degradation process. This was done by random sampling (**Figure 48**), which divides the soil of interest into two layers: upper and bottom. From each layer of soil, three samples were taken at different locations. For each sample spot, 100 mg of soil was taken and extracted by a QuEChERS B.

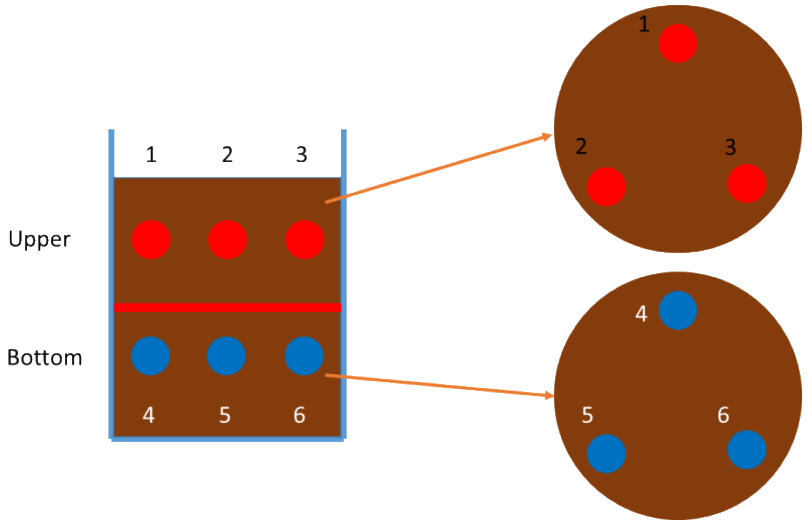


**Figure 48** Diagram of the random sampling used in section 4.2.2.7

### 4.2.3 Instrumentation

The LC-MS analyses of all the solutions obtained from QuEChERS extractions were performed on an Agilent Technologies 1260 High-Performance Liquid Chromatography (HPLC) system coupled with an Agilent 6520 Q-TOF mass spectrometer. (Agilent Technologies, CA, USA) The supernatant solutions from QuEChERS extraction were transferred to 2-mL Agilent amber screw-top glass LC vials (Part number: 5188-6535). To separate the potential leached-out reactive dye from the soil matrix, a gradient elution composed of water and acetonitrile (%B) was chosen. Starting at 98% for 1 minute, the percentage of acetonitrile then went down to 50 % in one minute and hold at 50% for two minutes. After that, the percentage of acetonitrile increased to 58% in one minute and then went back to 98% in two minutes. An Agilent ZORBAX SB-C18 (3.0 x 150mm, 3.5 μm) reverse-phase column was used as the stationary phase for the separation. The flow rate of the HPLC was set to 0.5 mL/min and the total run time for each sample was 10 minutes. Ionization was performed via electrospray ionization and was carried out in negative mode with the following parameters: gas temperature 350 ºC, drying gas 6 liters per minute, nebulizer 35 psi, $V_{cap}$ voltage 4000 V, and fragmentor voltage at 170 V.

## 4.3 Results and Discussions

### 4.3.1 Extraction of reactive dyes from solution

A simple test of extracting reactive dyes by using acetonitrile was performed, due that is the solvent used on QuEChERS. Extraction results with this organic solvent are summarized in **Table 2**, where it can clearly demonstrate that acetonitrile is not able to extract these dyes due to the nature of ionic compound and high polarity of reactive dye, which suggested that simple solvent extraction with organic solvent may have limited effect on the extraction of leached-out substances from soil. Thus, QuEChERS A extraction was tested on reactive dye solutions, and positive results were obtained ("Control without soil" column in **Table 2**), where all four reactive dyes were detected. These results showed that hydrophilic compounds like reactive dyes could be 'pushed' into an organic phase (acetonitrile) by saturating their environment by adding salts. Based on this outcome QuEChERS A method was selected to test the extraction of blank soil samples spiked with each reactive dye solution.

### 4.3.2 Extraction of reactive dyes from spiked soils

As is shown in Table 2, out of four reactive dyes tested, QuEChERS A extraction method was able to extract RB19 and RO35 from spiked soil. This result suggests that this extraction method still needs improvements. A modified QuEChERS method (B) was introduced, where to sonication steps were added to the extraction process. The extractions results using this modified method B (**Table 2**) clearly showed that all four reactive dyes can be detected after they were extracted from spiked soil. A possible explanation for this successful extraction is that by making smaller particles of soil through sonication, the extraction liquid (water and acetonitrile) will have a bigger surface area to interact with the dye, hence it can be extracted by the organic solvent.

Based on these results QuEChERS B is more efficient than the A method and it will be used for later experiments.

Table 2: Mass-to-charge ratio in selected reactive dyes and extraction results from preliminary tests

| Name | Ions generated | m/z (theo.) | m/z (exp.) | ppm error | Solvent only | Control without soil | QuEChERS A | QuEChERS B |
|---|---|---|---|---|---|---|---|---|
| RB19 | $[M-Na]^{-1}$ | 483.0326 | 483.0328 | -0.38 | ND | D | D | D |
| RO35 | $[M-3Na]^{-3}$ | 248.0058 | 248.0055 | 1.05 | ND | D | D | D |
| RB49 | $[M-2Na]^{-2}$ | 406.5198 | 406.5192 | 1.40 | ND | D | ND | D |
| RBlk5 | $[M-2Na]^{-2}$ | 352.4987 | 352.4980 | 2.11 | ND | D | ND | D |

Note: D = Detected, ND = Not detected, theo. = theoretical mass-to-charge ratio (m/z) based on structures shown in Figure 44, exp. =experimental m/z

Results from the recovery test are shown in **Table 3**. Here percent recovery was evaluated by measuring the absorbance peak area of each reactive dye at its $\lambda_{max}$ before extraction and comparing it against the absorbance area after extraction. It can easily be noticed that each reactive dye showed a different percent recovery as well as different degrees of matrix suppressing effect (ME <1). These results were expected due to the difference in the structures of each dye. Among all of the four dyes tested, RB19 showed the highest percent recovery and least level of matrix suppressing effect, this can be explained by its low molecular weight, low solubility (only one sulfonate group in its structure), low polarity (represented by Topological Polar Surface Area in Table 3), and high hydrophobicity (represented by XLogP in **Table 3**). On the contrary, bigger dyes molecules such as RB49, with three sulfonate groups, the highest number of hydrogen bond donors, the highest polarity among these four dyes, and lowest hydrophobicity showed lower recoveries. This means that RB49 has less affinity towards the organic phase during QuEChERS extraction, which leads to a lower recovery. In addition, the presence of NaCl also contributed to

the matrix suppression effect, which would result in ionization suppression and reduce the signal-to-noise ratio. [32-34]

Table 3: Percent recovery, matrix effect, and cheminformatics calculations on four reactive dyes

| Dye Name | RT: min | $\lambda_{max}$ | Recovery | Matrix Effect | Hydrogen Bond Acceptors | Hydrogen Bond Donors | Topological Polar Surface Area | XLogP |
|---|---|---|---|---|---|---|---|---|
| RB19 | 4.30 | 580 nm | 168.2 ± 3.0% | 0.347 ± 0.032 | 9 | 2 | 166.46 | 3.263 |
| RO35 | 4.39 | 430 nm | 57.9 ± 3.7% | 0.050 ± 0.007 | 18 | 2 | 281.41 | 3.197 |
| RB49 | 4.30 | 625 nm | 40.6 ± 2.1% | 0.015 ± 0.004 | 18 | 5 | 301.17 | 2.718 |
| Rblk 5 | 4.40 | 600 nm | 52.1 ± 0.7% | 0.009 ± 0.002 | 15 | 2 | 284.23 | 2.746 |

Note: Recovery and matrix effects are reported as Mean ± Standard Error. ME = Mean Peak Area (post-process)/Mean Peak Area (analyte). % Recovery = (Mean Peak Area (processed)/Mean Peak Area (unprocessed)) x100.

### 4.3.3 Extraction of reactive dyes from soil under ASTM D5988-03 test

A total of 20 different soil samples were extracted by QuEChERS B and analyzed by HRMS, three different types of substances were found that include the native dye without hydrolysis, the hydrolysis product of the reactive dye, and dye degradation products (**Table 4**).

The native dye and its hydrolysis products of Reactive Blue 49 and Reactive Orange 35 were only detected in all soil samples. The presence of unreactive dye can be explained by the presence of these dyes on the surface of the knitted cotton fabrics, which indicates that the fixation process during dyeing was incomplete, and even with the common after washing processes the unreactive dye remains on the fabrics. Therefore, these dyes can leach to soil and will have a heterogeneous distribution. In the case of hydrolyzed dye RO35, it will be produced during the fixation process where it is a common side reaction product. Hence, these can also remain on the surface of the fabrics and can leach to the soil. For dyes RB19 and RBlk5 that were not detected, it is likely that their concentration in soil were too low to be detected by the QTOF mass spectrometer or they have been washed away.

An interesting result from **Table 4** was the detection of dyes that did not correspond to the fabric type. The ion signal of doubly charged Reactive Blue 49 (m/z 406.5198) and Reactive Orange 35 (m/z 372. 5123) and their response in Diode Array Detector (DAD) at 625 nm and 430 nm respectively were found in the 45-days degradation soil of Reactive Black 5 (mass spectrum shown in **Figure 49**). This can be explained by the fact that different dyed fabrics were mixed together during the ASTM D5988-03 test. This result has a realistic meaning due that the mixing of different types of fabrics is common in the compost process.

In the case of dye degradation products, a series of potential unknown ions were found after extraction with QuEChERS B method. This includes ions with a m/z 393.0552 from Reactive Blue 19 (m/z 483.0326) 45-days degradation, m/z 321.0177 from Reactive Black 5 (m/z 352.4987) 45-days degradation, m/z 258.6757 from Reactive Orange 35 (m/z 248.0058) 45-days degradation, and m/z 247.9920 from Reactive Black 5 (m/z 352.4987) 90-days degradation. A series of corresponding molecular formulas were generated by MassHunter™ qualitative analysis software and structural elucidation of these products is currently underway. The observation of these mass-to-charge signals from soil after simulated compost process suggests that 45- or 90-days degradation could alter the shape of the cotton fabrics (see **Figure 45**) as well as generate reactive dye derivatives. It also proved that the QuEChERS B method can successfully extract and detect potential degradation products from soil.

**Table 4:** Extraction results of soil from degraded knitted cotton fabrics

| Sample | Degradation Time (Days) | Chromogen | Reactive group | Native dye | Hydrolysis product | Potential degradation product | Peak m/z | Formula generated |
|---|---|---|---|---|---|---|---|---|
| White | 45 | NA | NA | ND | ND | NA | NA | NA |
| RB19 | 45 | Anthraquinone | VS | ND | ND | D | 393.0552 | $C_{20}H_{14}N_2O_5S$ |
| RBlk 5 | 45 | Diazo | VS+VS | RB49 and RO35 | RO35 | D | 321.0177 | $C_{29}H_{20}N_6O_8S_2$ |
| RB49 | 45 | Anthraquinone | MCT | RB49 | ND | ND | NA | NA |
| RO35 | 45 | Diazo | MCT | RB49 | ND | D | 258.6757 | $C_{34}H_{29}N_5O_{11}S_3$ |
| White | 90 | NA | NA | ND | ND | NA | NA | NA |
| RB19 | 90 | Anthraquinone | VS | ND | ND | ND | NA | NA |
| RBlk 5 | 90 | Diazo | VS+VS | ND | ND | D | 247.9920 | $C_{19}H_{18}N_2O_8S_3$ |
| RB49 | 90 | Anthraquinone | MCT | ND | ND | ND | NA | NA |
| RO35 | 90 | Diazo | MCT | ND | ND | ND | NA | NA |

Note: VS = Vinyl Sulfone, MFT = Monofluorotriazine, MCT = Monochlorotriazine, ND = Not Detected, NA = Not Applicable

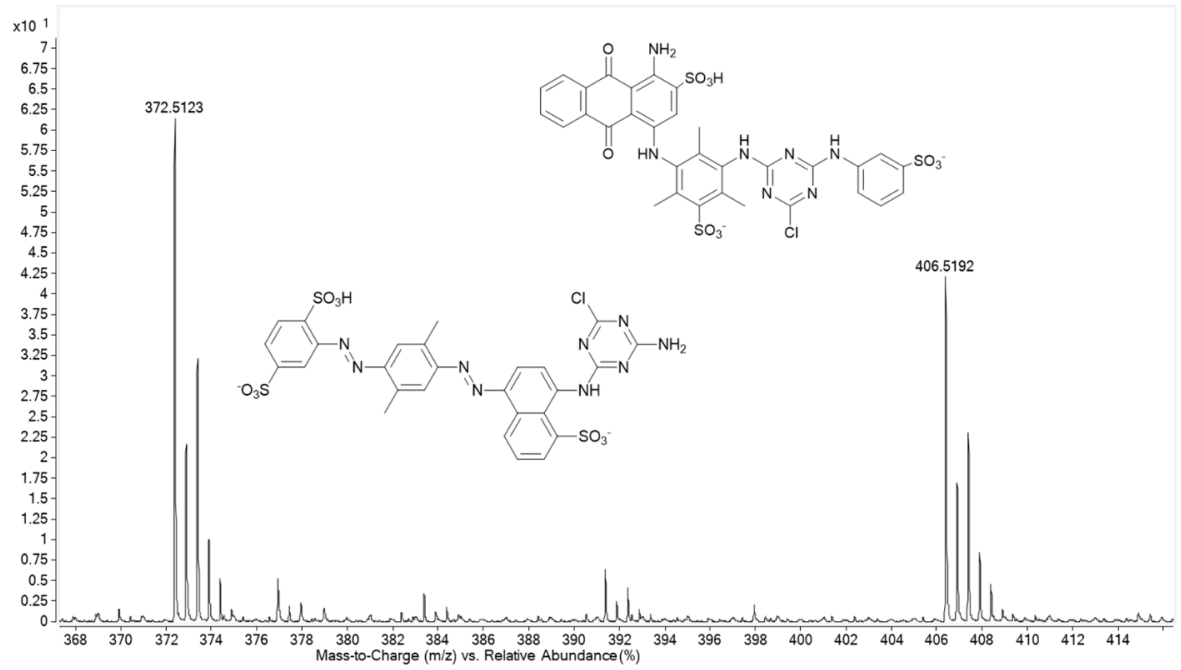


Figure 49: Reactive Blue 49 and Reactive Orange 35 mass spectrum after extraction from 45-day soil degradation process of Reactive Black 5 fabrics

## 4.4 Summary

It could be concluded that QuEChERS B method was efficient in the extraction of all four reactive dyes (Reactive Blue 19, Reactive Orange 35, Reactive Blue 49, and Reactive Black 5) as well as their corresponding hydrolysis products from soil. In addition, QuEChERS B was able to extract and detect 2 native dyes, 1 hydrolysis product, and 4 potential degradation products from the soil obtained from degraded cotton fabrics following ASTM Standard D5988-03. The overall experimental results showed that the combination of calculations (KNIME), high-resolution mass spectrometry with QuEChERS extraction method would greatly facilitate the study of traces of reactive dyes leaching to the soil. Results from this study indicate that despite their excellent colorfastness, reactive dyes on cotton fabrics could leach out and degrade during soil compost process. Based on the results from this project, further study could be conducted in two directions,

one is to try to quantify the amount of degradation product presence in soil. Another direction is to investigate the degradation of textile finishing after simulated composting process, which will be discussed in detail in the next chapter.

## Acknowledgments

The research work in this chapter was financially supported by Cotton Incorporated and Cotton Research and Development Corporation. Grant Number 16-430.

# References


1. Pellew C.E. Dyes and dyeing. Chandigarh: Abhishek Publications; 2007.

2. Clark M. Handbook of Textile and Industrial Dyeing, Volume 1 - Principles, Processes, and Types of Dyes. 2011

3. Environmental Protection Agency. Textiles: Material-Specific Data; Available at https://www.epa.gov/facts-and-figures-about-materials-waste-and-recycling/textiles-material-specific-data#TextilesTableandGraph. Accessed July 17, 2018.

4. Bolyard SC, Reinhart DR. Application of landfill treatment approaches for stabilization of municipal solid waste. Waste Manage (Oxford, U K ) 2016;55:22-30.

5. Frank RR, Davies S, Wagland ST, Villa R, Trois C, Coulon F. Evaluating leachate recirculation with cellulase addition to enhance waste biostabilisation and landfill gas production. Waste Manage (Oxford, U K ) 2016;55:61-70.

6. Grugnaletti M, Pantini S, Verginelli I, Lombardi F. An easy-to-use tool for the evaluation of leachate production at landfill sites. Waste Manage (Oxford, U K ) 2016;55:204-219.

7. Karanjekar RV, Bhatt A, Altouqui S, Jangikhatoonabad N, Durai V, Sattler ML, et al. Estimating methane emissions from landfills based on rainfall, ambient temperature, and waste composition: The CLEEN model. Waste Manage (Oxford, U K ) 2015;46:389-398.

8. Yadav P, Samadder SR. Assessment of applicability index for better management of municipal solid waste: a case study of Dhanbad, India. Environ Technol 2018;39(12):1481-1496.

9. Feltrim F, Izzo, Ronaldo Luis dos Santos, Rose JL, Mokdici R, Teixeira W. Effect of the MSW leachate in the traction strength of the soft plastic. Electron J Geotech Eng 2016;21.3:879-895.

10. Mazibuko M, Ndumo J, Low M, Ming D, Harding K. Investigating the natural degradation of textiles under controllable and uncontrollable environmental conditions. Procedia Manufacturing 2019;35:719-724.
11. Annamalai S, Santhanam M, Sudanthiramoorthy S, Pandian K, Pazos M. Greener technology for organic reactive dye degradation in textile dye-contaminated field soil and in situ formation of "electroactive species" at the anode by electrokinetics. RSC Adv 2016;6(5):3552-3560.
12. Gunasekar V, Ponnusami V. Plasmonic photocatalysis and kinetics of reactive dye degradation in aqueous solution using enzymatically synthesized Ag/ZnO. J Sol-Gel Sci Technol 2015;74(1):84-93.
13. Jamalluddin NA, Abdullah AZ. Reactive dye degradation by combined Fe(III)/TiO2 catalyst and ultrasonic irradiation: Effect of Fe(III) loading and calcination temperature. Ultrason Sonochem 2011;18(2):669-78.
14. Orha C, Lazau C, Dabici A, Bandas C, Olariu S, Manea F. Comparative photocatalytic performances of undoped/N-doped TIO2 under solar irradiation for a reactive yellow 125 azo reactive dye degradation from water. Environ Eng Manage J 2015;14(6):1355-1360.
15. Tomin MB, Kulic A, Kerkez D, Prica M, Rapajic S, Pilipovic DT, et al. Reactive dye degradation using fe-loaded bentonite as a fenton-like catalyst: from process optimization to effluent acute toxicity. Fresenius Environ Bull 2017;26(12):8184-8198.
16. Vu TA, Le GH, Dao CD, Dang LQ, Nguyen KT, Dang PT, et al. Isomorphous substitution of Cr by Fe in MIL-101 framework and its application as a novel heterogeneous photo-Fenton catalyst for reactive dye degradation. RSC Adv 2014;4(78):41185-41194.

17. Vera J, Correia-S L, Paga P, Bragana I, Fernandes VC, Domingues VF, et al. QuEChERS and soil analysis. An Overview. Sample Preparation 2013;1:54-77.

18. Bruzzoniti MC, Checchini L, De Carlo RM, Orlandini S, Rivoira L, Del Bubba M. QuEChERS sample preparation for the determination of pesticides and other organic residues in environmental matrices: a critical review. Analytical and Bioanalytical Chemistry 2014;406(17):4089-4116.

19. Abdel-Ghany M, Hussein LA, El Azab NF. Multiresidue analysis of five neonicotinoid insecticides and their primary metabolite in cucumbers and soil using high-performance liquid chromatography with diode-array detection. J AOAC Int 2017;100(1):176-188.

20. Han P, Shuai M, Feng X, Geng Q, Zhang W, Cao Y. Dissipation and residue determination of penflufen in soil by UPLC-MS-MS. Fresenius Environ Bull 2017;26(2):1520-1527.

21. Jia W, Chu X, Ling Y, Huang J, Lin Y, Chang J. Simultaneous determination of dyes in wines by HPLC coupled to quadrupole orbitrap mass spectrometry. Journal of Separation Science 2014;37(7):782-791.

22. Lee Y, Choi J, Abd El-Aty AM, Chung HS, Lee HS, Kim S, et al. Development of a single-run analytical method for the detection of ten multiclass emerging contaminants in agricultural soil using an acetate-buffered QuEChERS method coupled with LC-MS/MS. Journal of Separation Science 2017;40(2):415-423.

23. Meng M, He Z, Xu Y, Wang L, Peng Y, Liu X. Simultaneous extraction and determination of antibiotics in soils using a method based on quick, easy, cheap, effective, rugged, and safe extraction and liquid chromatography with tandem mass spectrometry. J Sep Sci 2017;40(16):3214-3220.

24. Wu X, Yu Y, Xu J, Dong F, Liu X, Du P, et al. Residue analysis and persistence evaluation of fipronil and its metabolites in cotton using high-performance liquid chromatography-tandem mass spectrometry. PLoS One 2017;12(3):e0173690/-e0173690/12.

25. Giaccone V, Cammilleri G, Macaluso A, Cicero N, Pulvirenti A, Vella A, et al. A LC-HRMS After QuEChERS Cleanup Method for the Rapid Determination of Dye Residues in Fish Products. Food Anal Methods 2018 Mar;11(3):625-634.

26. Zhu C, Wei J, Dong X, Guo Z, Liu M, Liang X. Fast analysis of malachite green, leucomalachite green, crystal violet and leucocrystal violet in fish tissue based on a modified QuEChERS procedure. Chinese Journal of Chromatography 2014;32(4):419.

27. Sultana N, Liu Y, Szymczyk M, Freeman HS, Vinueza NR. Dimerised heterobifunctional reactive dyes. Part 1: characterization using quadrupole time-of-flight mass spectrometry. Coloration Technology 2018 Dec;134(6):470-477.

28. Sultana N, Williams K, Ankeny M, Vinueza NR. Degradation studies of CI Reactive Blue 19 on biodegraded cellulosic fabrics via liquid chromatography-photodiode array detection coupled to high-resolution mass spectrometry. Coloration Technology 2019; 135: 475– 483. https://doi.org/10.1111/cote.12440

29. Standard A. D5988-03 (2003) Standard test method for determining aerobic biodegradation in soil of plastic materials or residual plastic materials after composting. ASTM International, West Conshohocken, PA, USA Edition.

30. Li L, Frey M, Browning KJ. Biodegradability Study on Cotton and Polyester Fabrics. Journal of Engineered Fabrics & Fibers (JEFF) 2010;5(4).

31. Preisach C, Burkhardt H, Schmidt-Thieme L, Decker R, editors. KNIME: The Konstanz Information Miner. Data Analysis; Machine Learning and Applications; Berlin, Heidelberg: Springer Berlin Heidelberg; 2008.

32. Constantopoulos TL, Jackson GS, Enke CG. Effects of salt concentration on analyte response using electrospray ionization mass spectrometry. J Am Soc Mass Spectrom 1999;10(7):625-634.

33. Metwally H, McAllister RG, Konermann L. Exploring the Mechanism of Salt-Induced Signal Suppression in Protein Electrospray Mass Spectrometry Using Experiments and Molecular Dynamics Simulations. Anal Chem 2015;87(4):2434-2442.

34. Kebarle P, Verkerk UH. Electrospray: From ions in solution to ions in the gas phase, what we know now. Mass Spectrometry Reviews 2009 Nov;28(6):898-917.

**CHAPTER 5**

**Quantification of docusate antimicrobial finishing after simulated compost degradation via Tandem Mass Spectrometry and QuEChERS extraction**

# 5.1 Introduction

As is mentioned in Chapter 1, to enhance the properties of textile products, different types of textile finishing could be applied to cotton fabrics. An example is anti-microbial finishing, which is used to protect cotton material from the growth of microorganisms[1-4]. Antimicrobial agents such as silver docusate use silver ion ($Ag^+$) to denature the thiol group in the protein by bonding to it and suppressing the growth of the microorganisms colony.[5,6] Despite its effectiveness against microorganisms, the extensive application of silver docusate anti-microbial finishing could bring problems as these antimicrobial agents may leach out during soil decomposition (in fact, 11,150 US tons of textile wastes were landfilled in 2017).[7] According to existing literature, docusate contamination in environmental matrices such as soil and water could be linked to human health issues including *Burkholderia cepacia* complex infections and there is no existing method featuring the quantification of docusate in soil.[1-6] Thus, the degradation of docusate antimicrobial finishing needs to be investigated.

Generally, a good quantification method requires a combination of an effective analyte extraction method and a sensitive analytical technique.[8] In recent years, the combination of QuEChERS and tandem mass spectrometry quantification has proven to an effective tool to quantify analytes in soil and multiple studies have been found featuring QuEChERS extraction of soil contaminants including mineral dye, pesticide, and veterinarian medicine followed by tandem mass spectrometry quantification reinforced by isotopically-labeled internal standards.[9-14] Despite these extensive previous applications, a quantification system for docusate has not been reported.

Thus, in this study, a quantification method based on QuEChERS extraction and tandem mass spectrometry was established to measure the concentration of docusate antimicrobial agents in soil after simulated compost degradation of cotton fabrics. After the establishment of the calibration system, this quantification method was then validated according to a guideline from the U.S. Food and Drug Administration. A series of variables for were validated including coefficient of determination ($R^2$ = 0.989±0.002), percent error (% error = 3±4%), coefficient of variation (% CV = 6±1%), limit of detection (LOD = 8±2 ng/mL), lowest limit of quantification (LLOQ = 27±5 ng/mL) and matrix effect (matrix effect = 0.944±0.026). Those parameters were obtained from the inter- and intra-day measurements for both calibration and the quality control sample. Posterior to this, actual samples extracted from a simulated compost degradation of cotton fabrics applied with sliver docusate antimicrobial finishing were measured, and it was observed that the concentration measured (51±5 ng/mL) fell into the ranges defined from the method development with good precision (% CV = 4±1%). This quantification method could potentially benefit both textile and environment fields as it could deepen the understanding of degradation of textile finishing in soil and benefit future studies related to docusate contamination in soil.

## 5.2 Experimental

### 5.2.1 Materials

#### 5.2.1.1 Solvents

ACS grade acetonitrile (ACN) and methanol (MeOH) used for QuEChERS extraction were purchased from Sigma-Aldrich (Sigma-Aldrich, MO, USA) and used without any further purification. ACS grade ethyl acetate used during solvent extraction on cotton fabrics was purchased from Sigma-Aldrich (Sigma-Aldrich, MO, USA) and used without any further

purification. HPLC grade water was acquired from a Pure Lab Ultra water purification system from ELGA Lab Water (ELGA Lab Water, High Wycombe, UK). LC-MS Grade acetonitrile was purchased from Thermo Fisher Scientific. (Fisher Scientific, PA, USA).

### 5.2.1.2 Chemicals

Isotopically labeled sodium docusate (Sodium bis(2-ethylhexyl-d17) sulfosuccinate, docusate-$d_{34}$, purity ⩾98.0%) and unlabeled sodium docusate (purity ⩾99.0%) used to prepare stock solutions and establish calibration curves were purchased from Sigma-Aldrich (Sigma-Aldrich, MO, USA) and used without further purification. The chemical structures of these two compounds are shown in Figure 50. ACS grade magnesium sulfate ($MgSO_4$) powder was purchased from Sigma-Aldrich (Sigma-Aldrich, MO, USA) and used without further purification.

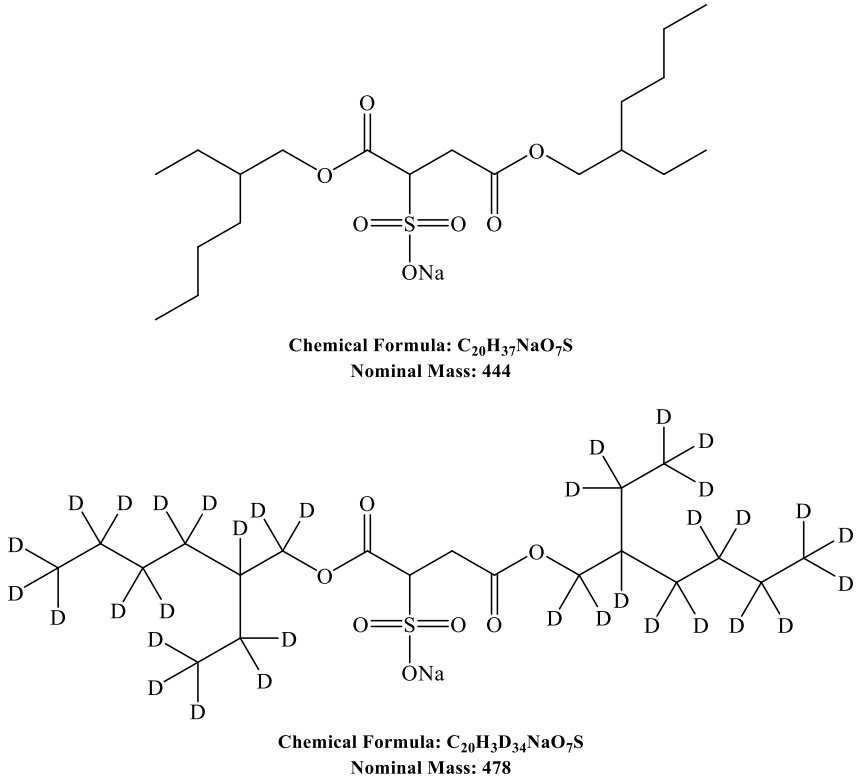


Figure 50: Structures of sodium docusate and docusate-$d_{34}$

### 5.2.1.3 Other Supplies

Disposable Luer-slip plastic syringes (1 mL) were purchased from Sigma-Aldrich. (Sigma-Aldrich, MO, USA) PTFE 0.2 µm Non-Sterile Syringe Filters were purchased from Fisher Scientific (Fisher Scientific, PA, USA). Snap-Cap™ Flat-Top Graduated Microcentrifuge Tubes were purchased from Fisher Scientific. (Fisher Scientific, PA, USA) 2 mL Amber Glass Screw Vials for HPLC were purchased from Fisher Scientific. (Fisher Scientific, PA, USA).

## 5.2.2 Methods

### 5.2.2.1 Simulated compost degradation

The simulated compost degradation process on cotton fabrics was conducted by Cotton Incorporated, USA. These single knit jersey clothes were made from 100% cotton. They were then bleached and applied with silver docusate antimicrobial finishing (Polygiene® AT300) at the Dyeing and Finishing Application Laboratory at Cotton Incorporated. The fabrics were cut into 2 inches by 2 inches fabric pieces and mixed with blank soil and stored at the bottom of a desiccator. The compost soil was purchased from Lowes and contained a blend of composted manure, wood compost, and sand. The soil was sieved to less than 2 mm particle size and stored at 4°C for 7 days to achieve a homogenous condition before use. Additionally, preliminary tests such as pH, moisture content, as well as the elemental composition was conducted to ensure an appropriate composition. During degradation, a beaker with KOH solution was placed on a perforated plate above the soil in the dedicator to control the humidity as well as to absorb carbon dioxide. The laboratory conditions were controlled according to standard ASTM D 5988-03.[15] The room temperature during degradation was controlled between 20°C and 21.1°C. The degradation time was 150 days.[16] After degradation, the fabrics, and the surrounding soil, along with a batch of

blank soil were collected and stored at 5 °C before being transferred to North Carolina State University for analysis.

### 5.2.2.2 Preparation of stock solutions

A 100 ppm (μg/mL) calibration stock solution of sodium docusate was prepared by dissolving 5 mg of sodium docusate powder into a 50 mL volumetric flask using HPLC grade water. A second stock solution of lower concentration (1 ppm) was prepared by diluting the 100 ppm (μg/mL) stock solution with a 10-mL volumetric flask and HPLC grade water. Then a series of spiking solutions were prepared at 8 concentrations including 10, 20, 50, 100, 150, 200, 15, and 180 ppb (ng/mL). Among them, the first six are calibration standards and the other two are quality control (QC) standards.

For the internal standard (IS) solution, one 1000 ppm docusate-$d_{34}$ solution was prepared with HPLC grade water and diluted in a 10-mL volumetric flask to a concentration of 10 ppm. Then this 10-ppm solution was diluted to a 0.1 ppm spiking solution in a 10-mL volumetric flask. All resulting solutions were stored in a refrigerator at 5 °C before use.

### 5.2.2.3 QuEChERS extraction on soil after simulated compost degradation

A diagram showing the workflow of QuEChERS extraction on the soil after simulated compost degradation was shown in Figure 51 A.[17] 200 mg of soil sample after degradation was loaded into a microcentrifuge tube and added with 100 μL of HPLC grade water and 100 μL of IS solution. Then the system was sonicated for 15 minutes by Branson 2210 sonicator. After that, 800 μL of QuEChERS extraction solvent made up of 90% acetonitrile and 10% methanol, along with 160 mg of $MgSO_4$ powder, were added into the tube. The system was then stirred well by a VWR vortex mixer at 2500 rpm for 20 seconds before being sonicated again for 15 minutes. After

sonication, the system was centrifuged by a VWR® Mini Centrifuge at 8500 rpm for 5 minutes and filtered by using a syringe filter before being MS/MS measurement.

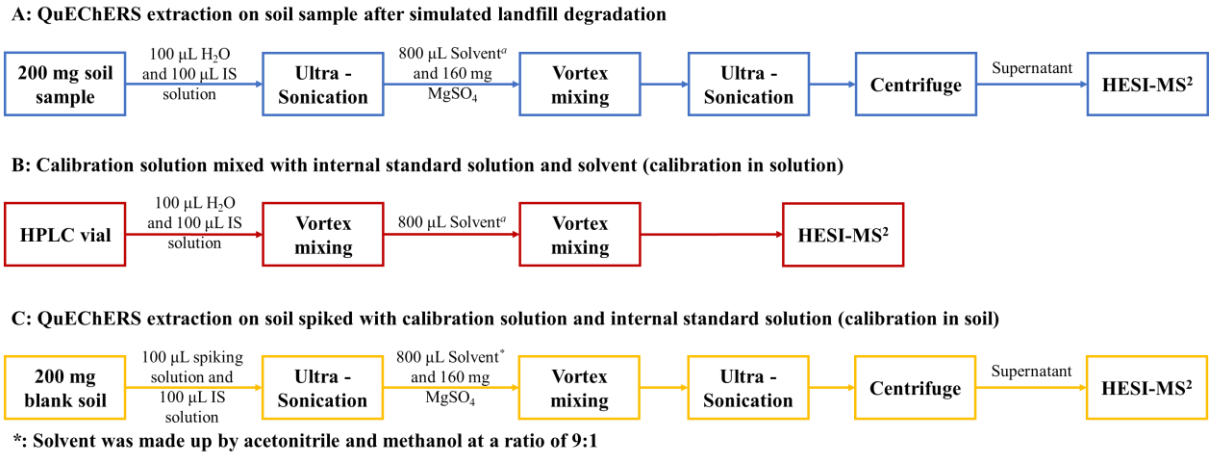


Figure 51: Diagram showing the workflow of QuEChERS extraction on the soil after simulated compost degradation, the establishment of the calibration curve in soil, and establishment of the calibration curve in solution

### 5.2.2.4 Establishment of calibration curves

To minimize the variation brought by the difference in a matrix, a calibration system was created in blank soil using the same extraction method as the one used in Section **2.2.3**. The procedure was shown in Figure 51 C. Every step was the same except HPLC grade water was replaced with docusate spiking solution at 8 concentration levels including 6 calibration samples and 2 QC samples. After extraction and sample preparation, both calibration and QC samples were stored in a refrigerator at 5 °C before analyses. The quantification trials were performed on a Velos Pro Linear Ion Trap Mass Spectrometer (LTQ-MS) from Thermo Fisher Scientific (Fisher Scientific, PA, USA), where all calibration samples and QC samples were measured by MS/MS to create a calibration curve. To facilitate method validation, the preparation of calibration solutions and quantification were repeated multiple times on the same day (**intra-day repeats**) and different days (**inter-day repeats**). Also, to evaluate the matrix effect, a reference calibration

curve was created in solution (Figure 51 B) where spiking solution and IS solution were mixed with QuEChERS extraction solvent to generate a non-matrix scenario.

### 5.2.2.5 Method validation on docusate quantification system

Following the establishment of the calibration system, this quantification method was validated according to the guidance published by the FDA in May 2018.[18] Consequently, a series of parameters were chosen for validation of this work: linearity, sensitivity, matrix effect, accuracy, and precision.

Linearity is represented by the coefficient of determination ($R^2$) obtained from intra-day and inter-day repeats. Sensitivity is evaluated by the limit of detection (LOD) and the lowest limit of quantification (LLOQ). The matrix effect is obtained by comparing the change of slope (***m*** in **y = mx+b**) between the calibration curve in solution versus the calibration curve in soil. Accuracy is evaluated by the mean percent error of calibration standard and QC standard against their nominal concentration from intra-day and inter-day repeats. Finally, precision is evaluated by the mean coefficient of variance (% CV) from the performed replications.

### 5.2.2.6 Solvent extraction on cotton fabrics with antimicrobial finishing

To evaluate the origin of docusate antimicrobial finishing in soil, a solvent extraction procedure was performed on cotton fabrics obtain before and after the simulated compost process. 50 mg of fabric sample was cut into smaller pieces and placed in a Fisher 5-ml vial before added with 2.5 mL of ACS grade ethyl acetate. Then the vials were sonicated on a Branson 2210 sonicator for 10 minutes. Then ethyl acetate solvent was evaporated on a Buchi RE121 rotavapor coupled with Buchi 461 water bath and Brinkmann B-169 Vacuum Aspirator. The fabrics then were removed from the vials and 1 ml of HPLC graded menthol was added to dissolve the residue. The

sample was then filtered by a Phenex-PTFE 4mm syringe filter and transferred into a 2 ml HPLC vial for QTOF-MS analysis.

### 5.2.3 Instrumentation

#### 5.2.3.1 QTOF

Qualitative detection of docusate antimicrobial finishing on samples obtained from sections **5.2.2.3** and **5.2.2.6** was performed on an Agilent Technologies 1260 High-Performance Liquid Chromatography (HPLC) system coupled with an Agilent 6520 Q-TOF mass spectrometer. (Agilent Technologies, CA, USA) The mobile phase was made up of acetonitrile and water in gradient elution and an Agilent ZORBAX SB-Aq C18 (3.5 μm, 3.0 x 150mm) reverse-phase column was used as the stationary phase. The flow rate of the HPLC was set to 0.5 mL/min and the total run time for each sample was 10 minutes. Ionization was performed via dual electrospray ionization (ESI) source from Agilent Technologies and was carried out in negative mode with the following parameters: gas temperature 350 ºC, drying gas 5 liters per minute, nebulizer 50 psi, capillary voltage 3500 V, fragmentor voltage 175 V, skimmer voltage: 65 V, and octupole voltage: 750 V. To improve the mass measurement accuracy, a solution of mass reference mix, obtained from Agilent Technologies, was introduced via a secondary ESI needle.

#### 5.2.3.2 Ion trap

Measurements of MS/MS abundance ratios in the calibration system and samples from QuEChERS extraction were carried out on an LTQ Velos Pro linear ion trap mass spectrometer coupled with Ultimate 3000 UHPLC system from Thermo Scientific (Fisher Scientific, PA, USA). Samples were introduced via an autosampler, with an injection volume of 30 μL. The mobile phase was made up of 98% LC-MS grade acetonitrile and 2% LC-MS grade water. The system was configured to bypass the column. The total run time for each sample was three minutes. Ionization

was performed in negative mode via a commercial heated electrospray (HESI) source (Fisher Scientific, PA, USA). The following source parameters are used including source heater temperature: 40 °C, sheath gas (nitrogen gas): 20 arb. (arbitrary units), auxiliary gas (nitrogen gas): 6 arb., sweep gas: 0 arb., electrospray voltage 3.5 kV, capillary temperature: 260 °C, and S-lens RF level of 68.2%. For quantification, the best MS/MS conditions were reached by optimizing the collision energy to obtain the highest signal, and the following MS/MS transitions were selected: m/z 421 to 81 for docusate and m/z 455 to 81 for docusate-$d_{34}$. For Higher-energy Collision Dissociation (HCD), normalized collision energy of 90% as described by the manufacturer was used. Data were collected by Tune Plus software (Thermo Scientific) and data processing was performed by using Xcalibur software (version 4.0.27.19).

## 5.3 Results and Discussions

### 5.3.1 Qualitative detection of docusate antimicrobial finishing

MS spectra on samples obtained from QuEChERS extraction on soil after simulated compost degradation and solvent extraction on cotton fabrics applied with docusate antimicrobial finishing before and after degradation were shown in Figure 52. As is shown in these spectra, docusate anion (m/z = 421.2265) could be detected after extraction on cotton fabrics and in soil with good mass measurement accuracy and correct isotopic distribution. Thus, it would be reasonable to claim that docusate anion detected in soil could be related to the antimicrobial finishing applied to cotton fabrics and it would be worthwhile to develop a quantification method to measure the concentration of docusate antimicrobial finishing in soil after simulated compost degradation.

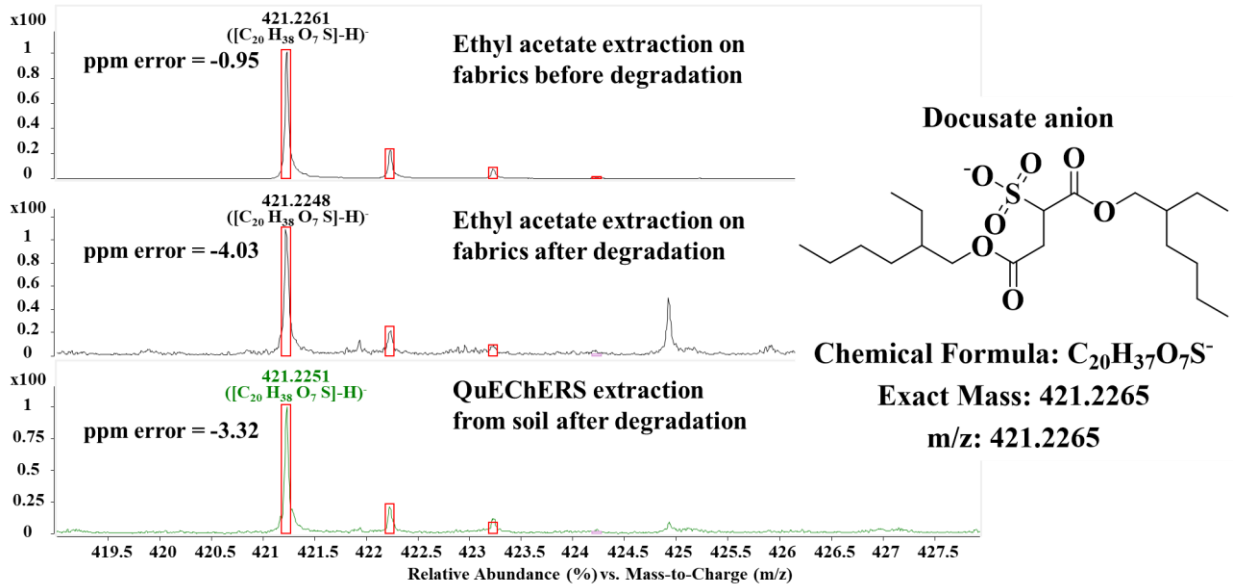


**Figure 52:** MS spectra showing the qualitative detection of docusate anion from cotton fabrics and in soil

## 5.3.2 Establishment of the calibration system

Table 5 summarizes the linear calibration data obtained from MS/MS quantification. Fifteen linear regression models were generated, and the mean coefficient of determination ($R^2$) was 0.989 ± 0.002. This value suggests that, under these experimental conditions, the change of docusate concentration in solution after QuEChERS extraction is highly proportional to the product ion abundance ratio between docusate and docusate-$d_{34}$. This expected linearity between analyte concentration and product ion abundance ratio could be explained by the reduction of ionization suppression and the introduction of an isotopically labeled internal standard. In an ideal scenario, there are infinite amounts of charges available at the ionization source and all molecules in the sample could be fully ionized. In that case, the peak height (absolute abundance) in a tandem mass spectrum is determined solely by the concentration of this molecule in solution. In the real-world scenario, however, because of the limitation of the ionization source, and the presence of a matrix such as soil, the amount of charge available is not unlimited. As a result, some molecules could be ionized better than other molecules, creating a higher peak height than others while the abundance

of other molecules gets reduced, which creates additional variation for quantification. With the introduction of internal standard, this variation could be overcome as despite the alteration of abundance brought by the fluctuation of instrument condition or insufficient ionization, the product ion abundance ratio between the analyte and internal standard would stay the same under the same ionization and tandem mass spectrometry conditions (e.g. isolation width, collision energy, and collision gas).

Table 5: Linear regression data obtained from HESI-LTQ-MS/MS calibration curves for docusate quantification

| | **m** | **b** | **$R^2$** |
|---|---|---|---|
| | 0.00125 | 0.0352 | 0.993 |
| **Day 1** | 0.00123 | 0.0416 | 0.978 |
| | 0.00122 | 0.0401 | 0.992 |
| | 0.00152 | 0.0441 | 0.979 |
| **Day 2** | 0.00143 | 0.0526 | 0.983 |
| | 0.00142 | 0.0553 | 0.997 |
| | 0.00106 | 0.0567 | 0.987 |
| **Day 3** | 0.00120 | 0.0433 | 0.995 |
| | 0.00113 | 0.0471 | 0.988 |
| | 0.00125 | 0.0521 | 0.992 |
| **Day 4** | 0.00140 | 0.0485 | 0.992 |
| | 0.00133 | 0.0469 | 0.973 |
| | 0.00151 | 0.0538 | 0.995 |
| **Day 5** | 0.00148 | 0.0524 | 0.999 |
| | 0.00139 | 0.0577 | 0.996 |
| **Mean** | 0.00132 | 0.0485 | 0.989 |
| **Std Error** | 0.00004 | 0.0017 | 0.002 |

Linear regression in form y = mx+b, values are displayed to three significant figures when available

### 5.3.3 Method validation

A series of validation parameters obtained from intra-day and inter-day repeats are shown in Table 6. The first parameter which needs to be evaluated during method validation is sensitivity, which is represented by the limit of detection (LOD) and the lowest limit of quantification (LLOQ). Among them, LOD is estimated by LOD=3σ/m, where σ is the standard deviation of the y-intercept of the linear regressions and m is the average slope of the linear regressions, and LLOQ is estimated by LOD=10σ/m.[19] Based on these equations, the LLOQ of this quantification method was determined to be 27±5 ng/mL and LOD was determined to be 8±2 ng/mL, which are noticeably lower than the mean docusate concentration obtained from the QuEChERS extraction on soil after simulated compost degradation (51±5 ng/mL). Another parameter that needs to be evaluated is the matrix effect, which generally describes the variation (enhancement or suppression) of analyte response because of matrix presence. In the case of docusate quantification in soil, the matrix effect is determined to be 0.944±0.026, which is expected as the introduction of the isotopically labeled internal standard could help to counter the variation of MS/MS abundance ratio cause by matrix presence. A figure demonstrating the difference between the calibration model established in soil and solution was shown in Figure 53.

Table 6: Validation parameters obtained from HESI-MS/MS calibration curves for docusate quantification

| | Intra-day repeats | Inter-day repeats |
|---|---|---|
| Linearity ($R^2$) | 0.997±0.001 | 0.989±0.002 |
| Matrix effect | 0.944±0.026 | |
| Sensitivity | | |
| *LLOQ* | 27±5 ng/mL | |
| *LOD* | 8±2 ng/mL | |
| accuracy (mean % error) | | |
| *quantitation standards* | 1±4 | 3±4 |
| quality control standards | | |
| *15 ng/mL* | -1±11 | -9±6 |
| *180 ng/mL* | -10±2 | -13±3 |
| *precision (mean CV%)* | 5±1 | 6±1 |

Accuracy and precision data are reported as the average across all quantitation standards

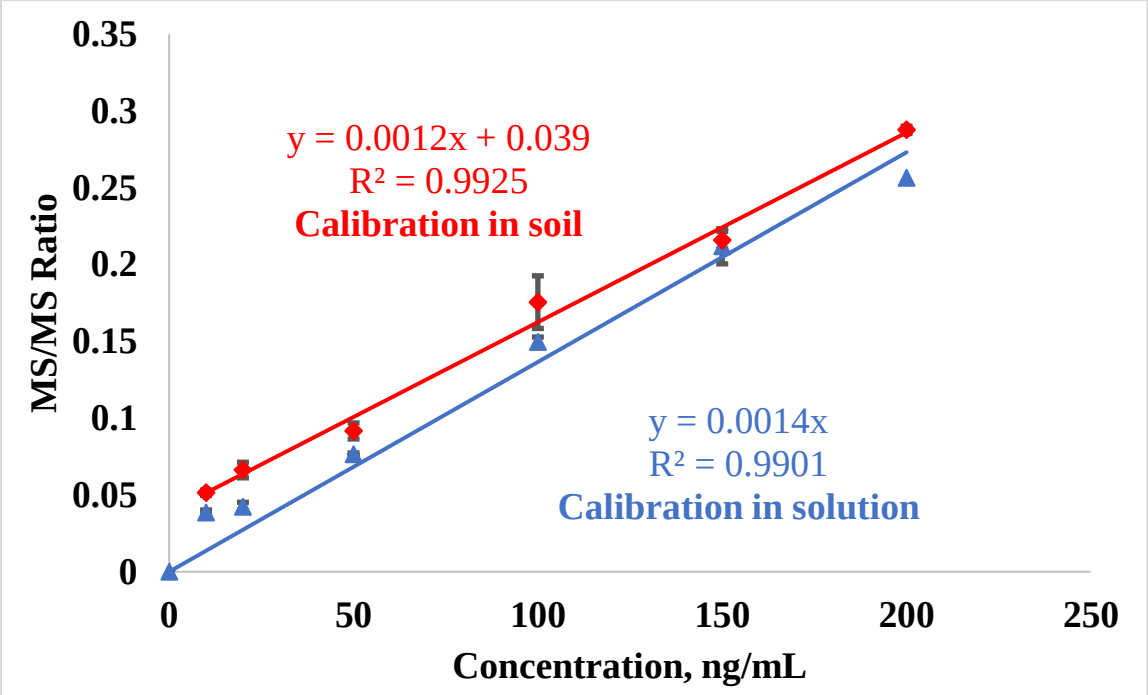


Figure 53: Docusate calibration model established from soil after the QuEChERS extraction versus calibration model established from solution

In addition to sensitivity and matrix effect, precision and accuracy of this method were also evaluated, and results were summarized in Table 7. Coefficient of Variation in percentage (% CV), alternatively called the Relative Standard Deviation in percentage (% RSD), was calculated based on the ratio between standard deviation and mean. According to the FDA guidance, % CV from intra-day and inter-day repeats should be within ± 15%, except for concentrations around the lowest limit of quantification (LLOQ), where the threshold can be widened to ± 20%. Here, it is noticeable that the %CV from all calibration levels, including QC standards, were below ± 15%, which suggests that this quantification method has sufficient accuracy, according to FDA guidelines. In terms of accuracy, all quantification standards showed a %error lower than the FDA threshold in which %error should be within ± 15%, except for concentrations around the LLOQ where the threshold can be widened to ± 20%. Across all concentration level tested, accuracy at 10, 20, 50 ng/mL level are relatively higher compared with other levels but still lower than the 15% threshold from FDA, which could be explained by the fact that measurements at lower concentrations are more susceptible to instrumental fluctuation and random error from QuEChERS extraction.

Table 7: Accuracy and precision of docusate quantification standards for the developed method with intra and inter-day repeats

| Concentration (ng/mL) | Intra-day repeats | | Inter-day repeats | |
|---|---|---|---|---|
| | Accuracy (% error) | Precision (% CV) | Accuracy (% error) | Precision (% CV) |
| **10** | 0.737 (10.1 ng/mL) | 3.46 | 16.1 (11.6 ng/mL) | 11.81 |
| **20** | 10.3 (22.1 ng/mL) | 7.71 | 12.3 (22.5 ng/mL) | 6.77 |
| **50** | -14.8 (42.6 ng/mL) | 5.68 | -11.3 (44.3 ng/mL) | 5.51 |
| **100** | 10.6 (111 ng/mL) | 9.77 | -0.0552 (99.9 ng/mL) | 7.03 |
| **150** | -4.49 (143 ng/mL) | 2.63 | 0.689 (151 ng/mL) | 4.73 |
| **200** | 0.692 (201 ng/mL) | 0.84 | -0.155 (200 ng/mL) | 2.15 |
| **15*** | -0.681 (14.9 ng/mL) | 5.09 | -8.65 (13.7 ng/mL) | 3.32 |
| **180*** | -9.63 (163 ng/mL) | 2.01 | -12.8 (157 ng/mL) | 3.84 |

Values reported to three significant figures, CV=coefficient of variation, *Quality Control standard

## 5.4 Summary

Although frequently used in textile industry, the degradation of docusate antimicrobial finishing in soil has not been studied before. Thus to solve this problem, a novel analytical measurement method based on tandem mass spectrometry and QuEChERS extraction was successfully developed to quantify the concentration of docusate antimicrobial agents in soil and this method was validated according to the quantification guideline published by the FDA. A modified QuEChERS extraction method removed analytes from soil matrix and reduced the complexity of the matrix. Then the combination of tandem mass spectrometry quantification and deuterated internal standard ensures the linearity of calibration curves. After that, method validation was performed where accuracy along with the precision of this method were evaluated

based on intra-day and inter-day repeats of calibration curves, and matrix effect was obtained by comparing the linearity from soil calibration against linearity from solution calibration. Besides, by performing intra-day and inter-day repeats, this docusate quantification method based on tandem mass spectrometry and the internal standard has shown good linearity ($R^2 > 0.99$), good accuracy (mean % error less than 15%), good precision (mean % CV less than 15%), good sensitivity (measured docusate concentration is 400% higher than LOD and 100% higher than LLOQ), and satisfying matrix effect. According to existing literature, docusate-related contamination in soil has been reported by multiple studies but and no literature has been found studying the degradation of docusate antimicrobial finishing in soil.[20,21] Thus, this quantification method would greatly benefit both the textile and environmental field as the combination of QuEChERS extraction and MS/MS quantification provides an accurate and precise measurement of docusate quantification in soil.

## Acknowledgments

This work in this chapter was financially supported by Cotton Incorporated and Cotton Research and Development Corporation. Grant Number 20-718.

## Reference

1. Almeida, L. *Functional finishes for textiles: improving comfort, performance, and protection;* Cambridge, England, Woodhead Publishing, 2015.
2. Mather, R. R.; Wardman, R. H. *The chemistry of textile fibers;* Cambridge: Royal Society of Chemistry, 2015.
3. Olson, E. S. *Textile wet processes;* Noyes Publications: Park Ridge, N.J., U.S.A., 1983.

4. Choudhury, A. K. R. *Principles of Textile Finishing electronic resource;* Woodhead Publishing: S.l., 2017.

5. Tomšič, B.; Klemenčič, D.; Simončič, B.; Orel, B. Influence of antimicrobial finishes on the biodeterioration of cotton and cotton/polyester fabrics: Leaching versus bio-barrier formation. *Polymer Degradation and Stability* 2011, *96*, 1286-1296.

6. Mittal, K. L.; Bahners, T. *Textile Finishing: Recent Developments and Future Trends;* Wiley: 2017.

7. Environmental Protection Agency Textiles: Material-Specific Data. *https://www.epa.gov/facts-and-figures-about-materials-waste-and-recycling/textiles-material-specific-data#TextilesTableandGraph* (accessed August 29, 2020).

8. Sui, X.; Terán, J., E.; Feng, C.; Wustrow, K.; Smith, C. J.; Vinueza, N. R. Quantification of anthracene after dermal absorption test via APCI-tandem mass spectrometry. *Analytical Methods* 2020.

9. Jia, W.; Chu, X.; Ling, Y.; Huang, J.; Lin, Y.; Chang, J. Simultaneous determination of dyes in wines by HPLC coupled to quadrupole orbitrap mass spectrometry. *Journal of Separation Science* 2014, *37*, 782-791.

10. Han, P.; Shuai, M.; Feng, X.; Geng, Q.; Zhang, W.; Cao, Y. Dissipation, and residue determination of penflufen in soil by UPLCMS-MS. *Fresenius Environ. Bull.* 2017, *26*, 1520-1527.

11. Abdel-Ghany, M.; Hussein, L. A.; El Azab, N. F. Multiresidue analysis of five neonicotinoid insecticides and their primary metabolite in cucumbers and soil using high-performance liquid chromatography with diode-array detection. *J. AOAC Int.* 2017, *100*, 176-188.

12. Lee, Y.; Choi, J.; Abd El-Aty, A. M.; Chung, H. S.; Lee, H. S.; Kim, S.; Rahman, M. M.; Park, B.; Kim, J.; Shin, H.; Shim, J. Development of a single-run analytical method for the detection of ten multiclass emerging contaminants in agricultural soil using an acetate-buffered QuEChERS method coupled with LC-MS/MS. *Journal of Separation Science* 2017, *40*, 415-423.

13. Meng, M.; He, Z.; Xu, Y.; Wang, L.; Peng, Y.; Liu, X. Simultaneous extraction and determination of antibiotics in soils using a method based on quick, easy, cheap, effective, rugged, and safe extraction and liquid chromatography with tandem mass spectrometry. *J. Sep. Sci.* 2017, *40*, 3214-3220.

14. Song, S.; Chen, Z.; Wei, J.; Lei, Y.; Deng, C.; Zhang, Y.; Tan, H.; Li, X. Residue and degradation of dodine in cucumber and soil investigated by QuEChERS-high performance liquid chromatography-triple quadrupole tandem mass spectrometry. *Huanjing Huaxue* 2017, *36*, 2165-2171.

15. Standard, A. D5988-03 (2003) Standard test method for determining aerobic biodegradation in soil of plastic materials or residual plastic materials after composting. *ASTM International, West Conshohocken, PA, USA Edition*.

16. Li, L.; Frey, M.; Browning, K. J. Biodegradability Study on Cotton and Polyester Fabrics. *Journal of Engineered Fabrics & Fibers (JEFF)* 2010, *5*.

17. Sui, X.; Feng, C.; Chen, Y.; Sultana, N.; Ankeny, M.; Vinueza, N. R. Detection of reactive dyes from dyed fabrics after soil degradation via QuEChERS extraction and mass spectrometry. *Analytical Methods* 2020, *12*, 179-187.

18. Anonymous, Bioanalytical Method Validation Guidance for Industry. *U.S. Food & Drug Administration* 2018.

19. Boes, K.; Boes, K.; Roberts, M.; Roberts, M.; Vinueza, N.; Vinueza, N. Rapid Quadrupole-Time-of-Flight Mass Spectrometry Method Quantifies Oxygen-Rich Lignin Compound in Complex Mixtures. *J. Am. Soc. Mass Spectrom* 2018, *29*, 535-542.
20. Rosal, R.; Rodea-Palomares, I.; Boltes, K.; Fernández-Piñas, F.; Leganés, F.; Petre, A. Ecotoxicological assessment of surfactants in the aquatic environment: Combined toxicity of docusate sodium with chlorinated pollutants. *Chemosphere* 2010, *81*, 288-293.
21. Glowicz, J.; Crist, M.; Gould, C.; Moulton-Meissner, H.; Noble-Wang, J.; Man, T. J. B.; Perry, K. A.; Miller, Z.; Yang, W. C.; Langille, S.; Ross, J.; Garcia, B.; Kim, J.; Epson, E.; Black, S.; Pacilli, M.; Lipuma, J. J.; Fagan, R. A multistate investigation of healthcare-associated Burkholderia cepacia complex infections related to liquid docusate sodium contamination, January - October 2016. *American journal of infection control* 2018, *46*, 649-655.

**CHAPTER 6**

**C.I. Reactive Blue 19 degradation products in aquatic medium via QuEChERS extraction: A high-resolution mass spectrometry study**

# 6.1 Introduction

As is has been discussed in previous chapters, the inventory of reactive dye greatly reshapes the cotton industry as it provides cotton fabrics with enhanced availability of color and excellent colorfast against washing thanks to covalent bonding with the cellulose polymer.[1-4] Despite those beneficial properties, the extensive applications of reactive dye in the cotton industry have also resulted in an increment in its environmental persistence due to their disposal in the liquid phase (dyeing bath residues[5, 6]) or solid-phase (used and not used garments in composts[7-9]). These conditions could generate degradation of reactive dye molecules which may impose potential environmental hazards during the decomposition process in soil and water.[10, 11] Recently, in a published article by Sultana et al., they identified and quantified the degradation products of a reactive dye (C. I. Reactive Blue 19) after simulated compost degradation[7]. This article opened the opportunity to learn more about the degradation of dyes in solid mediums and to evaluate the soil matrix itself. Then, in the study of Sui et al, the application of the QuEChERS extraction procedure allowed the extraction of reactive dyes and its degradation products for identification and quantification purposes.[12-16]

In addition to soil, the degradation of clothing dyed with reactive dyes and other chemical species could be performed in a simulated aquatic medium to evaluate the behavior of reactive dyes under those conditions. Moreover, these studies evaluated how several types of chemical treatments affect the rate of degradation of the fabrics in aquatic mediums.[17-20] Thus, besides investigating the degradation of reactive dyes in the soil, it would also be interesting to evaluate those aquatic media to identify and characterize reactive dyes and its potential degradation

products, which could help to better understand their environment and pollution consequences. [21, 22]

Due to the nature and the application of the reactive dyes, these chemicals are highly soluble in water, presenting a challenge in terms of analyzing the aquatic matrix directly since we have to separate the dye and its degradation products for analysis. Recently, the QuEChERS extraction method has been popular in environmental matrix analyses since this method can push the target analyte out of the matrix into an organic solvent. Moreover, high-resolution mass spectrometry, reinforced by tandem mass spectrometry, provides has been effective in determining structure-specific identification on degradation products and other dyestuff related chemicals.[12, 13, 23-25]

Thus, in this chapter, the QuEChERS extraction, identification, and characterization of reactive dyes (C.I. Reactive Blue 19 (RB19)) by high-resolution Quadrupole Time Of -Flight mass spectrometry (QTOF-MS) in combination with tandem mass spectrometry (MS/MS) was performed. Results from this study could deepen our understanding of reactive dye degradation in river water conditions and benefit future toxicology and environmental studies.

# 6.2 Experimental

## 6.2.1 Materials

### 6.2.1.1 Dyes

Standards of C.I. Reactive Blue 19 (RB19) and Acid Blue 25 (AB25) were purchased from Sigma-Aldrich (Sigma-Aldrich, MO, USA) and used without further purification. The chemical structures of these two dyes are shown in Figure 54.

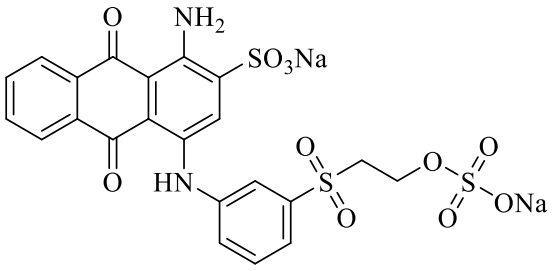

**C.I. Reactive Blue 19-** *Sulfatoethylsulfone form* **(SES)**
**Chemical Formula:** $C_{22}H_{16}N_2Na_2O_{11}S_3$
**Exact Mass:** 625.9712

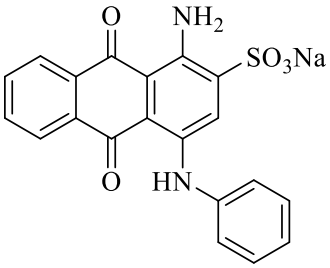

**C.I. Acid Blue 25**
**Chemical Formula:** $C_{20}H_{13}NaN_2O_5S$
**Exact Mass:** 416.0442

Figure 54: Chemical structures of C.I. Reactive Blue 19 and C.I. Acid Blue 25

### 6.2.1.2 Solvents

ACS grade acetonitrile (ACN) and methanol (MeOH) used for QuEChERS extraction were purchased from Sigma-Aldrich (Sigma-Aldrich, MO, USA) and used without any further purification. HPLC grade water was acquired from a Pure Lab Ultra water purification system from ELGA Lab Water (ELGA Lab Water, High Wycombe, UK). LC-MS Grade acetonitrile was purchased from Thermo Fisher Scientific. (Fisher Scientific, PA, USA).

### 6.2.1.3 Chemicals

ACS grade magnesium sulfate ($MgSO_4$) powder was purchased from Sigma-Aldrich and used without further purification.

### 6.2.1.4 Water samples

Water samples from aqueous degradation of cotton fabrics dyed with RB19 reactive dye were provided by the Department of Forest Biomaterials at NC State University. Those water samples were collected in a 50 mL centrifuge tube after the degradation process and stored in a refrigerator at 5 °C before being processed by QuEChERS extraction method and characterized by HPLC-DAD-QTOF MS.

### 6.2.1.5 Other Supplies

Disposable Luer-slip plastic syringes (1 mL) were purchased from Sigma-Aldrich. 0.2 µm PTFE Non-Sterile Syringe Filters were purchased from Analytical (Analytical Sales and Services Inc., NJ, USA). 15 x 45 mm Fisherbrand™ Snap-Cap™ Flat-Top Graduated Microcentrifuge Tubes were purchased from Fisher Scientific (Fisher Scientific, PA, USA.) 2 mL Amber Glass Screw Vials for HPLC & Marking Spot were purchased from Analytical.

## 6.2.2 Method

### 6.2.2.1 Aquatic degradation of C.I. Reactive Blue 19 dye-dyed fabrics

The procedure for the aquatic degradation of cotton fabrics with Reactive Blue 19 was performed by the Department of Forest Biomaterials at NC State University using the standard method ISO 14851on an RSA PF-8000 respirometer. The degradation media included an inoculum from the Neuse River wastewater treatment plant (activated sludge, 30 ppm Total Suspended Solids), along with nutrients. The containers were prepared within 24 hours after the collection of the inoculum, generating triplicates for every sample. After one week of incubation, the samples were analyzed and extracted for further characterization.[18, 20]

### 6.2.2.2 QuEChERS extraction on aquatic matrices

The application of reactive dyes during dyeing is facilitated by their water solubility brought by the introduction of sulfonate solubilizing groups.[1] This behavior applies as well to its degradation products. Thus, considering the composition complexity of degradation media, it is important to employ a procedure that could remove reactive dyes and its degradation products from this aqueous matrix. The QuEChERS extraction method employs a large enough amount of $MgSO_4$ salt along with HPLC compatible organic solvents to force the saturation of the aqueous

phase. This saturation allows that everything compatible with this organic solvent (the solubility of dyes is based mostly on their sulfonic groups, having most of the time nonpolar structures) to be transferred from the aqueous phase to the organic phase. Therefore, the complexity of the analyzed system is reduced, and the feasibility of characterization increases.[12]

In brief, 200 µL of a water sample was loaded into a 15 x 45 mm, Fisherbrand™ Snap-Cap™ Flat-Top Graduated Microcentrifuge Tube and combined with 160 mg of $MgSO_4$ powder and 800 µL of QuEChERS extraction solvents made up by acetonitrile to methanol ratio of 9:1. The mixture in the tube was then agitated using a VWR vortex mixer for 30 seconds at 2300 rpm (rotation per minute) and sonicated for 10 minutes using a Branson 2210 sonicator. Next, the system was centrifuged using a VWR microcentrifuge for 5 minutes at 8500 rpm. After the centrifuge process, the supernatant liquid was taken using a disposable Luer-slip plastic syringe and filtered into a 2 mL Amber Glass Screw Vials for HPLC-MS analyses using a 0.2 µm PTFE non-sterile syringe filter. A summary of this procedure is shown in Figure 55.

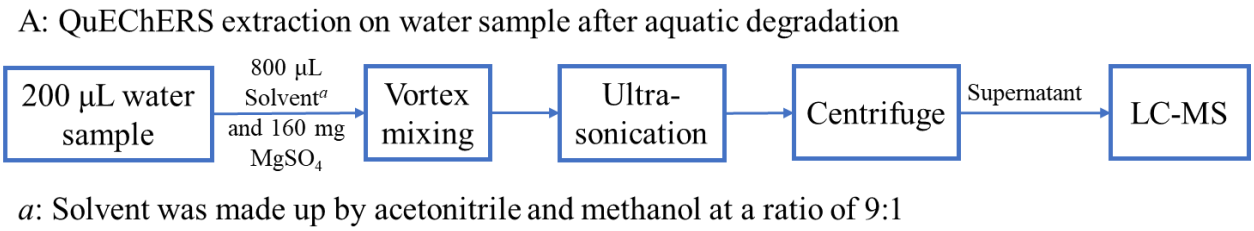


Figure 55: Diagram showing the procedure for QuEChERS extraction on aqueous biodegradation media

### 6.2.3 Instrumentation

The LC-MS analyses of all the samples obtained from QuEChERS extractions on aquatic matrices were performed using an Agilent Technologies 1260 A high-Performance Liquid Chromatography (HPLC) system that was coupled with a Diode Array Detector (DAD) and an Agilent 6520 Quadrupole Time-Of-Flight (QTOF) mass spectrometer (Agilent Technologies, CA,

USA). An isocratic elution composed of HPLC grade water with 0.1% formic acid (A) and LC-MS grade acetonitrile with 0.1% water (B) was chosen as the mobile phase. An Agilent ZORBAX SB-C18 (3.0 x 150mm, 3.5 μm) column was used for the separation. The flow rate of the HPLC was set to 0.5 mL/min, and the total run time for each sample was 5 minutes. Ionization was performed via dual electrospray ionization (ESI) source from Agilent Technologies and was carried out in negative mode with the following parameters: gas temperature: 300 ºC, drying gas flow rate: 10 liters per minute, nebulizer: 60 psi, capillary voltage: 4000 V, fragmentor voltage: 160 V, skimmer voltage: 65 V, and octupole voltage: 750 V. To improve the mass measurement accuracy, a solution of mass reference mix, obtained from Agilent Technologies, was introduced via a secondary ESI needle. Tandem mass spectrometry (MS/MS) analysis was performed by collision-induced dissociation (CID) with nitrogen as the collision gas. The collision energy was set to a level of 40 eV in MassHunter™ Acquisition software, and the isolation window was set to narrow (1.3 mass-to-charge ratio). After each sample run, the corresponding data file was processed using Agilent MassHunter Qualitative Analysis B.06.00.

## 6.3 Results and Discussions

### 6.3.1 Identification of RB19 degradation products from in aquatic matrices

Based on the current knowledge regarding the degradation products of C.I. Reactive Blue 19, and their presence in soil, this study evaluated the possibility of finding the same or additional forms of degradation products in this aquatic matrix.[12, 13, 26] Considering the complexity of the signals on the analyses, an additional QuEChERS extraction was performed on an aquatic degradation sample from a white cotton fabric without dye treatment. This sample served as a blank and it was characterized using the same analytical methodology described in section **6.2.3**. Then, the MS spectra obtained were subtracted from all the presented spectra as background.

After the analysis of these MS spectra, four forms of RB19 were identified using high-resolution mass spectrometry after aquatic degradation. These forms include unreacted RB19 with a vinyl sulfone reactive group (**VS** in **Figure 56**), RB19 hydrolysis form (**H** in Figure 56), and two forms of degraded RB19 (**D1** and **D3** in Figure 56). Detailed information about these species is summarized in Table 8.

Table 8: Compounds identified from aqueous degradation of RB19 cotton fabrics

| Experimental m/z | Proposed formula | Theoretical m/z | Ion species | ppm error | Identification |
|---|---|---|---|---|---|
| 483.0346 | $C_{22}H_{16}N_2O_7S_2$ | 483.0326 | [M-H]- | -4.14 | RB19 VS form (**VS**) |
| 501.0443 | $C_{22}H_{18}N_2O_8S_2$ | 501.0432 | [M-H]- | -2.20 | RB19 Hydrolysis form (**H**) |
| 393.0549 | $C_{20}H_{14}N_2O_5S$ | 393.0551 | [M-H]- | 0.51 | RB19 Degraded form 1 (**D1**) |
| 471.0331 | $C_{21}H_{16}N_2O_7S_2$ | 471.0326 | [M-H]- | -3.00 | RB19 Degraded form 3 (**D3**) |

Note: VS = Vinyl Sulfone, ppm error was calculated by equation: (Experimental Exact Mass - Theoretical Exact Mass)/ Theoretical Exact Mass * 100 %, m/z = mass-to-charge ratio

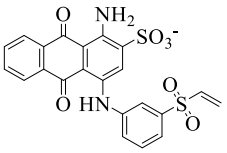

**C.I. Reactive Blue 19 -** *Unreacted form* (**VS**) - Deprotonated ion
**Chemical Formula:** $C_{22}H_{15}N_2O_7S_2^-$
**m/z:** 483.0326

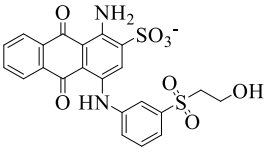

**C.I. Reactive Blue 19 -** *Hydrolysis form* (**H**) - Deprotonated ion
**Chemical Formula:** $C_{22}H_{17}N_2O_8S_2^-$
**m/z:** 501.0431

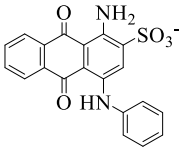

**C.I. Reactive Blue 19 -** *Degraded 1 (**D1**)* - Deprotonated ion
**Chemical Formula:** $C_{20}H_{13}N_2O_5S^-$
**m/z:** 393.0551

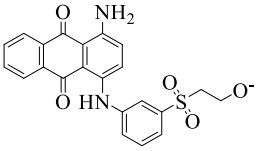

**C.I. Reactive Blue 19 -** *Degraded 2* (**D2**) **-** Deprotonated ion
**Chemical Formula:** $C_{22}H_{17}N_2O_5S^-$
**m/z:** 421.0864

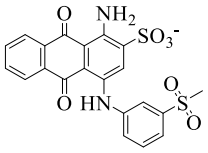

**C.I. Reactive Blue 19 -** *Degraded 3 (**D3**)* **-** Deprotonated ion
**Chemical Formula:** $C_{21}H_{15}N_2O_7S_2^-$
**m/z:** 471.0326

Figure 56: Chemical structures of different forms of RB19 identified in soil and water matrices

Four aspects were evaluated to prove whether the detected ion is a degradation product related to RB19: the response from DAD, mass-to-charge ratio value (m/z), chemical formula generated by MassHunter software, and fragmentation pattern under CID. In the case of **D1**, for example, the response from DAD showed a maximum absorption wavelength ($\lambda_{max}$) of 595 nm which corresponded to the range where the blue color is visible. In terms of the mass spectrometry response, as is shown in Figure 57, this ion has an m/z of 393.0549. Based on this m/z value, a series of chemical formulas with different levels of double bond equivalent (DBE, also called unsaturation number) and mass measurement accuracy (MMA, represented by ppm error) were generated by using the formulation generation function in MassHunter$^{TM}$ qualitative analysis software. By considering of DBE of RB19 in VS form (DBE = 16) and MMA of QTOF MS (ppm error within ± 5), the chemical formula of $C_{20}H_{14}N_2O_5S$ was selected for **D1** because it has a reasonable DBE (DBE = 15) and appropriate MMA (ppm error = 0.51). Then by comparing this

formula and corresponding mass spectrum to a Personal Compound Database and Library (PCDL) on commercial acid and reactive dyes, a match was found on C. I. Acid Blue 25.

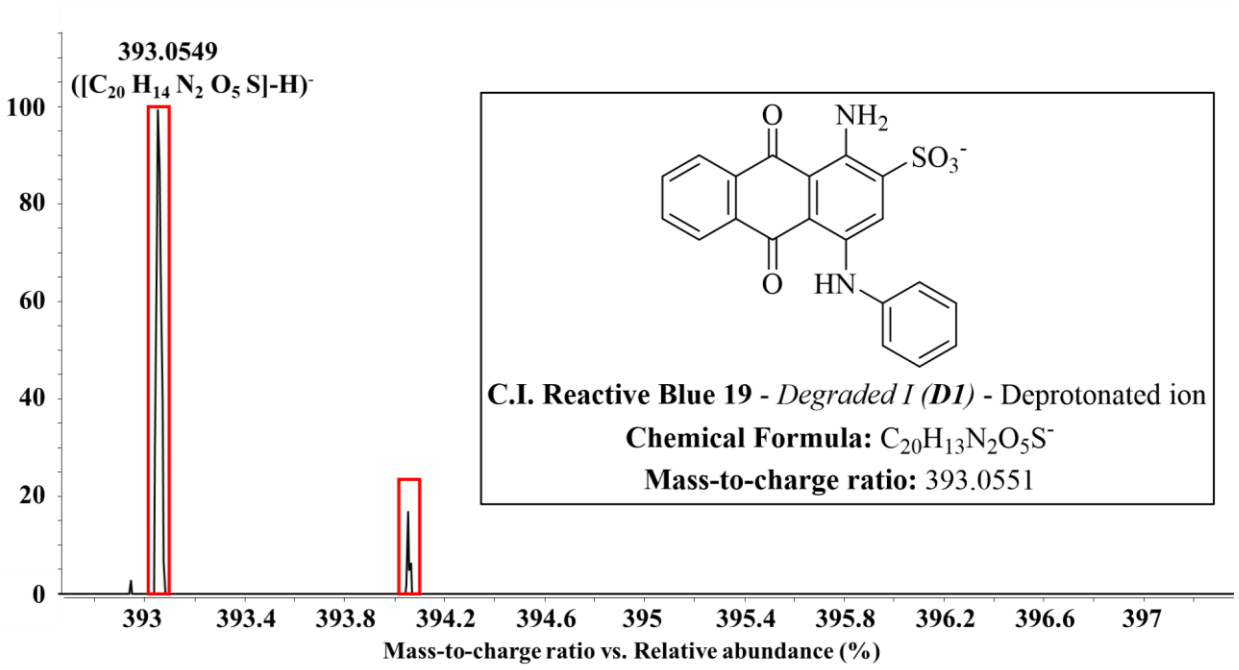


Figure 57: Mass spectrum showing the detection of RB19 degraded form 1 (**D1**) in aqueous degradation media

Posterior to this analysis, to elucidate the structure of this degradation product, LC-MS/MS analysis via CID was performed on this sample and a commercial AB25 standard. As is shown in **Figure 58**, after CID, the same MS/MS transition could be observed from both degradation product and AB25 standard where major product ion of m/z 329.0932 was observed, corresponding to a mass difference of 63.9319. Considering the nature of CID as a structure-specific process, this exact match of (shown in **Figure 58**) MS/MS spectra proves that this product found after the aquatic degradation of RB19 cotton fabrics is Acid Blue 25.

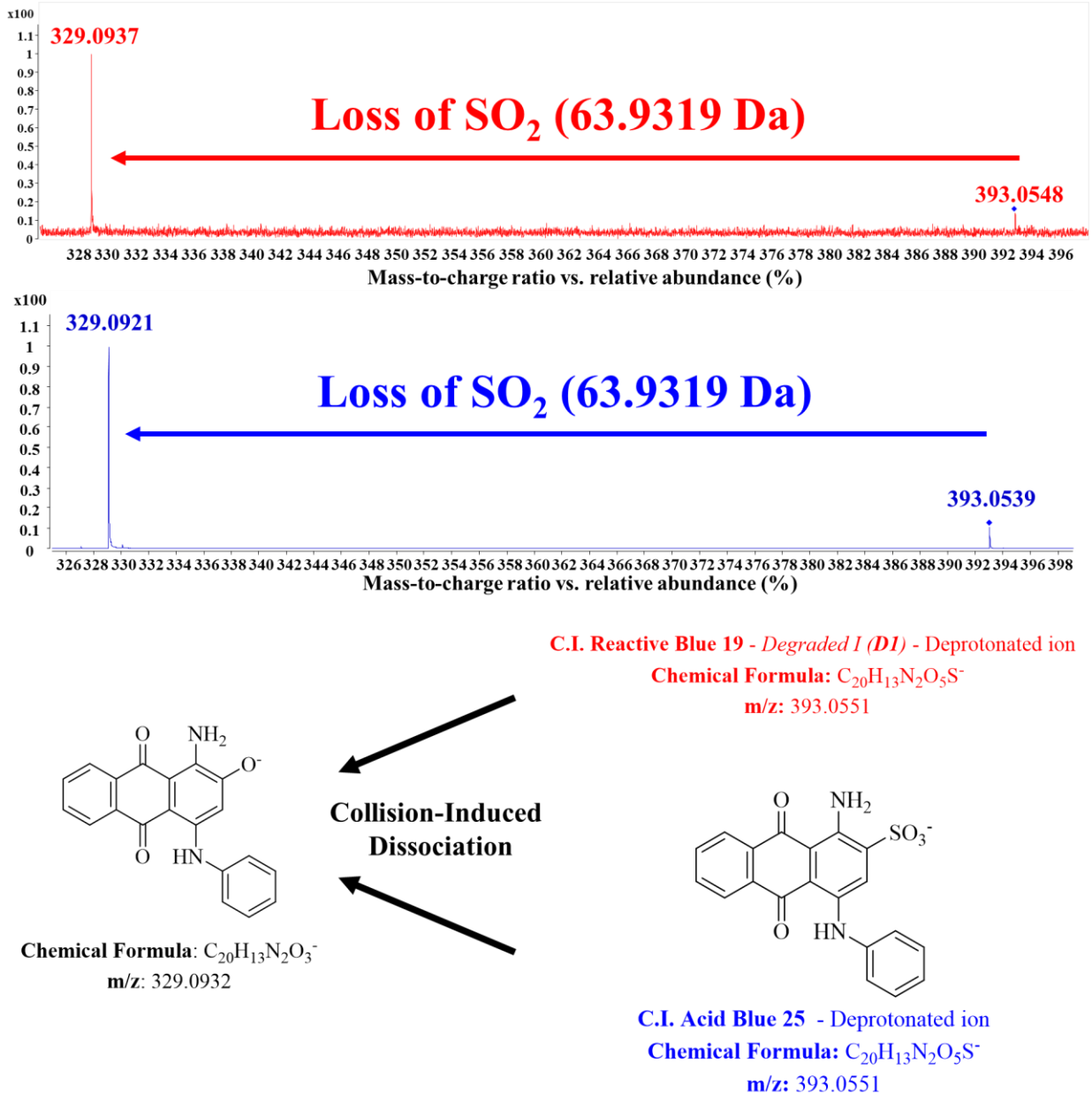


Figure 58: MS/MS spectra of RB19 degraded form 1 (D1) in aqueous degradation media and commercial AB25

Additionally, by following the same methodology mentioned above, another degradation product (m/z 471.0343 in Table 8, corresponding to D3 in Figure 56) was detected and identified, suggesting that in addition to the previously identified structure (m/z 393.0549 in Table 8), there could be an additional way (loss of -$CH_2OH$ group from hydrolysis product (product H in Figure 56)) in which RB19 degrades in an aqueous environment.

In summary, the degradation of Reactive Blue 19 in different mediums, such as soil and water, shares certain similarities however, every medium showed its uniqueness. For instance, the cleavage of vinyl sulfone reactive group (**D1** in **Figure 56**) was observed first in soil degradation and it was also identified from aqueous degradation, suggesting that degradation of RB19 in the different environment could result in the same product. On the other hand, degradation of RB19 in aqueous media possesses some uniqueness against soil degradation as degradation product **D3** representing the loss of $CH_2OH$ from hydrolysis form (**H**) was only identified in aqueous degradation. This difference in degradation products found in this study indicates that differences in the disposal environment would result in a variation of the process of RB19 degradation, which could be beneficial to future environmental or toxicology studies.

## 6.4 Summary

The combination of QuEChERS extraction, High-Resolution Mass Spectrometry, and Tandem Mass Spectrometry was proved to be useful to identify several species (unreacted dye and its degradation products) from aqueous degradation of cotton fabrics dyed with Reactive Blue 19 samples. Moreover, the identification of different forms of RB19, including one degradation product indicating the loss of vinyl sulfone (D1 in Table 8) (which was identified as well in the studies considering fabrics and soil extraction) and another degradation product representing the loss of $CH_2OH$ group (D3 in Table 8) (which has been unique to this type of matrix), was achieved based on a series of information obtained from LC-DAD-QTOF-MS and MS/MS including $\lambda_{max}$, exact mass, chemical formula, DBE, MMA, and fragmentation pattern under CID. This corroboration could be important in terms of further toxicological and mutagenic evaluations for these identified dye related degradation products.

In terms of future steps, we have been working on is the quantification of RB19 degradation product (D1 in Table 8) identified in the soil after simulated compost degradation, where a calibration system based on absorption area from Diode Array Detector (DAD) on commercial AB25 standard will be established and validated to measure the concentration of RB19 degradation product after a simulated compost process.

## Acknowledgments

This work in this chapter was financially supported by Cotton Incorporated and Cotton Research and Development Corporation. Grant Number 20-718.

## References

1. Zollinger, H., 1919-2005 *Color chemistry: syntheses, properties, and applications of organic dyes and pigments;* Verlag Helvetica Chimica Acta; Wiley-VCH: Zürich; Weinheim, 2003.
2. Christie, R. M. *Colour chemistry;* Cambridge, England: Royal Society of Chemistry, 2015.
3. Gürses, A. *Dyes, and pigments;* Cham, Switzerland: Springer, 2016.
4. Pellew, C. E., author. *Dyes and dyeing;* Abhishek Publications: Chandigarh, 2007.
5. Montagner, C.; Sodré, F.; Acayaba, R.; Vidal, C.; Campestrini, I.; Locatelli, M.; Pescara, I.; Albuquerque, A.; Umbuzeiro, G.; Jardim, W. Ten Years-Snapshot of the Occurrence of Emerging Contaminants in Drinking, Surface and Ground Waters and Wastewaters from São Paulo State, Brazil. *Journal of the Brazilian Chemical Society* **2018**.
6. Vacchi, F. I.; Vendemiatti, J. A. S.; Brosselin, V.; Ferreira da Silva, B.; B. Zanoni, M. V.; DeMeo, M.; Bony, S.; Devaux, A.; Umbuzeiro, G. A. Combining different assays and chemical analysis to characterize the genotoxicity of waters impacted by textile discharges. *Environmental and Molecular Mutagenesis* **2016**, *57*, 559-571.

7. Bolyard, S. C.; Reinhart, D. R. Application of landfill treatment approaches for stabilization of municipal solid waste. *Waste Manage. (Oxford, U. K. )* **2016**, *55*, 22-30.

8. Karanjekar, R. V.; Bhatt, A.; Altouqui, S.; Jangikhatoonabad, N.; Durai, V.; Sattler, M. L.; Hossain, M. D. S.; Chen, V. Estimating methane emissions from landfills based on rainfall, ambient temperature, and waste composition: The CLEEN model. *Waste Manage. (Oxford, U. K. )* **2015**, *46*, 389-398.

9. Mazibuko, M.; Ndumo, J.; Low, M.; Ming, D.; Harding, K. Investigating the natural degradation of textiles under controllable and uncontrollable environmental conditions. *Procedia Manufacturing* **2019**, *35*, 719-724.

10. Environmental Protection Agency Textiles: Material-specific Data. *https://www.epa.gov/facts-and-figures-about-materials-waste-and-recycling/textiles-material-specific-data#TextilesTableandGraph* (accessed August 29, 2020).

11. Bechtold, T.; Pham, T. *Textile chemistry;* Berlin ; Boston : De Gruyter, 2019]: 2019; .

12. Sui, X.; Feng, C.; Chen, Y.; Sultana, N.; Ankeny, M.; Vinueza, N. R. Detection of reactive dyes from dyed fabrics after soil degradation via QuEChERS extraction and mass spectrometry. *Analytical Methods* **2020**.

13. Sultana, N.; Williams, K.; Ankeny, M.; Vinueza, N. R. Degradation studies of CI Reactive Blue 19 on biodegraded cellulosic fabrics via liquid chromatography-photodiode array detection coupled to high-resolution mass spectrometry. *Coloration Technology* **2019**.

14. Anastassiades, M.; Lehotay, S. J.; Stajnbaher, D.; Schenck, F. J. Fast and easy multiresidue method employing acetonitrile extraction/partitioning and "dispersive solid-phase extraction" for the determination of pesticide residues in produce. *Journal of AOAC International* **2003**, *86*, 412-431.

15. Bruzzoniti, M. C.; Checchini, L.; De Carlo, R. M.; Orlandini, S.; Rivoira, L.; Del Bubba, M. QuEChERS sample preparation for the determination of pesticides and other organic residues in environmental matrices: a critical review. *Analytical and Bioanalytical Chemistry* **2014**, *406*, 4089-4116.

16. Vera, J.; Correia-S, L.; Paga, P.; Bragana, I.; Fernandes, V. C.; Domingues, V. F.; Delerue-Matos, C. QuEChERS, and soil analysis. An Overview. *Sample Preparation* **2013**, *1*, 54-77.

17. Berradi, M.; Hsissou, R.; Khudhair, M.; Assouag, M.; Cherkaoui, O.; El Bachiri, A.; El Harfi, A. Textile finishing dyes and their impact on aquatic environs. *Heliyon* **2019**, *5*, e02711.

18. Zambrano, M. C.; Pawlak, J. J.; Daystar, J.; Ankeny, M.; Goller, C. C.; Venditti, R. A. Aerobic biodegradation in freshwater and marine environments of textile microfibers generated in clothes laundering: Effects of cellulose and polyester-based microfibers on the microbiome. *Marine Pollution Bulletin* **2020**, *151*, 110826.

19. Zambrano, M. C.; Pawlak, J. J.; Daystar, J.; Ankeny, M.; Cheng, J. J.; Venditti, R. A. Microfibers generated from the laundering of cotton, rayon, and polyester-based fabrics and their aquatic biodegradation. *Marine Pollution Bulletin* **2019**, *142*, 394-407.

20. Zambrano, M. C.; Pawlak, J. J.; Daystar, J.; Ankeny, M.; Venditti, R. A. Impact of Dyes and Finishes on the Aquatic Biodegradability of Cotton Textile Fibers and Microfibers Released on Laundering Clothes: Correlations between Enzyme Adsorption and Activity and Biodegradation Rates, Marine Pollution Bulletin. *Marine Pollution Bulletin, (Submitted for Publication)*.

21. Boyd, B.; Basic, C.; Bethem, R. *Trace quantitative analysis by mass spectrometry;* John Wiley & Sons: Hoboken, N.J, 2008.

22. Watson, J. T. *Introduction to mass spectrometry: instrumentation, applications, and strategies for data interpretation;* John Wiley & Sons: Chichester, England; Hoboken, NJ, 2007.

23. Wu, X.; Yu, Y.; Xu, J.; Dong, F.; Liu, X.; Du, P.; Wei, D.; Zheng, Y. Residue analysis and persistence evaluation of fipronil and its metabolites in cotton using high-performance liquid chromatography-tandem mass spectrometry. *PLoS ONE 12(3):* e0173690.

24. De Vijlder, T.; Valkenborg, D.; Lemière, F.; Romijn, E. P.; Laukens, K.; Cuyckens, F. A tutorial in small molecule identification via electrospray ionization-mass spectrometry: The practical art of structural elucidation. *Mass Spectrometry Reviews* **2018**, *37*, 607-629.

25. Sultana, N.; Liu, Y.; Szymczyk, M.; Freeman, H. S.; Vinueza, N. R. Dimerised heterobifunctional reactive dyes. Part 1: characterization using quadrupole time-of-flight mass spectrometry. *Coloration Technology* **2018**, *134*, 470-477.

26. Terán, J. E.; Millbern, Z.; Shao, D.; Sui, X.; Liu, Y.; Demmler, M.; Vinueza, N. R. Characterization of Synthetic Dyes for Environmental and Forensic Assessments: A Chromatography and Mass Spectrometry Approach. *Journal of Separation Science*. **2020.**

**CHAPTER 7**

**Conclusions and recommendation for future research**

# 7.1 Conclusions

In this dissertation, through a joint force of wet chemistry, extraction process, and different analytical chemistry techniques including HPLC, HRMS, and MS/MS, the degradation of textile dyes and auxiliaries in soil after composting was examined qualitatively and quantitatively. First, through a combination of modified QuEChERS extraction method and QTOF mass spectrometry, four degradation products were identified based on exact mass measurement after a simulated composting process on cotton fabrics dyed with four commonly used reactive dyes including RO35, RB49, Rblk 5, and RB19. Then a quantification method aiming to measure the concentration of docusate antimicrobial in soil after the simulated composting process was developed through a combination of QuEChERS extraction, quantitative tandem mass spectrometry, and isotopically labeled internal standard. After establishment, this method was validated according to FDA guidelines, and results suggested that this method have good linearity ($R^2 > 0.99$), good accuracy (mean % error less than 15%), good precision (mean % CV less than 15%), good sensitivity (measured docusate concentration is 400% higher than LOD and 100% higher than LLOQ), satisfying matrix effect, and the concentration of docusate (51±5 ng/mL) falls within the linear range of calibration. Finally, two degradation products from the aqueous degradation of RB19-dyed cotton fabric were extracted by QuEChERS extraction and identified based on QTOF mass spectrometry and qualitative tandem mass spectrometry against the standard. Results obtained from this project would benefit both academia and the textile industry disposal of unwanted cotton textiles by compost or landfill could be complicated by the addition of reactive dye and textile

finishing because those chemicals could be leaching out and degrade under the decomposition process.

## 7.2 Recommendation for future works

**A.** Toxicology studies could be implemented to assess the toxicity of degradation products identified in both soil and aqueous environment. With the presence of these products confirmed and even quantified, the toxicity to microbes or aquatic animals should be evaluated to check their environmental impacts.

**B.** To help explain the generation of degradation products from their parent structure. Electronic structure calculation could be performed, which includes the 3D structure of intact dye (e.g. RB19) is optimized using Density Function Theory (DFT) and split valance triple zeta basis set, benchmarking of theory and basis set against experimental UV-Vis spectrum using time-dependent DFT (DFT), and evaluation of bonding energy among different products.

**C.** In this study, the degradation study of textile dye and finishing in soil was performed independently but in a real-world scenario, the fabrics could have both dye and finishing. Thus, it would be necessary to study the degradation of cotton fabrics with reactive dye and finishing in soil and investigate any potential interaction between these two types of chemicals.